Organic Implantable Probes for in vivo Recordings of Electrophysciological Activity and Drug Delivery

Ilke Uguz

▶ **To cite this version:**

Ilke Uguz. Organic Implantable Probes for in vivo Recordings of Electrophysciological Activity and Drug Delivery. Other. Université de Lyon, 2016. English. NNT : 2016LYSEM027 . tel-01665182

HAL Id: tel-01665182
https://theses.hal.science/tel-01665182

Submitted on 15 Dec 2017

HAL is a multi-disciplinary open access archive for the deposit and dissemination of scientific research documents, whether they are published or not. The documents may come from teaching and research institutions in France or abroad, or from public or private research centers.

L'archive ouverte pluridisciplinaire **HAL**, est destinée au dépôt et à la diffusion de documents scientifiques de niveau recherche, publiés ou non, émanant des établissements d'enseignement et de recherche français ou étrangers, des laboratoires publics ou privés.

N°d'ordre NNT : **2016LYSEM027**

THESE de DOCTORAT DE L'UNIVERSITE DE LYON
opérée au sein de
l'Ecole des Mines de Saint-Etienne

Ecole Doctorale N° 488
Sciences, Ingénierie, Santé

Spécialité de doctorat : Microelectronique
Discipline : Bioelectronique

Soutenue à huis clos le 21/11/2016, par :
(Uguz Ilke)

Organic Implantable Probes for in vivo Recordings of Electrophysiological Activity and Drug Delivery

---

Devant le jury composé de :

Christophe Bernard	Ingénieur de Recherche	Aix-Marseille Université	Président du Jury
Salleo Alberto	Professeur associé	Stanford University	Rapporteur
Lacour Stéphanie	Professeur	Ecole Polytechnique Fédérale de Lausanne	Rapporteure
Sahika Inal	Maitre Assistant	KAUST	Examinateur
Malliaras George	Professeur	Ecole des Mines de Saint-Etienne	Directeur de thèse
Hervé Thierry	C.E.O	Microvitae Technologie	Invité

Spécialités doctorales	Responsables :	Spécialités doctorales	Responsables
SCIENCES ET GENIE DES MATERIAUX	K. Wolski Directeur de recherche	MATHEMATIQUES APPLIQUEES	O. Roustant, Maître-assistant
MECANIQUE ET INGENIERIE	S. Drapier, professeur	INFORMATIQUE	O. Boissier, Professeur
GENIE DES PROCEDES	F. Gruy, Maître de recherche	IMAGE, VISION, SIGNAL	JC. Pinoli, Professeur
SCIENCES DE LA TERRE	B. Guy, Directeur de recherche	GENIE INDUSTRIEL	A. Dolgui, Professeur
SCIENCES ET GENIE DE L'ENVIRONNEMENT	D. Graillot, Directeur de recherche	MICROELECTRONIQUE	S. Dauzere Peres, Professeur

EMSE : Enseignants-chercheurs et chercheurs autorisés à diriger des thèses de doctorat (titulaires d'un doctorat d'État ou d'une HDR)

ABSI	Nabil	CR	Génie industriel	CMP
AVRIL	Stéphane	PR2	Mécanique et ingénierie	CIS
BALBO	Flavien	PR2	Informatique	FAYOL
BASSEREAU	Jean-François	PR	Sciences et génie des matériaux	SMS
BATTAIA-GUSCHINSKAYA	Olga	CR	Génie industriel	FAYOL
BATTON-HUBERT	Mireille	PR2	Sciences et génie de l'environnement	FAYOL
BERGER DOUCE	Sandrine	PR2	Sciences de gestion	FAYOL
BIGOT	Jean Pierre	MR(DR2)	Génie des Procédés	SPIN
BILAL	Essaid	DR	Sciences de la Terre	SPIN
BLAYAC	Sylvain	MA(MDC)	Microélectronique	CMP
BOISSIER	Olivier	PR1	Informatique	FAYOL
BONNEFOY	Olivier	MA(MDC)	Génie des Procédés	SPIN
BORBELY	Andras	MR(DR2)	Sciences et génie des matériaux	SMS
BOUCHER	Xavier	PR2	Génie Industriel	FAYOL
BRODHAG	Christian	DR	Sciences et génie de l'environnement	FAYOL
BRUCHON	Julien	MA(MDC)	Mécanique et ingénierie	SMS
BURLAT	Patrick	PR1	Génie Industriel	FAYOL
COURNIL	Michel	PR0	Génie des Procédés	DIR
DAUZERE-PERES	Stéphane	PR1	Génie Industriel	CMP
DEBAYLE	Johan	CR	Image Vision Signal	CIS
DELAFOSSE	David	PR0	Sciences et génie des matériaux	SMS
DELORME	Xavier	MA(MDC)	Génie industriel	FAYOL
DESRAYAUD	Christophe	PR1	Mécanique et ingénierie	SMS
DOLGUI	Alexandre	PR0	Génie Industriel	FAYOL
DRAPIER	Sylvain	PR1	Mécanique et ingénierie	SMS
FAVERGEON	Loïc	CR	Génie des Procédés	SPIN
FEILLET	Dominique	PR1	Génie Industriel	CMP
FRACZKIEWICZ	Anna	DR	Sciences et génie des matériaux	SMS
GARCIA	Daniel	MR(DR2)	Génie des Procédés	SPIN
GAVET	Yann	MA(MDC)	Image Vision Signal	CIS
GERINGER	Jean	MA(MDC)	Sciences et génie des matériaux	CIS
GOEURIOT	Dominique	DR	Sciences et génie des matériaux	SMS
GONDRAN	Natacha	MA(MDC)	Sciences et génie de l'environnement	FAYOL
GRAILLOT	Didier	DR	Sciences et génie de l'environnement	SPIN
GROSSEAU	Philippe	DR	Génie des Procédés	SPIN
GRUY	Frédéric	PR1	Génie des Procédés	SPIN
GUY	Bernard	DR	Sciences de la Terre	SPIN
HAN	Woo-Suck	MR	Mécanique et ingénierie	SMS
HERRI	Jean Michel	PR1	Génie des Procédés	SPIN
KERMOUCHE	Guillaume	PR2	Mécanique et Ingénierie	SMS
KLOCKER	Helmut	DR	Sciences et génie des matériaux	SMS
LAFOREST	Valérie	MR(DR2)	Sciences et génie de l'environnement	FAYOL
LERICHE	Rodolphe	CR	Mécanique et ingénierie	FAYOL
LI	Jean-Michel		Microélectronique	CMP
MALLIARAS	Georges	PR1	Microélectronique	CMP
MAURINE	Philippe	Ingénieur de recherche	Microélectronique	CMP
MOLIMARD	Jérôme	PR2	Mécanique et ingénierie	CIS
MONTHEILLET	Frank	DR	Sciences et génie des matériaux	SMS
MOUTTE	Jacques	CR	Génie des Procédés	SPIN
NEUBERT	Gilles	PR	Génie industriel	FAYOL
NIKOLOVSKI	Jean-Pierre	Ingénieur de recherche		CMP
NORTIER	Patrice	PR1		SPIN
OWENS	Rosin	MA(MDC)	Microélectronique	CMP
PICARD	Gauthier	MA(MDC)	Informatique	FAYOL
PIJOLAT	Christophe	PR0	Génie des Procédés	SPIN
PIJOLAT	Michèle	PR1	Génie des Procédés	SPIN
PINOLI	Jean Charles	PR0	Image Vision Signal	CIS
POURCHEZ	Jérémy	MR	Génie des Procédés	CIS
ROBISSON	Bruno	Ingénieur de recherche	Microélectronique	CMP
ROUSSY	Agnès	MA(MDC)	Génie industriel	CMP
ROUSTANT	Olivier	MA(MDC)	Mathématiques appliquées	FAYOL
ROUX	Christian	PR	Image Vision Signal	CIS
STOLARZ	Jacques	CR	Sciences et génie des matériaux	SMS
TRIA	Assia	Ingénieur de recherche	Microélectronique	CMP
VALDIVIESO	François	PR2	Sciences et génie des matériaux	SMS
VIRICELLE	Jean Paul	DR	Génie des Procédés	SPIN
WOLSKI	Krzystof	DR	Sciences et génie des matériaux	SMS
XIE	Xiaolan	PR1	Génie industriel	CIS
YUGMA	Gallian	CR	Génie industriel	CMP

ENISE : Enseignants-chercheurs et chercheurs autorisés à diriger des thèses de doctorat (titulaires d'un doctorat d'État ou d'une HDR)

BERGHEAU	Jean-Michel	PU	Mécanique et Ingénierie	ENISE
BERTRAND	Philippe	MCF	Génie des procédés	ENISE
DUBUJET	Philippe	PU	Mécanique et Ingénierie	ENISE
FEULVARCH	Eric	MCF	Mécanique et Ingénierie	ENISE
FORTUNIER	Roland	PR	Sciences et Génie des matériaux	ENISE
GUSSAROV	Andrey	Enseignant contractuel	Génie des procédés	ENISE
HAMDI	Hédi	MCF	Mécanique et Ingénierie	ENISE
LYONNET	Patrick	PU	Mécanique et Ingénierie	ENISE
RECH	Joël	PU	Mécanique et Ingénierie	ENISE
SMUROV	Igor	PU	Mécanique et Ingénierie	ENISE
TOSCANO	Rosario	PU	Mécanique et Ingénierie	ENISE
ZAHOUANI	Hassan	PU	Mécanique et Ingénierie	ENISE

Mise à jour : 29/06/2015

Organic Implantable Probes for in vivo Recordings of Electrophysciological Activity and Drug Delivery

Ilke Uguz

Department of Bioelectronics

École nationale supérieure des mines de Saint-Étienne

This dissertation is submitted for the degree of

Doctor of Philosophy

Gardanne November 2016

Declaration

I hereby declare that except where specific reference is made to the work of others, the contents of this dissertation are original and have not been submitted in whole or in part for consideration for any other degree or qualification in this, or any other University. This dissertation is the result of my own work and includes nothing which is the outcome of work done in collaboration, except where specifically indicated in the text.

Ilke Uguz
November 2016

Acknowledgements

I would like to express my sincere gratitude to the following people:

First of all my supervisor George Malliaras for giving me the opportunity to work in the field of organic bioelectronics and also for creating an encouraging working environment.

To Sahika Inal, Mary Donahue, Jonathan Rivnay, Liza Klots, Xenofon Strakosas, Anna-Maria Pappa and Jolien Pas -whom I worked very closely with during my PhD- for all their help and friendships. To Thomas Lonjaret and Eloise Bihar for their helps not only scientifically but also for all the administration processes. To Vincenzo Curto and Christopher Proctor for their invaluable input for the projects we worked together and Adel Hama for keeping the laboratory together. To all members of BEL for discussions and the friendship they offered throughout my PhD.

I would like to thank Christophe Bernard for the possibility of validating our devices in his laboratory. All the in vivo experiments in this thesis were conducted by Pascale Quilichini and Antoine Ghestem. I would like to conduct my gratitude to them.

I would like to thank to the cleanroom stuff for all their helps -especially Thierry Camilloni and Sylvan Nolot.-

Finally, I would like to thank the Région Provence Alpes Côte d'Azur for financial support, and -Microvitae the économic partner in this project-.

Abstract

Recordings and stimulation of in vivo neural activity are necessary for diagnostic purposes and for brain-machine interfaces. Organic electronic devices constitute a promising candidate due to their mechanical flexibility and biocompatibility. Local control of neuronal activity is central to many therapeutic strategies aiming to treat neurological disorders. Arguably, the best solution would make use of endogenous highly localized and specialized regulatory mechanisms of neuronal activity, and an ideal therapeutic technology should sense activity and deliver endogenous molecules simultaneously to achieve the most efficient feedback regulation. Thus, there is a need for novel devices to specifically interface nerve cells. Here, we demonstrate an organic electronic device capable of precisely delivering neurotransmitters in vitro and in vivo. In converting electronic addressing into delivery of neurotransmitters, the device mimics the nerve synapse. The inhibitory neurotransmitter, -aminobutyric acid (GABA), was actively delivered and stopped epileptiform activity, recorded simultaneously and colocally. These multifunctional devices create a range of opportunities, including implantable therapeutic devices with automated feedback, where locally recorded signals regulate local release of specific therapeutic agents. In addition, we demonstrate the engineering of an organic electrochemical transistor embedded in an ultrathin organic film designed to record electrophysiological signals on the surface of the brain. The device was applied in vivo and epidurally implanted could reach capabilities beyond similar sized electrodes allowing minimally invasive monitoring of brain activity.

Table of contents

List of figures

List of tables

Chapter 1

Introduction

Polymers have been utilized in the industury instead of materials such as metals, ceramic etc. as insulators over decades. However, it was not till 1977 that it was demonstrated polymers could serve as conductors as well by reaching conductivity values as high as high metals upon doping. First successful attempt to achieve that was by Nobel awarded Heeger, MacDiarmid and Shirakawa, when they reported freely standing polyacertylene films, which are typically electrically insulating, doped with Iodine can exhibit conductivity values of ca. 10 order of magnitude higher than the pristine state. Eventhough the films were not airstable and processable, it paved the way to the fundamental investigations in the field and started the hunt for polymers with similar properties. Since then, a large number of polymers was shown to possess similar characteristics and a new class of materials is identified which combines the properties of plastic with electrical conductivity of metals. These materials have been investigated for a variety of applications including actuators, photovoltaics, photonics, lasers, displays.[28], [64]

The most promising materials are conjugated polymers, which own conjugated double bonds between carbon atoms along the backbone, wherein the charge carriers can hop. The bonds in conjugation are alternately single and double. Each double bond contains a localized single sigma bond, which is a strong chemical bond and a less localized pi bond, which is weaker. Exploiting the presence of the weaker pi bonds, conjugated polymers can be oxidized and reduced more easily and reversibly, resulting in unusual electrical and optical properties. The effect of oxidation or reduction is called doping, conversion of an insulating polymer to a conductive one.[143]

The electrical properties of conductive polymers depend based on the nature of the dopants and level of doping. Understanding the nature of processes that regulate them during synthesis allows us to control the complex properties they have. Besides, those prop-

erties can be altered by application of optical and electrical signals which can be utilized in design and realization of sensor platforms.

1.1 Structure of Conducting Polymers

Electrical characteristics of solids such as conductive, non-conductive materials and semiconductors, are defined by the band theory of solids. When a large number of atoms or molecules are brought together to form a polymeric chain or a crystalline solid, energy bands are formed through the interaction of the constituent atomic or molecular orbitals. Since, the electronic properties of a semiconductor are dominated by the highest partially empty band and the lowest partially filled band, it is sufficient to only consider these bands. The band of the highest energy that is completely filled by the electrons is called the valence band. The electrons associated with valence band are involved in chemical bonding. They are consequently rather localized and not free to move through the solid. The lowest lying unoccupied levels form a band as well, which is called the conduction band. These unoccupied energy levels enable carriers to gain energy when moving in an applied field. Thus, the conductivity occurs at this band. There is a forbidden energy region between the valence band and the conduction band. This energy separation is called the energy gap or band gap, E_g. When the E_g is large the material behaves as an insulator. Figure 1.1 depicts the situation in a semiconductor. [3] An (intrinsic) semiconductor has a band gap that is smaller than that of an insulator and at room temperature a significant number of electrons can be excited to cross the band gap. Upon inducing impurities by doping , controlled change in their activity and number can be achieved. If donors can provide free electrons to a semiconductor, the semiconductor is known as an n-type; while acceptors can provide free holes instead, the semiconductor is then classified as a p-type. [72]

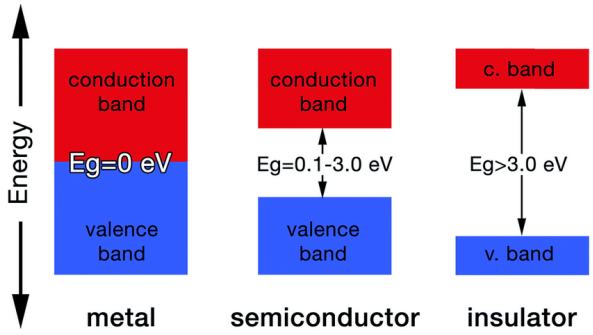

Fig. 1.1 Energy band diagram demonstrating different band gap energies for metals, semiconductors and insulators respectively.[3]

The energy diagram of a conjugated polymer is, on the other hand, is less usual. Conjugated polymers have delocalized electrons along the backbone, facilitating electrical conductivity. To have a more detailed perspective, we have to focus on the carbon atom being the main building block of organic compounds. Carbon has 4 orbitals in the ground state configuration. However, to be able to maintain more bonding with the surrounding atoms such as hydrogen, one electron can be moved to 2p orbital from 2s orbital upon excitation, therefore producing 4 singly occupied orbitals as illustrated in figure 1.2. For example, for the formation of molecule CH_2 , those 4 orbitals simply overlap with 1s orbitals of H atoms and form 4 sigma bonds which are equally distanced to each other. In the example of Ethene (C_2H_4), carbon atoms form a double bond with each other which requires a pi bond in between. As a result, the carbon atom forms 3 sp2 orbitals leaving one p orbital to maintain the π bonding with a second carbon atom. The sp2 orbitals overlap with s orbitals of the hydrogen atom to be able to form sigma bonds. [121]

In case of Sp3 hybridized polymers, the valence electrons of the molecules are bonded by the covalent interaction resulting in a electrically non-conductive material. On the other hand, for sp2 hybridized polymer chains, the valence electrons occupy the pi orbital. These delocalized orbitals alternate for the entire polymeric chain and the electrons occupying those delocalized orbitals are highly mobile along the chain. Upon oxidation and reduction, the polymer can be doped adding or removing delocalized electrons. Polymers are mainly doped p-type, by emptying the orbitals partially, which aims to create charge carriers along the chain axis to maintain charge transport.[87]

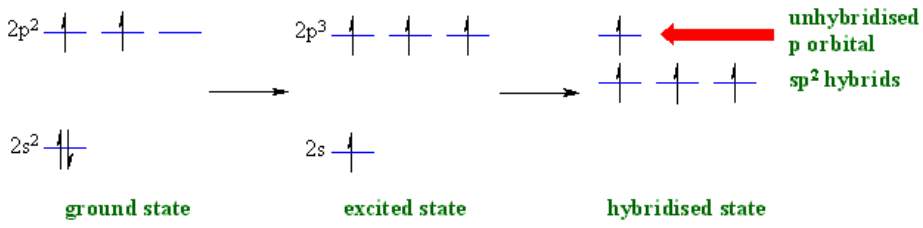

Fig. 1.2 In the ground state of the free carbon atom, there are two unpaired electrons in separate 2p orbitals. In order to form four bonds, four unpaired electrons in four separate but equivalent orbitals are needed. The single 2s, and the three 2p orbitals of carbon mix into four sp3 hybrid orbitals which are chemically and geometrically identical.[121]

1.2 Processing of Polymers

1.2.1 Coating

Precise deposition of thin films of polymers is extremely important as it governs to the subsequent electrical, photonic and mechanical properties. Regarding the coating of conjugated polymers, solution based processes, the vapor deposition and electrodeposition are the most common ones.

Chemical Vapor Deposition

Chemical vapor deposition (CVD) is a very useful method for deposition of polymers without any use of solvents. The idea is to directly convert the gas phase monomers of the polymer of interest into a polymerized thin film leading to a physically stable solid film. Polymers can be directly grown on substrates at low temperatures. CVD is especially very promising in coating polymers that would have high swelling or degradation inside solutions. [127] The deposition could take place as fast as 1 μm/min and could reach thicknesses as high as over 200 μm. Morevoer, through CVD, films that are pinhole-free and thinner than 10 nm were reported. Another novelty CVD offers is the high conformability for substrates that owns micro scale surface topography.[50]

Solution based Processes

Coating of the soluble polymers can be done using several methods depending on the required film parameters such as thickness. The simplest method to deposit a conducting polymer on a substrate is dip-coating. The substrate is placed and subsequently withdrawn from a coating solution with a defined withdrawal speed under controlled environmental conditions such as temperature and humidity, as they have a direct effect on the thickness and homogeneity of the film. The film is formed upon subsequent evaporation of the solvent resulting in the gelation or aggregation of the nonvolatile species in the solution. [21]

A popular technique to deposit films is spin coating. For spincoating, droplets of the solvent including the polymer are placed onto the substrate, which is fixed on a rotatable plate. As the plate rotates, the solution is spread on the substrate in a uniform way. Viscosity of the solution, rotational speed and the duration of the spinning define the film thickness. In case the polymer is insoluble, synthetic efforts are required to increase solubility.[178] Yet, such methods can decrease the electrical conductivities as a result of the change in the polymer structure in the film. Spin coated films can be exposed to further post-processing methods such as annealing to enhance molecular ordering within the film and controlling the

evaporation speed of the solvent. The processing parameters such as solution concentration, evaporation rate and surface properties of the substrate are at utmost importance, as they have direct effect on the quality and physical stability of the film.[113]

Another coating method that is widely used is spray coating. The solution is nebulized into air and made into an aerosol with a particle size of around 10 μm. The aerosols, in a first chamber filled with nitrogen, shrink upon heating and are transferred through nozzles to a second chamber by a pressure driven process, where they are directed to the substrate. Such methods are reported to have low coating yield as the highly accelerated droplets may rebound from the surface.[48] To overcome such problems, one alternative way is using electro-spray coating. In electro-spray coating, atomization is induced by an electric field eliminating the need of high pressure gas.[86]

For all solution based processes one important point is the wetting behavior of the solution. For the solution to wet the surface, the surface tension of the solution should be lower than the surface energy of the substrate. Surfactants can be included in solutions to improve the wetting or the substrate can be activated by plasma treatment for introducing chemical groups on the substrate surface prone to interactions with the polymer.

Laser Ablation

Pulsed laser deposition (PLD) is one of the most versatile tools for coating organic semiconductors. A focused ultraviolet laser pulse is utilized to ablate or vaporize the bulk polymer under vacuum, which depends on the absorption properties of the polymer. Subsequently, vaporized polymer is collected onto a substrate, where the thin film is grown.[124] However, the intense interaction between the focused UV light and the polymer can cause a photo-modification of the deposited film, causing an undesired chemical structure. An alternative approach to overcome such issues is using matrix-assisted pulsed laser evaporation (MAPLE). For MAPLE, the polymer is dissolved inside a solvent and the solution is frozen. The frozen target is processed as PLD. The approach aims to limit the direct interaction between the polymer and laser, therefore avoids the degradation of the organic compounds.[146] The properties of synthesized nanostructures can be efficiently controlled by parameters of laser ablation such as pulse duration, wavelength and properties of the environment. This offers an accurately controlled growth of the polymer film from a completely solvent-free source.[40]

Electrospinning

Novel approaches, such as, electrospinning of the polymers has started to take increasing attention. The method is similar to electro-spraying in principle except that it generates fibers

of the polymer upon application of an electric field.[176] An high voltage (kV) is applied to the end of a capillary containing the polymer solution, creating conical shapes on the surface of the liquid. As the magnitude of the bias is increased, the repulsive electrostatic force is driven to such a value that it overcomes the surface tension. As a result, the solution undergoes a process of lengthening, forming fibers, during which solvent evaporates. Finally, voltage driven charge threads of the polymer solutions with fiber diameter scaling down to 10 nm are directed on to a substrate. The method leads to the possibility of obtaining one dimensional devices. [26]

Electrodeposition

Electrodeposition of polymers is of great practical interest as it combines a simple electrical technique, which can be controlled, even automated with the inherent possibility of coating various substrates with polymers of broadly varying properties.[106] By electrodeposition, conductive polymers can be directly deposited on the conductive surfaces, such as gold or aluminium. The surface to be coated is made an anode and immersed inside a solution that contains the monomer of the polymer to be coated and the doping agent, typically an an/cation. The monomers, driven by the applied electric field, are accumulated on the surface, where they lose their charge and are deposited as thin films. [14]

Insulation layers to be employed on conducting polymer based devices are deposited in similar ways. Dielectric materials such as silicon oxide or parylene can be deposited using CVD.[111] Materials such as poly-4-vinylphenol (PVP) can be spincasted and further crosslinked upon thermal treatment.[61]

1.2.2 Patterning Techniques of Conducting Polymers

The most important part of fabrication of conducting polymer based devices is governed by the capabilities of patterning them micron-scale. For both soluble and insoluble materials, patterning of the organic semiconductors is challenging. The structure of the materials is generally optimal prior to the deposition and most treatments degrade the structure of the materials. However, none of the existing patterning techniques is satisfactory for all types of organic semiconductors and their particular applications. For example, materials, which are intolerant to wet processing or thermal exposure etc. arises the need of employing the right patterning techniques. Therefore, patterning process to be employed should specifically be chosen for the material in focus. Besides, obtaining high precision is crucial for avoiding cross talks and parasitic leakage, which would otherwise lead to low device performance.

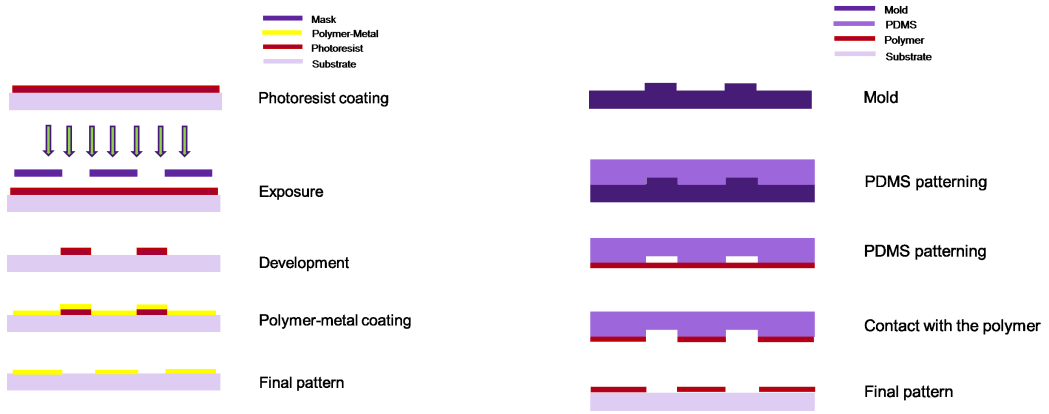

(a) Photolithography.

(b) Softlithography.

Fig. 1.3 a) Typical sequence of photo lithographic processing steps, illustrated for a positive resist. b) Typical sequence of softlithography steps illustrated for microcontact printing.[186]

The method employed shall preferably let the user scale down the device to the smallest size possible along with the ability to process over a large area.[96]

Lithography-based Techniques

One of the most well developed techniques in terms of precise and reproducible patterning is optical lithography. The process is based on exposing a light sensitive polymer, called photoresists, that are materials which lose or gain resistance against solvents when exposed to light. In photolithography photoresists are exposed to a specific wavelength range of light by using a mask that carries the desired pattern at its surface. Through the mask, the pattern is transferred into a three dimensional structure on the photoresist as depicted in figure 1.3a.[186] Optical lithography can be used to pattern conductive polymers and metals by depositing them on the patterned resist and removing the resist by the lift off process to keep only the polymer/metal of interest on the substrate with the right pattern. Alternatively, the photoresist can be coated and patterned onto a previously coated polymer and patterning can be achieved by etching. The residuals of the photoresist are removed by the solvent, which shall be compatible to the polymer to avoid any degradation. Through optical photolithography, figures scaling down to 100nm can be obtained. However, the large number of lithography steps are needed for patterning each compound, which increases the cost of manufacturing remarkably.[69]

Another lithography-based patterning technique is soft lithography, which is based on transferring a pattern on a master structure to the polymer.(Figure 1.3b) The master structures such as silicon are obtained by using conventional lithography techniques. Subse-

quently, master molds are used to make elastomeric replicas using materials such as poly (dimethyl siloxane) (PDMS). Replicas, coated with the polymer of interest, are pressed against the substrate to transfer the polymer in the exact required pattern to the substrate as shown in figure 1.3b.[126] Soft lithography is especially useful for patterning onto curved, soft and flexible substrates since the elastomeric molds are used. A big number of patterning techniques offering prospect for polymer patterning such as microcontact printing (uCP)[189], replica molding (REM)[51], microtransfer molding[191] etc. form the basis of soft lithography. They are based on printing, molding and embossing with an elastomeric stamp.

Printing-based Techniques

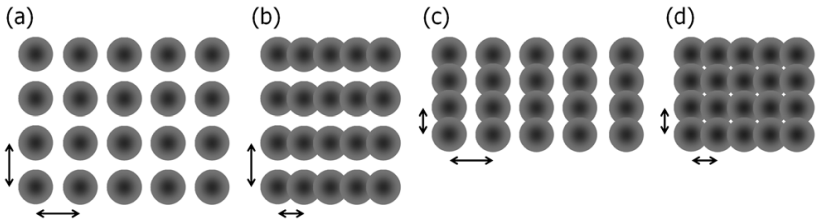

Fig. 1.4 Schematic representation of variations in dot spacing, indicated by the arrow: (a) single droplets when the dot spacing in the x- and y-direction is larger than the droplet diameter on the substrate, (b) horizontal lines when the dot spacing in the x-direction is reduced and (c) vertical lines for a reduced dot spacing in the y-direction. Continuous films (d) are formed when in both x- and y-directions the dot spacings are smaller than the droplet diameter on the substrate.[126]

Being a process that does not employ any masks and offering contact free patterning, inkjet printing is increasingly being utilized in conductive polymer patterning. In this technique, the pressure driven drops of the solution are pushed out of fine nozzles of the tool on top of the substrate.(Figure 1.4) The method has high material efficiency since only a little portion of waste is produced. The printing pattern is controlled by the printer software, which eliminates the need of using a mask. The figure dimension is strictly governed by the size of the nozzles and printing speed is determined by the amount of the nozzles.[166] The thickness of the coating can easily be adjusted from films with a thickness of tens of nanometers to films with tens of micrometers. To reach such fine resolution hydrophobic dewetting patterns can be utilized. For inkjet printing, most crucial point is the optimization of solution parameters such as ink viscosity and surface tension for obtaining a good morphology and homogeneity of the polymer. For each polymer of interest, concentration, dot spacing and blend ratio etc. shall be strictly evaluated and characterized. However,

upon optimization, inkjet printing allows an easy and reproducible path to pattern and coat polymers.[109]

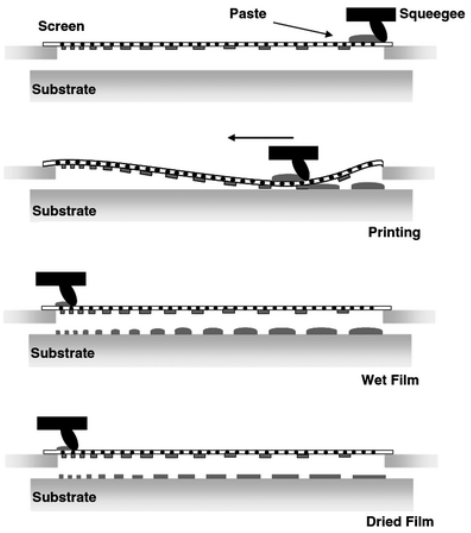

Fig. 1.5 Schematic diagram of screen printing process.1.4

Screen printing is widely employed for high volume technology in graphic printing and recently becoming a tool for polymer patterning. For the screen printing process, the ink is forced through a screen by applying mechanical pressure with a spueegee resulting in the formation of homogeneous films. However, the system has some drawbacks. If a different printing layout is aimed, the unique screen should be first modified for that particular layout. Moreover, the high viscosity solutions required for printing triggers the production of more waste. Yet, the method is compatible to roll to roll processes and offers great prospect for mass production of conducting polymer based devices.[8]

1.2.3 Applications of Conducting Polymers

Owing to their multifunctional and unique optical, electrical and mechanical properties, conducting polymers find applications in numerous fields such as chemical and biological sensing, electrophysiology, biomedicine etc. The ability to be processed at low temperatures and from simple organic or aqueous solutions makes them a natural competitor of silicon used in the conventional microelectonics field. In addition, the mechanical flexibility of organic materials makes them naturally compatible with plastic substrates for lightweight and foldable products.[38]

Organic Field Effect Transistors

The first transistor was invented in 1947 and shapened the microelectronics industry since then.[172] From simplest analog circuits to the most sophisticated computers they are the key elements of the operation processes. Ever since polymers were engineered to be electrically conductive, field effect transistors based on conducting polymers are started to become interesting for the industry. Especially the compressibility of organic semiconductors at low temperatures compare to silicon based ones makes them attractive in the area. Besides, the capability of using solution based techniques such as spin coating and printing offers prospect in commercializing the products, as it makes the large scale fabrication feasible. [63]

The first organic field effect transistor is reported in 1986 by Tsimura, who used polythiophene as semiconductor. The idea is simply to employ an organic semiconductor as the channel material. Basically, a FET operates as a capacitor where one plate is a conducting channel between two ohmic contacts, the source and drain electrodes, and the second plate is the gate. The source drain current can be controlled via the electric field introduced by the gate. For conventional inorganic electronics, the semiconductor is doped silicon. For a p-type channel as the gate voltage is applied, the holes are accumulated on the insulator/silicon interface, therefore it forms a passage along the semiconductor for the source-drain bias injected carriers. In case of OFETs, a layer of thin film deposited organic polymer replaces the silicon at the channel. Examples include pentacene or poly-3-hexylthiophene (P_3HT) as p-type channel or benzobisimidazobenzophenanthroline (BBL) or perfluorinated copper-phthalocyanine ($F_{16} - CuPc$) as n-type channel.[128]

OFETs are three terminal devices , source, drain and the gate. The devices consists of the contacts which are fabricated out of metals or doped-organic conductors, insulator and the organic semiconductor. The working principle is similar to the silicon based FETs. When a sufficiently high positive bias (compare to the source which is grounded) is applied, an high charge density is created next to the insulator interface, which significantly reduces the resistance between the source and the drain. That results in the current flow on the thin film, thus turning the device on.

The improvements in the field over last decades assisted OFET technology to be utilized for industrial usage. Examples include OFET enabled flexible displays and e-paper displays. [156]

Organic Photovoltaics

In the field of renewable energy, photovoltaics are maintained to be a very important player among others. The research and development in the field is increasingly growing along with the need of improving the technology. A relatively younger technology, organic photovoltaics (OPVs) recently emerged employing organic materials, which shows great potential in terms of cost, simplicity in processing and high electrical performance.[116] Since conjugated polymers can be designed such that they can have E_g´s at a range which allows most of the sun light to be absorbed, the OPVs can have high yields. Organic photovoltaic devices based on pi conjugated polymers, having energy gaps of 1 to 3 eV between the LUMO and HOMO, leads to strong interactions with the visible light. Maximum absorption coefficients of typical organic semiconductors are on the order of $10^5 cm^{-1}$, which suggests that the use of 100 nm thick films can absorb most of the incident light. [25]

The working principle of OPVs is as follows. Upon absorption of an incident photon, which has higher energy than the optical gap of the organic polymer as the active material, an electron is excited from HOMO to LUMO leaving an hole behind. The electron hole pair is subsequently separated over a built-in gradient in the electrochemical potential of the solar cell. Finally, the electron and hole is collected at opposite electrodes and led to recombine after being put to work in an external circuit.[115]

The research efforts aiming to develop solar cells made out of organic semiconductors are significantly on the rise. Although their performance is still considerably lower than that of cells based on crystalline silicon (around 5 % efficiency as compared with 15 % for silicon cells), they present numerous advantages. Unlike crystalline silicon, which has to be produced at very high temperatures, they can be processed and synthesized using inexpensive, room temperature processes and their optical and electrical properties can be tuned for the particular application. Moreover, the compatibility with solution based processes (for instance from inks or paints) makes it possible to cover large areas and flexible substrates such as films and fabrics. Due to their compatibility with flexible substrates, they could be used in many applications such as packaging, clothing, flexible screens, or for recharging cell phones and laptops.[140],[138]

Organic Light Emitting Diodes

Light emitting diodes have been dominating the industrial areas such as automotive use, back-light sources for consumer electronics, display screens for advertising, electronic equipment, and general lighting. However, having certain limitations like cost and difficulty of production triggered the research in technologies based on organic materials. Organic light

emitting diodes (OLED) technology is proven itself as a promising candidate for its low cost, ease of fabrication, brightness, speed, wide viewing angle, low power consumption and contrast. This has changed the LED market with commercialized products such as displays for mobile phones and portable digital media players, car radios and digital cameras among others.[67] Among the use of organic semiconductors in FETs or PVs, OLEDs have been the most successful and already been in the market.

The structure of a typical OLED consists of a thin film of organic semiconductor sandwiched between the layers of metal acting as anode and cathode. When a bias is applied between the electrodes, the semiconductor emits light which strictly depends on the level of the applied bias. Application of a voltage causes the current to flow through the device as electrons are injected into the LUMO of the semiconductor at the cathode and withdrawn from HOMO at the anode. Electrostatic forces bring the electrons and the holes towards each other and they recombine forming an exciton, a bound state of the electron and hole. The decay of this excited state results in a relaxation of the energy levels of the electron, accompanied by emission of radiation whose frequency is in the visible region.[79],[139]

1.3 Electrophysiology

Electrophysiology is the study of the electrical properties of biological cells and tissues. It involves measurements of electric current and voltage changes on a wide variety of scales from single ion channels to whole organs like the brain. [145]

The nervous system is organized into two parts: the central nervous system, which consists of the brain and the spinal cord, and the peripheral nervous system, which connects the central nervous system to the rest of the body. The nervous system is a complex collection of nerves and specialized cells known as neurons, which are responsible for generation and propagation of electrical pulses. These specialized cells are the information-processing units of the nervous system conducting reception and transmission of information. Each neuron has a small role in transferring the information throughout the body. [80]

1.3.1 Structure of a Neuron

The neuron structurally has three important sections; soma ,dendrite and axon as show in figure 1.6. The body of a neuron is called soma, which contains the organelles such as nucleus, ribosomes, mitochondria and other miscellaneous organelles. There are structures branching out from soma in a treelike fashion called dendrites. The primary goal of a dendrite is to serve for reception of the signals from other neurons. Dendrites have numerous

spines on them, providing a greater surface area for other neurons to attach. The incoming signals can be classified as excitatory, meaning this signal is generated to make the neuron fire and inhibitory, meaning it is generated to keep the neuron from firing. Axon is a long, slender projection of a nerve cell, or neuron, that typically conducts electrical impulses away from the neuron's cell body. It transfers the chemical information received by the dendrites to the next neuron. They are usually long (0.1 mm to 2 m) and contain numerous vesicles which hold neurotransmitters. They are wrapped by myelin sheaths, acting as an insulator during the conduction of electrical pulses. The estimated number of neurons in human brain is 10^{10} and each neuron might have hundreds, even thousands of synapses on its dendrites.[Lodish H]

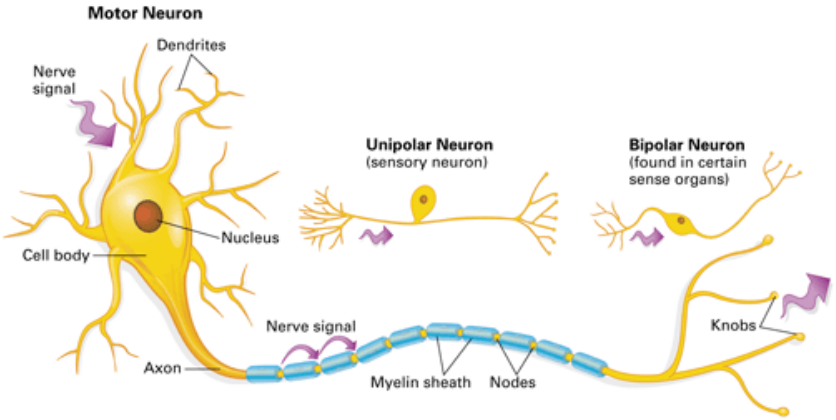

Fig. 1.6 The basic structure of a single neuron consisting of soma, containing organelles, dentrites responsible of receiving signals and axons responsible of conducting the signals.[Lodish H]

The information transfer between two neurons is achieved at the interface of the dendrites of one and cell body of the other. This connection where the transfer occurs is called synapses and those synapses does not only exist between neurons but also between neurons and skeletal muscles cells to be able to convert the electrical impulse to movement.

At the synapses, the information transfer is done by the chemical messengers called neurotransmitters. When an electrical signal travels down the axon and reaches the axon terminal, it triggers the release of neurotransmitters. The membrane around the dendrites is covered with specialized protein molecules called receptors that can detect the neurotransmitters. Neurotransmitters cross the synapse and bind to those receptors, conveying the inhibitory or excitatory signal.

1.3.2 Neural Activity

Microscopic- Action Potentials

The communication among neurons occurs due to generation and propagation of electrical pulses, which are called action potentials and they are of great importance in understanding electrophysiological properties of cells. The electrical activity at the cellular level occurs due to the movement of the charges such as sodium, potassium, calcium and chloride through the neuronal surface membranes. The neurons are wrapped by the membranes, which are mainly composed of 10 nm-thick liquid-crystal bilayer of phospholipids and semipermeable to the ionic flow. The permeability is mediated by channel protein assemblies specific to each ion. It serves as a diffusion barrier and can pump the ions out by the channel proteins to generate a potential difference between inside and outside of the cell. The membrane potential is held at a relatively stable values of around -70 mV called resting potential, which is in-between the reversal (equilibrium) potentials for both K + (-100 mV) and Na + (+41 mV).

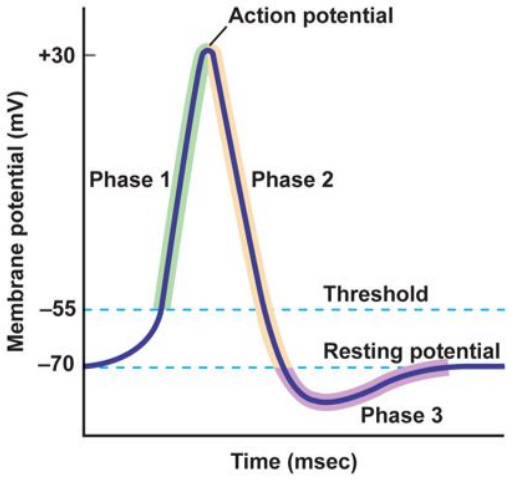

Fig. 1.7 The stages of an action polential, upon stimuli depolarization of the membrane by Na uptake, hyperpolarization by K pumping and reaching back to the resting potential.[Lodish H]

Action potential represents the changes of the membrane potential that occurs during excitation of a neuron. The process starts with the opening of the channels responsible of Na transport in the membrane. Na concentration is around 10 times higher outside of the cell than inside. Therefore, opening of the channels results in an huge diffusion of na ions inside the cell. Na, being positively charged, causes the membrane potential to be less and less negative till it reaches +30 mV and causes depolarization. As the membrane

potential reaches +30mV, the channels, responsible of potassium transport are open. As the concentration gradient of potassium is opposite of sodium, the potassium ions diffuses out and the membrane potential starts to repolarize towards its resting potential. Potassium channels are slightly delayed in closing and a short period of hyperpolarization occurs. (Fig 1.7)

The actuator of this process is the opening of Na channels which have different types and mechanisms. One type is called the ligand gated Na channels, which opens upon binding of a neurotransmitter. Another type is the voltage gated Na channel. With an external stimulus, the membrane potential can be depolarized till a certain level (-55mV). Once the membrane reaches this voltage, the voltage gated Na channels will open and continue the depolarization process via diffusion of Na within the cell.

The process is conducted by two type of channels Na and K channels. Voltage gated Na channels have 2 gates and open when membrane potential becomes -55mv and closes within around 1 ms. K channels have only one gate, which is sensitive to the membrane potential and opens with little delay when the Na concentration within the cell peaks. The total process is around slightly more than a millisecond.

The action potential is initiated at the beginning of the axon. The high density of Na channels rapidly depolarizes the membrane which triggers the other Na channels to open along the axon axis, thus conducts the signal.

Chemical modulation is achieved by neurotransmitters, which can be classified as inhibitory and excitatory. Some of the examples are;

- GABA, being an inhibitory neurotransmitter, binds to the transmembrane receptors and causes the ions channels to allow the flow of negatively charged chloride ions inside the cell. Therefore, it makes a negative change in the membrane potential, causing hyperpolarization. Due to an excitatory neurotransmitter, if neurons are firing too often in the brain, GABA will be sent out to attempt to balance this stimulating over-firing.

- SEROTONIN is another inhibitory neurotransmitter, which balances any excessive excitatory (stimulating) neurotransmitter firing in the brain. Adequate amounts of serotonin are necessary for a stable mood.

- DOPAMINE is a special neurotransmitter because it is considered to be both excitatory and inhibitory. When dopamine is either elevated or low, it can induce serious focusing issues. Dopamine is also responsible for our drive or desire to get things done or motivation. Stimulants such as caffeine cause dopamine to be pushed into the

synapse so that focus is improved. Unfortunately, stimulating dopamine consistently can cause a depletion of dopamine over time.

- NOREPINEPHRINE is an excitatory neurotransmitte, which is responsible for stimulatory processes in the body. Norepinephrine can cause effects such as anxiety at elevated excretion levels. Low levels of norepinephrine are associated with low energy and decreased focus ability.

- EPINEPHRINE is an excitatory neurotransmitter that is reflective of stress. Long term stress or insomnia can cause epinephrine levels to be depleted. Epinephrine also regulates HEART RATE and BLOOD PRESSURE

Mesoscopic- Local Field Potentials

Initial neurophysiology efforts mainly focus on recordings with action potentials as they are the basic source of any activity. However, last decades the interest has been directed to the use of LFPs for studying cortical function. The most important reason of it is, LFPs and their different band-limited components (known e.g. as alpha, beta or gamma bands) are invaluable as they carry information about the state of the cortical network and the local intracortical processing, including the activity of excitatory and inhibitory interneurons and the effect of neuromodulatory pathways. Another reason is LFPs contain information from a very broad spectrum of oscillations ranging from less than one Hz to one Hundred, all of which reflects contribution of several neural processing pathways.[110]

The local field potential is the electrical potential recorded in the extracellular space in brain tissue, by micro electrodes arrays in a localized area. They represent the information from localized populations of neurons as the signal can differ a lot for electrodes spaced by 1 mm distances. It has been shown that action potentials have a limited participation in generation of LFPs. They are generated by summated postsynaptic potentials arising from the synchronized oscillations of membrane potential of neurons. Large scale oscillations that can be measured with macroscopic electrodes are due to larger populations of neurons. As for a bigger area the signal has to propagate through various media such as cerebrospinal fluid, durameter, muscle skin etc., it is subject to filtering and diffusion phenomena across these media. However, they display the same type of oscillations during wake and sleep states.[73]

The mesoscopic oscillations of the brain can be divided in to groups based on their frequency response. Each of those groups represent the state of the brain. The five brain waves in order of highest frequency to lowest are as follows: gamma, beta, alpha, theta, and delta.

- Gamma waves are involved in higher processing tasks as well as cognitive functioning. They are important for learning, memory and information processing. 40-100 hz.
- Beta are high frequency low amplitude brain waves and commonly observed during awake state. They are involved in conscious thought and logical thinking and having the right amount is crucial for maintaining focus. Stimulators such as caffeine increases it remarkably. 12-40 hz
- Alpha waves are the gap between subconscious mind and conscious thinking. It is responsible of feelings inducing relaxation. Over stress induced alpha waves to be blocked. 8-12 hz
- Theta waves are present during deep meditation and light sleep, including the REM dream state. It is only experienced momentarily as you drift off to sleep from Alpha and wake from deep sleep (Delta) 4-8 Hz
- Delta waves are the slowest brain waves and observed during deep, dreamless sleep. 0-4 Hz. [168]

1.3.3 Approaches for Interfacing Neurons

The purpose of the chapter is to focus on the methods used in animal studies to understand electrical functioning in CNS. Neural activity inside the brain triggers transmembrane currents that can be measured in the extracellular medium. The improving technology in the field along with new data processing tools and computation models provide insight in understanding the dynamics of the brain. The methods differ from in vitro approaches such as patch clamp method, micro electrode arrays to in vivo methods such as electroencephalography (EEG), electrocorticography (ECoG) or depth probes.

A cross section of a mammalian skull is illustrated in figure 1.8. The meninges is the fluid-filled sac surrounding the brain, which provides both a protective cushion and a means of waste removal. The two outermost layers of the meninges, i.e. the dura mater and the arachnoid, which follow the inside of the skull, and are separated from the third layer, the pia mater, which follows the contours of the cortex, by continuously flowing cerebrospinal fluid (CSF). CSF is a clear, colorless body fluid found in the brain and spine. It is produced in the choroid plexuses of the ventricles of the brain. It acts as a buffer for the brain's cortex, providing basic mechanical and immunological protection to the brain inside the skull.

The cerebral cortex is the cerebrum's (brain) outer layer of neural tissue in humans and other mammals. It is divided into two cortices, along the sagittal plane: the left and right cerebral hemispheres divided by the medial longitudinal fissure. The cerebral cortex plays a

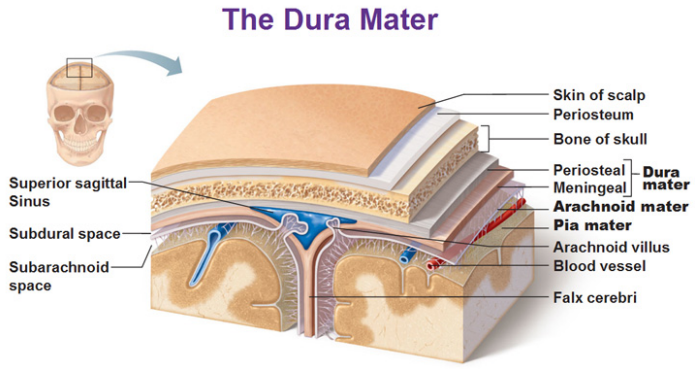

Fig. 1.8 The brain is protected from injuries by skull, meninges, cerebrospinal fluid and the blood-brain barrier. [41]

key role in memory, attention, perception, awareness, thought, language, and consciousness. The human cerebral cortex is 2 to 4 millimetres thick. [41]

Interfacing the brain requires removal of one or multiple of the protective layers. Alternatively the brain can be extracted for subsequent investigation. The approaches are divided in to sections based on if they are with living organisms or cells, microorganisms etc..

In Vitro Models

Patch Clamp

Patch clam technique was first introduced by Neher and Sakman in 1976 to resolve the ionic currents through acetylcholine-activated channels. Since then, the method has shown great developments and being extensively used in studying ion channels in cells.

The principle is to suck a portion of the membrane of a cell by a micropipette which is filled with a suitable electrolyte, thus to maintain a good sealing between the electrolyte and the bath the cell is located in. (Fig. 1.9) Subsequently, by using two electrodes, one being inside the pipette and one in the batch, the cell can be recorded or stimulated electrically. Deciding the diameter of the tip of the pipette is crucial as it defines the area of the membrane to investigate.

It can be applied in many different configurations. In cell-attached configuration, after the seal is performed the recordings is done without any further disruption of the cell. In inside-out configuration, after the seal is formed, the patch of the membrane is pulled away, and the patch remain attached to the pipette with the inner surface of the membrane exposed to the bath. Another configuration is whole-cell clamp, which is based on rupturing the membrane partially to be able to record summed currents flowing through all channels in the membrane.

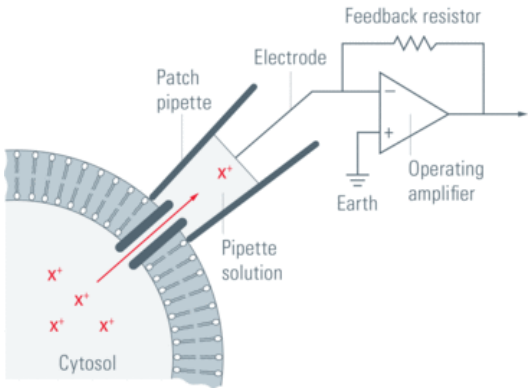

Fig. 1.9 General principle of patch-clamp recordings; A glass pipette containing electrolyte solution is tightly sealed onto the cell membrane and thus isolates a membrane patch electrically. Currents fluxing through the channels in this patch hence flow into the pipette and can be recorded by an electrode.[39]

The patch clamps study is ideal for studying mechanism at the single channel level. As the cell is isolated, toxins, neurochemicals and ions can be applied and their effect can be studied in defined concentrations. Several drugs or ion concentrations can be tested on one patch to obtain concentration response curves.[39],[Gary S. Aston-Jones]

Microelectrode Arrays

Application of patch clamp concerns the parts of cells or individual channels. Even though, it is at utmost importance to understand the function of individual components, it has small effect on the overall activity of a neuron. A neuron usually receives synapses from thousands of other neurons, and many of those inputs may be active at approximately the same time. The most efficient way of investigating in vitro neuron populations are by micro electrode arrays (MEA). Since the development of first MEAs the technology showed a great improvement in terms of quality of recordings and became one of the most common techniques used to record and stimulate large populations of neurons. The technique employs tightly packaged sets of electrodes in contact with a neural cell population, allowing to observe not only one neuron but also its interaction with the others. New generation in vitro MEAs may have up to 10000 electrodes, increasing the spatial resolution remarkably.

MEAs can be used to perform electrophysiological experiments by using cell culture of neurons to study central nervous system. It allows the researchers to investigate the neural activity in a controlled environment, than an in vivo one. The neurons are typically cultured from rat neurons and can be extracted locally based on the region that would like to be investigated including cortical, hippocampal or spinal neurons. Another method is to use

brain slices, which are extracted from the skull and rapidly cooled to survive for many hours. Again the slice can be cut from the area of the interest for a more specialized study.

One of the main advantages of MEA based electrophysiology is the ability to use known concentration of drugs (upon perfusion), the effect of it can be solely studied. One other is they allow study of neuronal properties and cellular integrative mechanisms without outside influence (e.g., from other neurons or hormones, etc.). However, lacking connections between sets of functioning neurons decreases the utility of this approach for studying neuronal networks or the interactions between brain regions.[157]

In Vivo Models

The in vivo approaches for interfacing brain can be classified as their invasivities as illustrated in the figure 1.10.

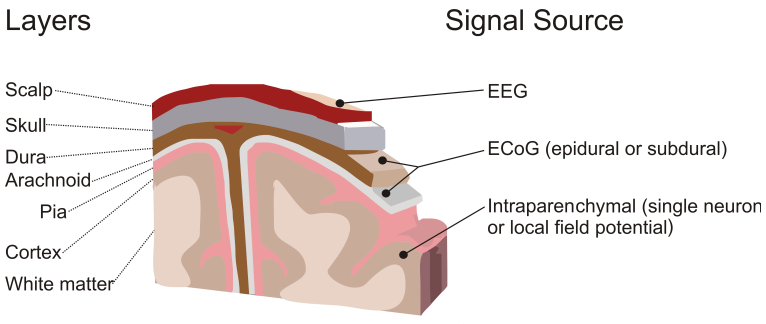

Fig. 1.10 Macroscopic recording are done via electroencephalography (EEG) by placing arrays on the scalp. Mesoscopic recording are done through electrocorticography (ECoG) by placing the arrays epi or subdurally on the surface of the brain and implantable electrodes by penetrating the arrays inside the brain. [57]

Depth Probes

Using depth electrodes, the local field potential of a neural population in a sphere with a radius of 0.5–3 mm around the tip of the electrode can be captured. With a sufficiently high sampling rate (more than about 10 kHz), depth electrodes can also measure action potentials. In which case the spatial resolution is down to individual neurons, and the field of view of an individual electrode is approximately 0.05-0.35 mm.[57]

The commercially available electrodes typically consist of electrolytically sharpened wires that are less than 100 μm in diameter and are completely insulated except for a small exposed area at the tip which forms the recording or stimulation site. Increasing the number of recording sites requires increasing the number of electrodes which results in a linear

increase in overall probe size and causes undesirable neural tissue damage. Further, it is difficult to insert a large number of probes accurately into a small volume of brain tissue. Depth probes are employed extensively for detecting neural disorders and brain machine interfaces, as well as for deep brain stimulation for patients with Parkinson's disease.[144]

Electroencephalography

Neuroimaging studies of human cognitive, sensory, and motor processes are usually based on techniques such as electroencephalography (EEG), which is the least invasive among all the in vivo approaches to evaluate the electrical activity of brain. The idea is to place electrodes on the scalp of the subject and record mesoscopic activity. These methods can be used to resolve functional connectivity among brain regions. For example, EEG detects spontaneous or evoked electrical activity from the scalp with low spatial resolution (cm range). It is used to detect, seizure disorders such as epilepsy, traumatic head injuries, brain tumor, memory problems etc. [119]

Electrocorticography

Electrocorticography (ECoG) is a well-established electrophysiological monitoring technique that typically utilizes electrode arrays placed on the cerebral cortex of the brain. The technique involves a surgical operation that removes a piece of scull to be able to place the arrays directly on the brain. Higher invasivity comes with the advantage of both higher spatial and temporal resolution compare to EEG systems. Conventional systems offer a temporal resolution of approximately 5 ms and a spatial resolution of 1 cm.[9]

Techniques like EEG have either inherently low temporal or low spatial resolution, and suffer from low signal-to-noise ratio or poor high-frequency sensitivity. Therefore, for exploring the short-lived spatio-temporal dynamics of many of the underlying brain processes they are not practical. In contrast, the invasive technique of electrocorticography provides brain signals that have an exceptionally high signal-to-noise ratio, less susceptibility to artifacts than EEG, and a high spatial and temporal resolution. It has been especially proven to be useful for advancing brain-computer interfacing (BCI) technology for decoding a user's intentions to enhance or improve communication and control. Besides, ECoGs are being used to identify epileptogenic zones of the cortex that generate epileptic seizures. Nevertheless, human ECoG data are often hard to obtain because of the risks and limitations of the invasive procedures involved, and the need to record within the constraints of clinical settings. Still, clinical monitoring to localize epileptic foci offers a unique and valuable opportunity to collect human ECoG data. [60], [Thakor]

1.4 Organic Bioelectronics

The brain consists of billions of neurons that are interconnected into a complex neural network. The communication throughout the brain is achieved when action potentials are generated and propagated among adjacent neurons. The brain processes information through spatiotemporal activity patterns of neural networks. Therefore a comprehensive analysis of neural activity is essential for understanding how brain functions. Certain irregularities in neural signaling network causes serious diseases.[42] Examples include:

- Epilepsy, in which abnormal electrical discharges from brain cells cause seizures,
- Parkinson's disease, which is a progressive nerve disease that affects movement,
- Multiple sclerosis (MS), in which the protective lining of the nerves is attacked by the body's immune system,
- Amyotrophic lateral sclerosis (ALS), is a motor neuron disease which weakens the muscles and progressively hampers physical function.

Carrying the existing knowledge in the field further would be of great importance in curing such diseases.[192] Moreover, extensive understanding of the brain functions can be employed for brain machine interfaces (BMI). Brain waves carry important and highly relevant information pertaining to the control of a prosthetic limb. The challenge is to record the brain waves, either from single neurons directly or from the whole brain in a precise manner, which could then be used to control the associated limb. It would be instructive to understand what these signal sources are and how they might be recorded for building a BMI.[Thakor]

Bioelectronics deals with the coupling of biological units to electronics with the aim of maintaining a better understanding or control over biological processes. Bioelectronics directly communicates with neuronal systems via electronic elements that transduce electric signals to and from bioelectric signals of neurons. The integration of electronics with biological entities to yield functional bioelectronic devices attracts substantial research efforts because of the basic fundamental scientific questions and the potential practical applications of the systems.[185] Because of its inherent interdisciplinary nature, bioelectronics is closely linked to many other fields in materials and life sciences. The biochemical and biotechnological progress in tailoring and synthesize of new materials provide a broad platform for their integration with electronic elements. The electronic elements may involve, for example, electrodes, field-effect transistor devices etc. [68]

Currently studies for neural interfacing are mainly being conducted by metal electrodes, which are capable of recording neural activity at a single-cell level with high temporal resolution. Besides, metal electrode technology offers simultaneous stimulation of the activity of a large number of neurons.[158] Over the past decades, electrical recordings by metal-based bioelectronics has significantly contributed to our basic understanding of neural activity. Today, implantable systems in the human body are becoming more widely acceptable and available for diagnostics and treatment of neurological disorders. They have wide applications on deep brain stimulation for Parkinsons disease, phrenic nerve stimulation, cochlear implants and electrical stimulation therapies for epilepsy. With a greater life expectancy and an increasing demand for medical healthcare, there is a growing demand on technology and biomedical engineers to develop implantable systems for a wide variety of medical diagnostics, treatments and therapies. [58]

Despite the common applications, conventional bioelectronic systems are suffering some major challenges for neural interfaces due to the usage of metals. First of all, the conventional inorganic probes are made of stiff materials such as platinum or silicon with high elastic modulus. Interfacing them with soft tissue comes with the risk of introducing inflammation and complicates the long term stability.[89] Besides, the neural systems carry information by ion fluxes whereas metals are only electrically conductive. This limits the communication transfer between the electronics and neurons, leading to devices with low performance. [158]

Ideally, neural interfaces should be able to enable effective and reliable signal transduction between neurons and electronic materials. Recent developments in the field of bioelectronics, driven by the advances in materials research paved the way for new technologies employing organic electroactive materials. Specifically, organic bioelectronics based on conducting polymers has been shown to provide more effective transduction interfaces to neurons than metals, thus enhancing the quality of both neural recordings and stimulation characteristics of organic bioelectronics.[42] Furthermore, organic bioelectronics is particularly promising to improve the long-term success of implanted neural interfaces due to their mechanical flexibility and biocompatibility.[7]

Recently, organic electronics based on poly(3,4-ethylenedioxythiophene) (PEDOT) doped with poly(styrenesulfonate) (PEDOT:PSS) have received tremendous attention for neural recordings and stimulation. PEDOT:PSS is a p-type semiconductor in which a negative sulfonate group on the PSS chain creates a hole carrier on the PEDOT as illustrated in figure 1.11.[135] The chain consists of (macro-)molecular blocks within which atoms are covalently bonded to each other, however these blocks are held together by means of weak van der Waals interactions and, in the case of doped materials, electrostatic interactions as

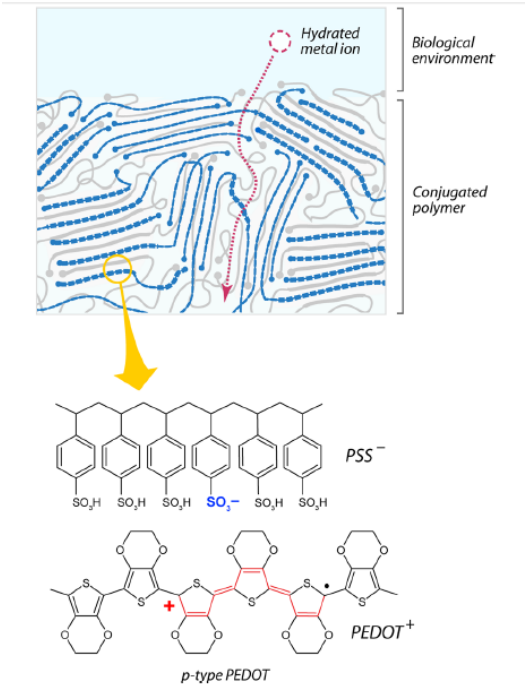

Fig. 1.11 Schematics of the organic semiconductor, PEDOT, at the interface with an electrolyte. The inset shows the action of p-type dopant, PSS in PEDOT.[135]

well. Upon application of a bias along the polymer axis, the hole carrier moves along the p-conjugated PEDOT backbone while the negative sulfonate group remains immobile, resulting in an high electrical conductivity around 100 Scm^{-1}, yet high chemical stability in solutions.[118] High electrical conductivity is combined with the ability of PEDOT:PSS to conduct ions, as they can penetrate the bulk of the PEDOT:PSS film from the electrolyte solution and modulate its doping level. By combining high ionic and electronic conductivities, PEDOT:PSS opens up a new communication channel with bionic signals and proves itself as one of the most attractive candidates for neural interfaces.[159]

1.4.1 Electrical sensing

The most commonly used electrical devices for interfacing neurons are electrodes and transistors.

Neural Recordings with Electrodes

The electrode performs the function of transduction from the ionic currents in the electrolyte to an electric current in the measurement system. The approach employs two metallic plates dipped inside the electrolyte, working electrode and the reference electrode. Upon applica-

tion of a small bias between two electrodes, a double layer of charge accumulation, called Helmholtz double layer is formed on the surface of both electrodes. The layer formed at the electrode-electrolyte interface is the region where electrical charge from the metal electrode is transduced into ionic charge in the surrounding electrolyte or vice versa. The transduction is based on non-Faradiac currents, which are capacitive in nature and involve charge redistribution at the electrode and in the surrounding electrolyte. Therefore, those double layers can be modeled as capacitors. Generally, the size of the electrolyte-working electrode interface is minimized to be able to dominate total capacitance, thus to achieve the sensing at this interface. [112]

The technological efforts improved the quality of information that can be gained from neural recordings by increasing the number and density of electrodes. However, the recording and stimulation quality of these platforms is reflected by the electrical coupling coefficient between single neurons and the device, which remained poor for traditional metal electrodes leading to a low signal-to-noise ratio. The charge capacity of the electrodes is related to their size, and miniaturization for single cell experiments limits the charge able to be applied before damaging either the electrode or the surrounding tissue.[158]

There are couple of parameters to be optimized to be able to reach the highest electrode performance. The most important parameter is the impedance of the probes as it decides sensitivity of recordings. The impedance at the electrode site is decided by the double layer capacitance, which scales linearly with surface area. Yet, the arrays shall be kept as small as possible to form a dense array on the recording area and get a better spatial resolution.[158] One way to decrease the impedance by keeping the surface area constant for metal probes is by introducing a surface topography. Another important point is the biocompatibility of the electrode material at the neural interface. Any mechanical mismatch between implanted electrodes and neural tissues can result in inflammatory response of the neural tissues. This chronic inflammation results in the formation of glial scars that insulate the electrodes from neural signals, which eventually leads to electrode failure in long-term studies.[30]

Conducting polymers are extensively studied to be able to overcome such issues. Earliest efforts in the field include electropolymerization of thick PPy coatings on gold and Ir electrodes. Due to its high stability and biocompatibility, polystryne sulfonate was used as dopant. Selective electrodeposition of the PPy/PSS resulted in low impedance, which was around 2 orders of magnitudes less than the bare electrode and good contact with the neural tissue. The thickness was adjusted during electropolymerization and film roughness is observed to increase with thickness, which contributed to the low impedance. The efficient surface area contributed in sensing was estimated to be around 30 times more than the bare gold, due to the porosity of the film.[35]

To further increase the communication of the electrode materials with the neural tissue, surface modification of the polymer offers an effective path. PPy with nona-peptide CDPGYIGSR is electrodeposited in the electrode sites to achieve patterning of bioactive molecules.[36] Such processes increase the contact between the electrode sites and the neurons to avoid inflammatory response and increase cell adhesion, paving the way for in vivo applications by increasing the lifetime of the recordings.

Despite the high performance as an electrode coating, PPy is chemically unstable and can be easily over-oxidized or decomposed in aqueous solutions. On the other hand, PEDOT has a dioxyethylene bridging group across the 3- and 4-positions of the hetero-ring, which blocks the possibility of decoupling and leads to superior electrochemical stability in aqueous solutions. Similarly electrochemically deposited PEDOT:PSS films showed more stable characteristics than PPy/PSS. [37]

PEDOT:PSS coated gold electrode arrays with low impedance values can be obtained upon spincoating/lithography processes. The devices were tested with rat hippocampus brain slices and could capture action potentials with minimum noise. Traditional MEAs do not conform to the curvilinear surface of the brain, decreasing the stability and efficiency of the electrical recordings due to poor mechanical contact.[152] Implementing the PEDOT:PSS arrays onto highly conformable parylene C substrates with couple of um thickness, let the device perfectly follow the cortical surface topography of the brain, leading a good coupling between the neural tissue and electrodes. Consequently, such electrodes could detect both LFPs and APs from superficial cortical neurons with high signal to noise ratios.[85]

Neural Recordings with Transistors

One branch of the organic field effect transistors is electrolyte gated transistors, which employs electrolyte as gate insulator. The technology utilizes an electrolyte between the channel and the gate, therefore increases the capacitance remarkably compared to the classical dielectrics(up to 3 orders of magnitudes).[18] Different types of electrolytes such as aqueous liquid electrolytes, hydrogels, ionic liquids or ionic gels can be utilized. The idea is based on the earlier efforts by Wrighton et al. of utilizing reversible electrochemical oxidation of organic semiconductors to fabricate electrochemical transistors, which can amplify the chemical signals. Since then, the devices with different formations are extensively being utilized such as organic electrochemical transistors (OECTs), ion-sensitive field-effect transistors (ISFETs), hygroscopic insulator field-effect transistors (HIFETs) and electrical double layer transistors (EDLTs). [183]

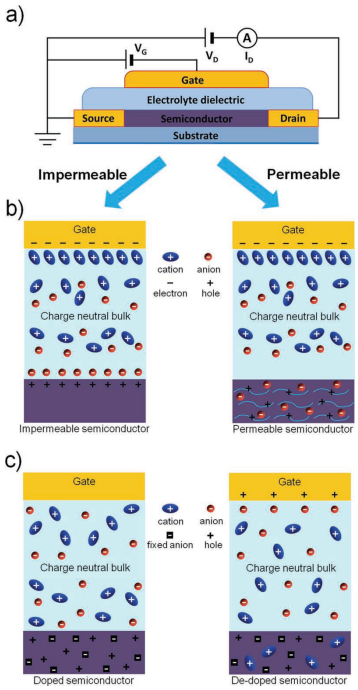

Fig. 1.12 (a) Cross-section of an Electrolyte gated transistor. (b) Carrier accumulation-mode operation of an EGT for un-doped ion-impermeable (left) and permeable semiconductors (right) and (c) depletion-mode operation for degenerately doped semiconductors without (left) and with (right) a gate voltage. 1.12

The operation mechanism can be classified in to two principles, depending on the organic semiconductors being permeable or non permeable to the ions inside the electrolyte as depicted in figure 1.12. If the semiconductor is impermeable, upon application of a gate voltage, the ions in the electrolyte migrate along the electrolyte and accumulate at the interface of the semiconductor and the gate. As a result at both interfaces an electrical double layer is formed. These double layers can be modeled as capacitors and the total capacitance of the gate-electrolyte-semiconductor stack is the capacitors in series. Reports have shown that a significant double layer formation can be obtained by low operating potentials resulting in high electrical field at the electrolyte-semiconductor interface, thus high sensitivity.

If the semiconductor is permeable, still an electrical double layer may be formed but the ions will be diffusing inside the organic film and compensate the induced charge carriers by a process called electrochemical doping. The electrochemical transistors functions by reversible oxidation and reduction of the semiconductor film upon application and removal of a gate potential. If the semiconductor is p-type polymer, the anions will diffuse inside the film and dope it by pairing with the holes upon application of a negative gate voltage. The mode is called accumulation mode and the the channel becomes conductive as the gate is applied. Devices can be operated in depletion mode as well by employing a n-type semiconductor as the channel. In this case application of a positive gate bias drives the cations inside the film and dedopes the channel, resulting in the source drain current decrease.

Neural signals can be efficiently recorded using such transistor arrays as the polymer is in direct contact with the neural tissue. The neural signal acts as gate and causes modulation in the source drain current. First neural recordings using transistor arrays were achieved using silicon FETs. The neuron is placed on the oxidized Si insulating n-type Si gate inside the electrolyte. As the neuron is stimulated to fire action potentials externally, the positive voltage change increases the surface potential and modulates the current flowing along the p-channel between source and drain. Even though the device could record neural activity, the low oxide capacitance dominates the high double layer capacitance, resulting in poor amplification.[47]

That difficulty can be overcome using organic transistors, as cation penetration inside the bulk of the film increases the double layer capacitance formation from a 2D plane as it is in silicon oxide to a 3D one. For OECTs, cations from the electrolyte can penetrate the polymer and dedope the semiconductor channel, modulating the carrier density and the source drain current. Such devices were tested in vivo in anesthetized rat and proven to get a superior signal to noise level compare to the electrodes due to local signal amplification and noise reduction. (Fig. 1.13)[84]

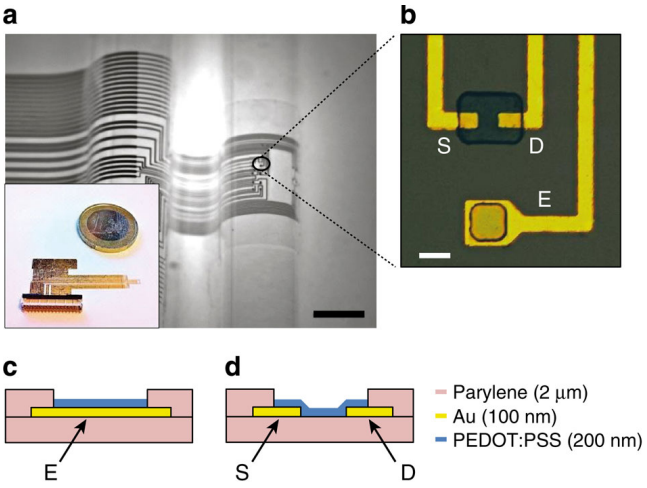

Fig. 1.13 Structure of the ECoG probe. (a) Optical micrograph of the probe conforming onto a curvilinear surface. (b) Optical micrograph of the channel of a transistor and a surface electrode. Scale bar, 10 mm. (c,d) Layouts of the surface electrode and of the transistor channel. [84]

1.4.2 Chemical-Biological sensing

EGOFETs can be used for sensing of (bio)chemical species in an electrolyte upon modification of the surface of the polymers. These devices work at relatively low potentials in aqueous media, converting the quantity of the analyte of interest to a change in current. The aqueous media including the analyte of interest can be employed as the electrolyte allowing the detection and quantification of the target molecules. Upon functionalization of the gate or the semiconductor, the sensing capabilities can be moved a step further. (Fig. 1.14) [164]

Immunosensors have attracted growing attention for the highly sensitive and fast immunological response they have. Immunosensors are affinity ligand-based biosensor solid-state devices in which the immunochemical reaction is coupled to a transducer. It relies on the strong recognition and affinity between antigens and antibodies, which are proteins generated by the immune system to identify bacteria, viruses, and parasites. The affinity between antibodies and antigens is very strong but of non-covalent nature. Subsequent to the affinity, the change in the resultant complex in terms of mass, optical or electrochemical signals allows sensitive quantification and characterization of the analyte.[100]

In electrochemical immunosensors, the antigen-antibody formation is translated into an electrical signal, which can be monitored as a change in electric current (amperometric immunosensors), a voltage difference (potentiometric immunosensors), or a resistivity change (conductimetric immunosensors). For amperometric immunosensors, being the most common type, the measurements of electrochemically active products rely on redox active en-

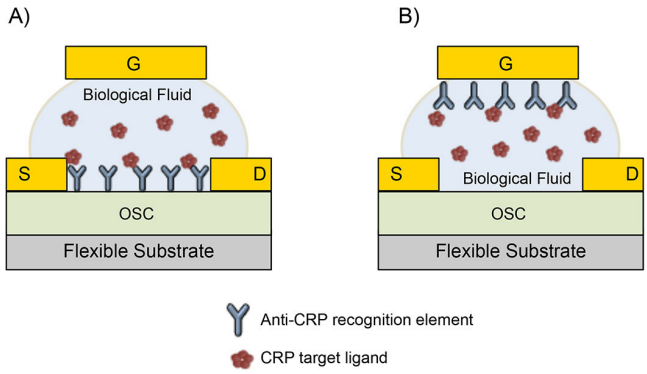

Fig. 1.14 Schematic of the electrolyte-gated organic field-effect transistor (EGOFET) biosensor structures. Antibodies are anchored on the organic semiconductor surface (A) or to the gate electrode (B). The devices enable selective CRP detection. G, S, D: Gate, source, and drain gold electrodes, respectively. OSC: Organic semiconductor. [164]

zymes. During the enzymatic reaction, electrochemically active products are either consumed or released and electrochemically detected at the electrode. Some of the enzymes which are used in the process are horseradish peroxidase (HRP), glucose oxidase (GOx), and catalase. Only the material that is bound to the electrode surface causes a catalytic reaction.[120]

In the fabrication of electrochemical immunosensors, conducting polymers have been playing an important role as biologically compatible and electrically conductive platforms in immobilizing biomolecules. Usually, the conducting polymers can easily be functionalized with amine groups or carboxylic acid groups to stably immobilize biomolecules through covalent bond. [108],[70]

Using this approaches analytes such as glucose, which have importance in brain functioning were precisely detected. By application of PEDOT:PSS based OECTs detection of glucose without modification of gate and the channel in solution with sensitivities of uM was achieved. For that research, the OECT was ran inside PBS, which includes GOx. Upon addition of glucose, hydrogen peroxide was produced, which subsequently modulated the channel current linearly with the added quantity.[163] Even though the model offers a good detection platform, modifying the gate electrode with enzymes and nanoparticles, such as carbon nanotubes and platinum nanoparticles, the device performance can be dramatically improved. The approach exploits the high electrocalatylic activity Pt nanoparticles shows to hydrogen peroxide, which is very crucial in sensing glucose based on detection of H2O2, which is a byproduct of glucose and glucose oxidase reaction. Moreover, Pt nanoparticles, due to their biocompatibility and large surface area, are very effective for enzyme mobilization. Pt nanoparticles were combined with glucose oxidase at the gate of an OECT along

with Chitosan, for its high water permeability and susceptibility to chemical modifications. During OECT operation, as the glucose is added to the media, the enzymatic reaction at the gate functionalized by Pt-Nps and the enzyme, produces an electron, which then contributes to the gating of the channel.[13] Same sensing principles was as well applied for enzymatic sensing of the two main neurotransmitters in the brain, glutamate and acetylcholine. OECTs, with their channels composing of the PEDOT:PSS/Pt NPs composite films could detect glutamate down to concentrations found in the extracellular fluid, which is very promising for potential in vivo applications. [81]

1.4.3 Chemical Stimulation

The communication among the nerve cells is dependent on the interplay of both electrical and chemical signals. One of the major challenges in all devices at the neural interface is to maintain successful communication between the signal carriers of the nervous system (ions and neurotransmitters) and those of conventional electronics (electrons). Since conjugated polymers can utilize both electrons and ions as charge carriers, using them can establish a novel communication interface between electronic components and biological systems.

Conducting electroactive polymers can be used to electrically manipulate molecular interactions for subsequent localized release of drugs. For instance, PPy can be mixed with an enzyme, antibody or even a living cell as dopant and the intermolecular interactions can be manipulated via electrical stimulation. Heparin, that is covalently bound onto PPy electrode can be re-bound from the surface under an applied constant current, which can be utilized in anti coagulation applications in implanted devices.[99] Another example is the electropolymerization of , dexamethasone (Dex), an anti-inflammatory drug with PPy. As PPy undergoes a reduction reaction, it releases its dopant:Dex. The release of Dex is achieved by using cyclic voltammetric stimulus and found out to be linear with the applied stimuli offering controlled amount of delivery.[179] Similar examples are tested also in vivo. Neurotrophins (a family of proteins) are important to induce development and function on spiral ganglion neurons, which serve to sense hearing. PPy /neurotrophin coated electrodes are implanted in deafened guinea pig and and led to an increase in neural density upon field-induced release of neurotrophin. However, for those devices the delivered amount is limited to the small electrode size and it is difficult to reach an adequate concentration.[131]

A device type that can overcome such issues is an organic electrophoretic ion pumps (OEIP). The device relies on electrophoretic delivery of ions from one PEDOT:PSS based electrode to the other, through an ion bridge. The approach utilized over-oxidative degradation of PEDOT:PSS, which breaks the conjugation and destroys the electronic conductivity of the polymer.[165] Therefore, along the ion bridge made of basically PSS, only cations

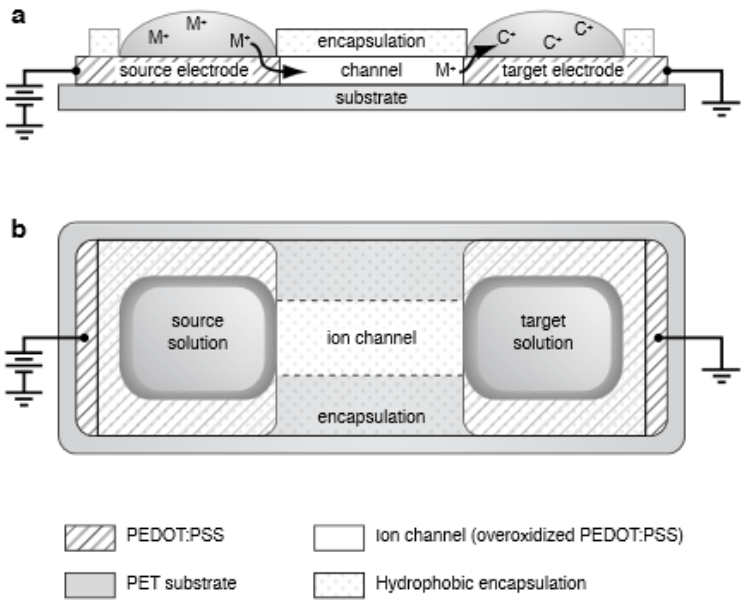

Fig. 1.15 The organic electronic ion pump. Side view of the planar device used in characterization and in vitro studies. The black arrow indicates the flow of charged species from the source electrolyte, S, through the anode, then through the over-oxidized channel, and finally out into the target electrolyte, T, via the cathode. [165]

(due to Donnan exclusion principle) can travel from one reservoir to another upon application of a bias. The devices are shown to deliver a variety of cations such as Potassium and calcium along with neurotransmitters such as ACh, one of the major neurotransmitters which affects synaptic plasticity and excitability. (Fig. 1.15) [155] The devices were tested with in vitro assays and upon pumping calcium, cells located around 100 um away from the pump outlet were successfully stimulated.[174] Besides, by pumping protons from an acidic source, controlled pH gradients were generated. By adjusting the applied voltages and pulse times, local ion concentration oscillations were generated, which might be very useful for cell signaling studies.[66]

Recently, OEIPs were demonstrated as a novel brain/machine interface integrated into an in vivo platform for the modulation of mammalian sensory function.(Fig. 1.16) The device, with the electrophoretic capability of GABA delivery was chronically implanted in rats with nerve injury. The device was shown to reduce pathological hypersensitivity by the highly localized delivery of the neurotransmitter GABA on the injury sites.[78]

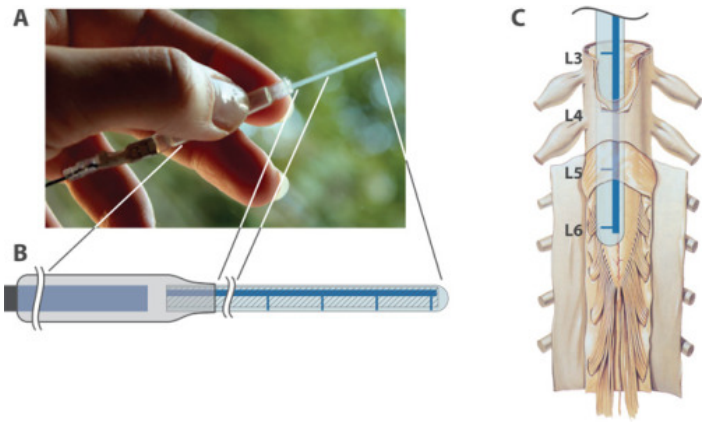

Fig. 1.16 (A) Photograph of the organic electronic ion pump device. (B) Schematic illustration: electrical connection (left); reservoir with internal electrode (center); delivery channel and outlets (right). Total length 120 mm; reservoir diameter 6 mm, length 60 mm; delivery tip width 1.2 mm, length 40 mm, thickness about 0.2 mm. [78]

Chapter 2

In Vitro Ion Pumps

2.1 Controlling Epileptiform Activity with Organic Electronic Ion Pumps

2.1.1 Introduction

Drugs constitute the classical therapeutic approach to treat diseases. Newly designed active substances can be very promising during preclinical testing, but later fail in the clinic because of their toxicity, side effects, rapid elimination/degradation, or failure to reach the desired target. Additionally, drugs are not usually administered specifically to the region of the body affected by the pathology. As a result, they can act elsewhere and have deleterious, undesired effects. In the case of neurological disorders, the situation is more complex as drugs need to cross the blood brain barrier before reaching their targets in the brain[2],[27]. In addition, the expression of multidrug transporters can effectively transport drugs back to the blood stream limiting their action in the nervous system. Novel strategies have been developed to circumvent these limitations in the field of neurological disorders. They include optogenetics, to control epilepsy[91],[122],[188] or psychiatric disorders[175], and designer receptors exclusively activated by designer drugs[44],[43]. These techniques allow on-demand interventions, where and when they are needed. However, both approaches require viral transfer of xenomolecules, which still limits their translation to the clinic.[92] In the immediate future, drugs still remain the best mode of action; therefore, progress must be made to by-pass all the above- mentioned problems. An ideal solution would be to deliver drugs directly where they are needed, on demand.

Small-scale systems for in vivo drug delivery are of wide interest.[97] Such devices reduce the necessary amount of the compound to be administered by localizing the delivery

directly in the target region. Since small amounts are delivered, they are less likely to interfere with the function of nearby "healthy" regions and have toxic effects. In addition, although concentrations can be high locally, the drug will be heavily diluted when returned to the circulation. Progress in the use of these micro- and nano-systems includes both the delivery of therapeutic compounds for combating disease and the delivery of compounds influencing cell proliferation, migration, and differentiation.[142] However, even in the case of microfluidic devices, some problems remain: biocompatibility, which is essential for long-term implantation of such devices in patients, increase of local pressure, which can produce damage, and delivery of both the drug and its solvent, since the solvent can have undesired effects on its own. Electrochemically controlled release of drugs from conducting polymer electrodes is another option. However, it is has been demonstrated for these devices that the rate of drug release is complicated to control and the lack of a reservoir results in a limited amount of the drug which can be delivered.[162],[180] This is not suitable for a device to be eventually implanted. We focus our work here on a device compatible with flexible organic (biocompatible) systems for neural implantation, an OEIP, which can deliver molecules without any fluid flow and thus with negligible increase in local pressure.

We used epilepsy as a model system to test the device. Epilepsy affects 1 % of the world population and remains drug-resistant in 30 % of the cases.[103],[95] Epilepsy is a prototypical example for which drugs have failed in the clinic because of their toxicity, side effects, or failure to cross the blood brain barrier, despite having strong antiepileptic effects.[136],[15] Controlling drug-resistant epilepsy may still be achieved with these compounds if they could be delivered locally. As a first step in this direction, we used hippocampal slices in which several pharmacological manipulations can be used to evoke epileptiform activity. Lowering the extracellular concentration of Mg^{2+} or blocking K+ channels with 4-aminopyridine (4AP) in the perfusion medium produces epileptiform activity that is resistant to common antiepileptic drugs.[5],[181] In order to test the efficacy of the OEIP, we chose to deliver gamma- aminobutyric acid (GABA), an endogenous neurotransmitter, which can have an inhibitory effect via its action on GABAA and GABAB receptors. In adult neurons, the activation of GABAA receptors leads to Clinflux into the cell, hyperpolarizing the cell membrane. In addition, the opening of these channels decreases the membrane resistance, creating a shunt effect, and limiting the effectiveness of excitatory inputs. The net effect is to decrease the firing probability of the cell. The advantages of using GABA are that it is endogenous and that it is quickly taken up and metabolized.[151] It is also particularly relevant in the context of epilepsy since many antiepileptic drugs have been designed to boost GABAergic neurotransmission.[107]

2.1.2 Results

Organic electronic ion pump

Organic electronic ion pumps (OEIPs) can be used to deliver ions and small charged molecules, such as neurotransmitters, with high spatial resolution, to stimulate cell activity locally.[65], [153] The OEIP key component is a cation exchange membrane (CEM), a polyanion, which, because of its high concentration of fixed negative charges, is permeable and selective to cations. This inclusion of cations and exclusion of anions is valid as long as the ionic concentrations of the electrolytes in contact with the CEM are low compared to the concentration of fixed charges in the CEM. To "pump" ions from one electrolyte, through the CEM to the other electrolyte, a voltage is applied across the CEM, and cations in the positively addressed electrolyte are electrophoretically transported through the polyanion. Since anions are excluded from the CEM, the majority of the current through the CEM is due to cation drift (typically for a fixed charge concentration of 1 M in a CEM and 0.1 M electrolytes, 99 % of the ions in the CEM are cations and 1 % are anions). This means that the number of cations that are released at the target electrolyte can be calculated from the current, with 1 μA translating to a delivery rate of 10 nanomol/second.

To run an ionic current through the CEM, two electrodes that can convert an electronic current into an ionic current are needed. We use poly(3,4-ethylenedioxythiophene) doped with polystyrene sulfonate (PEDOT:PSS) electrodes, labeled source electrode and target electrode (Figure 2.1a). The source electrode is positively biased, which means that holes are injected into the PEDOT of this electrode. To remain charge neutral, cations leave the PEDOT:PSS source electrode as the charge of the PEDOT increases due to the injection of holes. The target electrode is negatively biased, which means that holes are extracted from the PEDOT of this electrode. To remain charge neutral, cations move into the PEDOT:PSS target electrode as the charge of the PEDOT decreases due to the extraction of holes.

The reaction at the positive source electrode can be described by the reaction:

$$PEDOT^{x+} : mM^{+} : PSS^{x+m-} = PEDOT^{x+n+} : m-nM^{+} : PSS^{x+m-} + ne^{-} + nM^{+}$$

where M+ is an arbitrary monovalent cation in the electrolyte, m and n are integers, and eis an electron. At the negative target electrode the reverse reaction takes place:

$$PEDOT^{y+} : pM^{+} : PSS^{y+p-} + ne^{-} + nM^{+} = PEDOT^{y-n+} : p + nM^{+} : PSS^{y+p}$$

The lifetime of the device is limited by the capacity of the PEDOT in electrodes. The device can keep transporting ions, with the above mentioned electrode reactions, as long as there is PEDOT in the source and target to be oxidized and reduced, respectively. The amount of PEDOT that can be oxidized in a pristine 200 nm thick PEDOT:PSS film has been estimated to be 3.2 mC/cm^2 . Using a film thickness of 800 nm and an electrode area of 1 cm^2 gives 12.8 mC. Another study estimates the density of sulfonate groups involved in doping PEDOT in PEDOT:PSS to about 3 x 10^{20} cm^{-3}. For the same electrode this gives 2.4 x 10^{16} "active" doping sulfonate groups, each one bearing a charge of 1.602 x 10^{-9} C. This gives a total capacity of 3.8 mC. Based on theses estimates, running the device at a constant current of 1 μA would give a lifetime of 1-3 hours of continuous use.

Configuration of the experiment

The architecture of the OEIP used in this work is depicted in Figure 2.1a. It has a reservoir electrolyte that contains the cations to be transported (K + or GABA+ , 40 mM(aq)) to the chamber containing the neural tissue. The CEM is made from the polyanion poly(styrene sulfonate-co-maleic acid) (PSSA-co-MA) cross-linked with poly(ethylene glycol) (PEG) and is patterned into a large channel that then splits into an array of 32 separate outlets, each 20 μm wide. The pyramidal cell layer of the CA1 area of the mouse hippocampus was placed directly above the outlets of the OEIP (Figure 2.1b). A tungsten recording electrode was then inserted into the pyramidal cell layer directly above one outlet to record changes in electrophysiological activity of the cells close to the outlet. A voltage was sourced to induce a cationic current through the OEIP, and the tungsten electrode recorded extracellular field potentials and multiunit activity resulting from the cation delivery. In order to test the device, we first delivered K + , which should increase cell excitability and lead to increased pyramidal cell activity. In a second set of experiments, we applied GABA to test the efficiency of the device to suppress epileptiform activity.

In order to test the ability of the pump to deliver ions and interfere with neuronal function, we first used local K + delivery, a procedure known to induce hyperexcitability in mouse hippocampal slices.[141],[160] The outlet of the pump was placed in direct contact with the stratum pyramidale (SP) of the hippocampal CA1 area (Figure 2.2a). A tungsten recording electrode was inserted in SP, directly above the outlet of the pump, to provide immediate electrophysiological recordings of pyramidal cell firing (Figure 2.2b) and assess the effects of K + delivery. Recordings taken during K + delivery (black trace) are shown in Figure 2.2c, with the corresponding changes in mean firing rate superimposed (blue trace). Approximately 60 s after switching on the ion pump, there was a clear increase in firing rate.

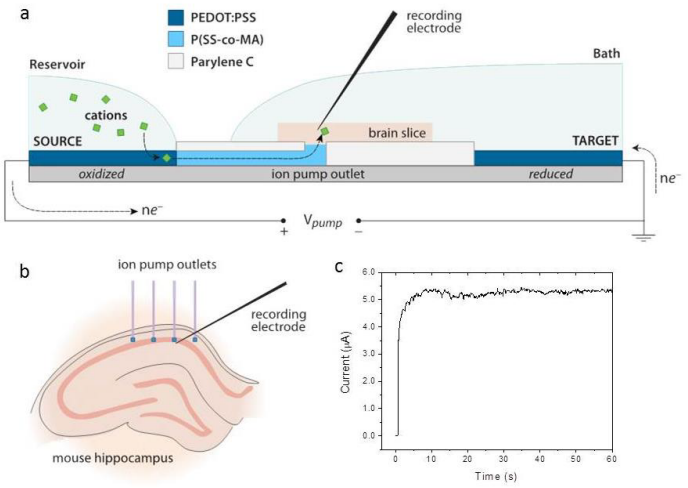

Fig. 2.1 Delivery of cations directly to neural tissue.(a) Cations are electrophoretically transported through the CEM and released at the outlets below the pyramidal cell layer of the CA1 area. Due to an applied bias voltage, Vpump, ions are electrophoretically delivered from the reservoir towards the target. For each ion being delivered, an electron is transferred from the source electrode to the target electrode, oxidizing the source and reducing the target. (b) The outlets of the pump are located below the pyramidal cell layer of CA1 area of the mouse hippocampus. A tungsten recording electrode is inserted in the pyramidal cell layer over the outlet of interest to record field potential and unitary spikes. (c) An ionic current flowing through the ion pump when a 20 V bias is applied.

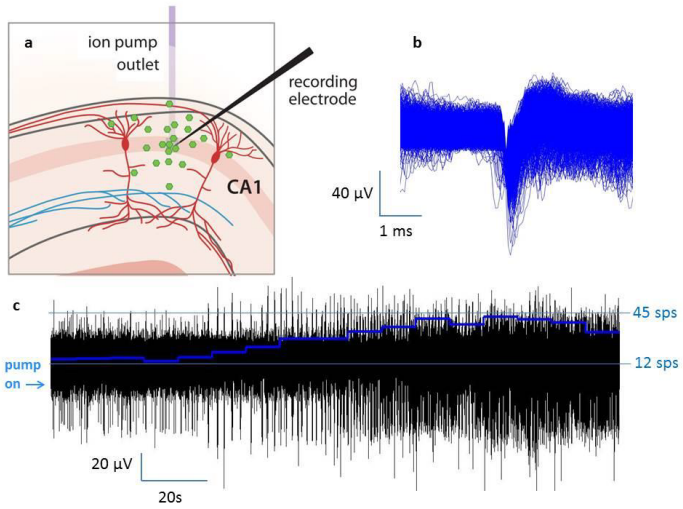

Fig. 2.2 Delivery of K+ to induce hyperexcitability.(a) The tungsten recording electrode was located in CA1, above the ion pump outlet, and spontaneous firing was measured. (b) Action potentials were sorted from the complete recording to obtain the change in mean firing rate, determining the approximate number of spikes per second (sps). (c) The pump was turned on at the beginning of the displayed recording, as indicated. After approximately 1 minute a significant increase in firing rate from 12 sps to over 40 sps was measured (blue trace).

Assuming similar delivery from the all outlets, the measured current through the device during the applied voltage corresponds to a delivery of 4.08 nanomol/second/outlet given an ideally permselective CEM. The concentration of ions in an area around the outlets can be estimated by modeling the diffusion of ions from the outlets in a half-sphere with radius equal to the maximum diffusion length of the ion during the delivery time. This concentration after 60 s of delivery is increased approximately 2.9 mM above the normal concentration in the ACSF. This concentration is an estimation since it does not take into account the uptake mechanisms of K+ by glial cells. [88]

To verify that the increase in activity was not due to the powering of the electronic device itself, we switched on the pump with no cation in the reservoir, only DI water. This did not increase neuronal activity (not shown). For comparison, direct addition of potassium chloride (3.5 mM) to the perfusion medium (with the ion pump turned off), resulted in similar increased neuronal activity (compare Figure 2.2c and Figure 2.3). We conclude that neuronal activity can be manipulated on-demand by the local delivery of cations with the OEIP.

To test the ability of the device to control epileptiform activity, we used three different models: high K +, low Mg^{2+} , and 4AP. GABA has an acidity (pKa) of 4.23 (carboxyl, COO) and 10.43 (amino, $+H_3N(CH_2)_3$). We added GABA to DI water in the reservoir of the

device, resulting in a pH of 6.67. However, the pH inside the PEDOT:PSS is higher, giving positively charged +H3N(CH2)3COOH ions for delivery. To test the delivery and effect of these GABA ions, hyperactivity was first induced by the addition of extra potassium chloride to the perfusion, elevating the external concentration of K+ from 3.5 mM to 7 mM. The tungsten recording electrode was again located in CA1, above the ion pump outlet. The OEIP was then turned on. After approximately 60 s of pumping, CA1 pyramidal cell hyperactivity was suppressed (Figure 2.3).

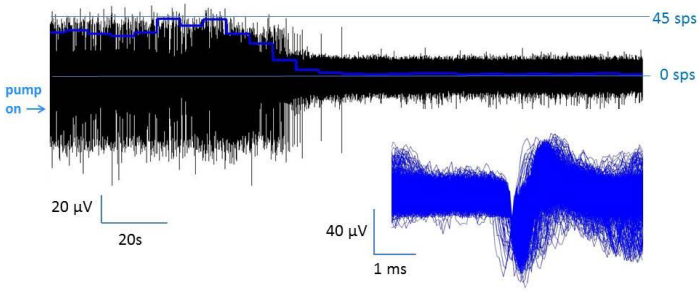

Fig. 2.3 Delivery of GABA to suppress hyperexcitability.Hyperexcitability was induced by adding 3 mM KCl to the perfusion. Spikes were sorted from the complete recording to obtain the change in mean firing rate. The pump was turned on at the beginning of the displayed recording, as indicated. After approximately 1 minute a significant decrease in mean firing rate (blue trace) was observed.

We obtained similar results in the low Mg^{2+} model. As seen in Figure 2.4 (top panels), the ion pump was again placed under CA1 SP with a corresponding tungsten recording electrode. For additional comparison, a second tungsten electrode was located in the SP of the CA3 area. Epileptiform discharges were abolished within one minute of pumping in the CA1 area, while remaining unaffected in the CA3 region. This demonstrates that the ion pump can control the activity of a given region without interfering with the activity of the nearby region. We chose to control the CA1 region, because the axons from the pyramidal neurons of CA1 do not extend back to CA3. This means that modification in the firing rate of neurons in CA1 cannot directly affect the firing of CA3 pyramidal cells. Finally, delivering GABA also abolished epileptiform activity induced by 4AP, in Figure 2.4 (bottom panels).

In these examples the delivery of GABA was estimated to be 1.75 picomol/second/outlet, corresponding to a local change of 4.5 μM extracellularly in CA1 (calculation details in the Discussion section below). This concentration change corresponds to the known quantities of extracellular GABA able to inhibit spontaneous activity, typically between 7 and 20 M.[77] Once completely diluted in the 500 ml perfusion, this delivered GABA is at a concentration of 3.36 nM, essentially insignificant. Hence, the effect of GABA is due to

its direct diffusion into the neuronal tissue, and not by its dilution into ACSF, a conclusion supported by the lack of effect on CA3 pyramidal cell activity.

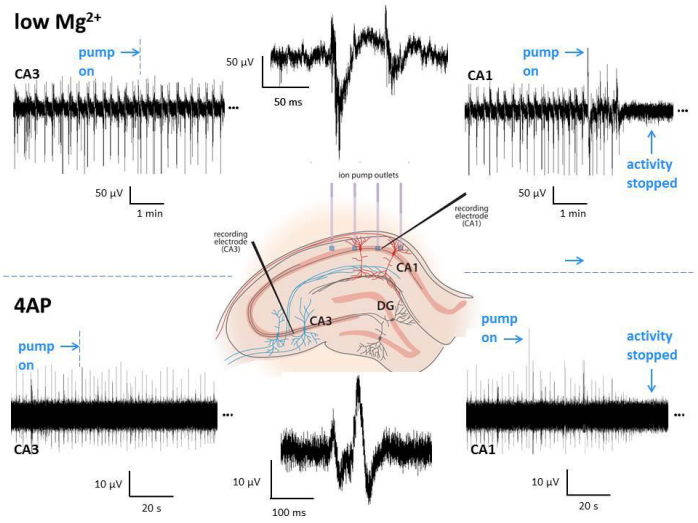

Fig. 2.4 Suppression of epileptiform activity in the hippocampus. Targeted delivery of GABA from an ion pump located in the CA1 of a mouse hippocampal slice locally inhibits epileptiform activity induced in low Mg^{2+} ACSF (top panels) or in the presence of 4AP (bottom panels). The middle traces shows examples of individual epileptiform discharges (field potential) recorded in both conditions. Note that epileptiform discharges stopped in CA1 (right panels) where the pump outlets were located 1 min after turning on the pump, but not in CA3 (left panels), which was not exposed to GABA. A small artifact was seen in CA1, the location of the pump, when the pump was turned on, no artifact was seen in CA3.

2.1.3 Discussion

We have shown that an OEIP can abolish abnormal electrophysiological activity by on-demand, local delivery of the inhibitory neurotransmitter GABA. Although the mechanisms underlying hyperexcitability induced by high-levels of K + , low Mg^{2+}, and 4AP are different, GABA delivery successfully blocked the pathological activity. This means that, despite the fact that there are multiple ways to generate hyperexcitability[71], local delivery of GABA may work as a general way to control epileptiform activity. This is consistent with the fact that seizures are prevented by GABA boosters in many patients.[34] Propagation of abnormal activity by the recruitment of additional brain regions is a defining feature of seizures.[150] Studies of such epileptiform propagation in vitro clearly show that, before the epileptiform wavefront, there are very large amplitude inhibitory currents.[171] Pyramidal cells essentially receive barrages of inhibitory inputs in advance of the epileptiform wave.

When present, these inhibitory barrages effectively block the intense excitatory synaptic currents that would normally exceed the threshold for action potentials.[170] The progressive loss of these inhibitory inputs to pyramidal cells coincides with the progressive increase in the propagation of epileptiform activity. Although the epileptiform wavefront itself generates large feedforward excitation, when feedforward inhibition is intact, epileptiform activity spreads more slowly and recruitment is effectively limited.[170]

Since this loss of inhibitory control occurs when GABAergic neurons enter into a depolarization block after the onset of epileptiform discharges[71], the local delivery of GABA could supplement the deficit of GABAergic neuronal activity and restore inhibitory restraint. Given the fact that brain cells are equipped with powerful transporters which pump GABA from the extracellular space to the intracellular milieu to be recycled,[19] the effect of GABA here is quite striking. Clearly, enough GABA is reaching GABAergic receptors, and not being recycled away. It is additionally striking, considering that these GABAergic receptors can desensitize[76] in the presence of high extracellular concentrations of GABA.

Whether the same effect can be obtained in vivo in chronic models of epilepsy remains to be determined. Transfering OEIP technology to the clinic is justified in drug resistant patients with partial onset epilepsy if neurosurgery cannot be performed (for example if it would remove/damage the eloquent cortex). The pumps could be incorporated into the electrodes routinely used in the clinic for long-term deep brain stimulations. The materials and fabrication scheme employed for the in vitro experiments used here for validation are compatible with similar approaches we have used to develop mechanically flexible organic bioelectronic devices for in vivo measurements.[84] Namely, the ion pump can be fabricated on a parylene-C support that would impart a low profile, conformability, implantability and durability[83], and which can also incorporate electrophysiology and selective biomolecule/ion sensors.

With the geometry used here, the pump could work intermittently to deliver GABA when needed for weeks. Increasing the size of the device (its thickness above 800 nm) should enhance its duty cycle, but the scaling of electrode capacity for very thick films has not been investigated, and may not be the limiting factor at such extremes. Additionally, it must be noted that we chose to deliver GABA, which is actively pumped up and recycled. The local delivery of potent drugs would require fewer molecules to be delivered, thus increasing the lifetime of the pump. Its usage would also be considerably extended by on-demand activation, similar to optogenetics control of seizures.

We conclude that organic electronic ion pumps represent a technological breakthrough for local and timed delivery of active molecules that cannot be delivered in a systemic way.

Using the body's endogenous molecules is an even a better solution, as seen here with the ability of delivered GABA to control epileptiform activity.

2.1.4 Methods

Electrophysiological recordings in vitro.

All protocols have been approved by the Institutional Animal Care and Use Committee of INSERM. All experiments were repeated twice. Electrophysiological recordings were made in the CA1 and CA3 of the mouse hippocampus. After decapitation of anesthetized mice, brains were rapidly extracted (postnatal day 14 to 18). Transverse hippocampal slices (350 μm) were prepared using a vibratome. Freshly-cut slices were placed in a chamber and perfused with oxygenated (95 % O_2 / 5 % CO_2) artificial cerebrospinal fluid (ACSF) (126 mM NaCl, 3.5 mM KCl, 2mM CaCl_2, 1.3 mM MgCl_2, 1.2mM NaH_2PO_4, 26.2 mM NaHCO_3, and 10 mM glucose). Slices were maintained in the chamber at room temperature and allowed to recover for one hour prior to experimental use. After this period of recovery, slices were transferred with a pipette to the surface of the ion pump. The chamber containing the ion pump and slice was continuously perfused with oxygenated ACSF warmed at 33°C. Tungsten electrodes (with a tip resistance of 1-3 M) were positioned in both the CA1 and CA3 region of the hippocampus. Recordings were made with a World Precision Instruments DAM80 AC amplifier, and acquired using an analog-to-digital converter (Digidata 1322B, Molecular Devices). Analysis was performed using using Clampfit (Molecular Devices) or Matlab (Mathworks)-based software. Ion pump fabrication and characterization. OEIPs were patterned on a glass wafer, which was first cleaned and oxygen plasma treated (Advanced Vacuum Reactive Ion Etch, O_2 400 sccm, 250 W, 30 s). A solution of 3-glycidoxypropyltrimethoxysilane (GOPS, 5 wt%) in a water:ethanol mixture (1:19) was spin coated to improve the adhesion of the PSSA-co-MA on glass. After 15 min, the wafers were rinsed in ethanol to remove excess GOPS. They were then baked at 110 °C for 20 min. PSSA-co-MA (5 wt% in a water:1-propanol mixture, 1:1) was mixed with polyethylene glycol (3 wt%, moleculate weight 400 $gmol^{-1}$) for crosslinking. The solution was then deposited by spin casting at 2000 rpm to obtain a thickness of 400 nm. The film was baked at 110 °C for 1 h. A thin layer of poly(methyl methacrylate) (PMMA) was deposited on top of the PSSA-co-MA film for a better adhesion of the S1818 photoresist. The photoresist was deposited and exposed using a MA6-BA6 Süss Mask and Bond Aligner and the final pattern was obtained by reactive ion etching (O_2 100 sccm, CF_4 200 sccm, 150 W, 100 s) and removal of S1818 and PMMA in acetone. Parylene-C was subsequently deposited using an SCS Labcoater 2 to a thickness of 2 μm with the use of an adhesion promoting

silane. Soap (solution of 1 % in water) was spun and followed by a subsequent parylene-C deposition (2 μm). Finally, the source/target PEDOT:PSS was patterned with the insulating parylene-C using photolithography and a sacrificial peel-off step. A thick layer of AZ9260 (MicroChemicals) photoresist was cast, baked and exposed using a SUSS MJB4 contact aligner, followed by reactive ion etching in an O2 plasma (160 W, 50 sccm O_2, 15 min) using an Oxford 80 plus plasma etcher. For the preparation of the PEDOT:PSS films, 20 ml of aqueous dispersion (PH 1000 from H.C. Stark) was mixed with 5 ml of ethylene glycol, 50 ml of dodecyl benzene sulfonic acid and 1 wt% of GOPS, and the resulting dispersion was spin-coated at 650 rpm, soft baked at 100°C for 60 s, and spun cast at 650 rpm to attain thicker PEDOT:PSS films. The film is patterned by peel-off of the top parylene C film and subsequently baked at 140 °C for 1 h and were immersed in deionized water to remove any excess low molecular weight compounds. The reservoir chambers, cut from cured polydimethylsiloxane, were affixed to the source (reservoir) and target (bath) areas. During pump operation, voltage (Vpump=20 V) was sourced and current measured using a Keithley 2400 source/measure unit, and customized LabView software.

2.1.5 Suplementary Information

Lifetime Calculations

The amount of PEDOT that can be oxidized in a pristine 200 nm thick PEDOT:PSS film has been estimated to be 3.2 mC/cm^2 . Using a film thickness of 800 nm and an electrode area of 1 cm 2 gives 12.8 mC. Another study estimates the density of sulfonate groups involved in doping PEDOT in PEDOT:PSS to about 3 x 10^{20} cm^{-3} . For the same electrode this gives 2.4 x 10^{16} "active" doping sulfonate groups, each one bearing a charge of 1.602 x 10^{-9} C. This gives a total capacity of 3.8 mC. Based on these estimates, running the device at a constant current of 1 μA would give a life time of 1 - 3 hours of continuous use.

With the geometry used here, the pump could work intermittently to deliver GABA when needed for weeks. Increasing the size of the device (its thickness above 800 nm) should enhance its duty cycle, but the scaling of ele ctrode capacity for very thick films has not been investigated, and may not be the limiting factor at such extremes. Additionally, it must be noted that we chose to deliver GABA, which is actively pumped up and recycled. The local delivery of potent drugs would require fewer molecules to be delivered, thus increasing the lifetime of the pump. Its usage would also be considerably extended by on-demand activation, similar to optogenetics control of seizures.

For example, the function of the OEIP could be used in place of deficient neuronal structures found in pathology. Propagation of abnormal activity by the recruitment of additional

brain regions is a defining feature of seizures. Pyramidal cells essentially receive barrages of inhibitory GABA in adva nce of the epileptiform wave. Brain cells are equipped with powerful transporters which GABA from the extracellular space to the intracellular milieu to be recycled. When present, these inhibitory barrages effectively block the intense excitatory sy naptic currents that would normally exceed the threshold for action potentials. Although the epileptiform wavefront itself generates large feedforward excitation, when feedforward inhibition is intact, epileptiform activity spreads more slowly and recruitment is effectively limited. The OEIP could supplement the loss of inhibitory barrages.

Neuronal activity returns after switching off the OEIP . Small - scale systems for in vivo drug delivery are of wide interest. Such devices reduce the necessary amount of the compound to be administered by localizing the delivery directly in the target region. Since small amounts are delivered, they are less likely to interfere with the function of nearby "healthy" regions and ha ve toxic effects. In addition, although concentrations can be high locally, the drug will be heavily diluted when returned to the circulation. Progress in the use of these micro - and nano - systems includes both the delivery of therapeutic compounds for comb ating disease and the delivery of compounds influencing cell proliferation, migration, and differentiation. However, even in the case of microfluidic devices, some problems remain: biocompatibility, which is essential for longterm implantation of such devices in patients, increase of local pressure, which can produce damage, and delivery of both the drug and its solvent, since the solvent can have undesired effects on its own. Electrochemically controlled release of drugs from conducting polymer electrodes is another option. However, it is has been demonstrated for these devices that the rate of drug release is complicated to control and the lack of a reservoir results in a limited amount of the drug which can be delivered. This is not suitable f or a device to be eventually implanted. The OEIP delivers molecules without any fluid flow (no solvent) and thus with negligible increase in local pressure (Fig. 2.5) .

Diffusion Calculations

Clearly, enough GABA is reaching GABAergic receptors, and not being recycled away or desensitizing the receptors. We calculated the concentration of GABA (both numerically and analytically), and see that the diffusion of GABA remained local enough to control the activity of CA1 pyramidal cells, without affecting the nearby CA3 region located 1000 μm away. Additionally, the delivered concentration is comparable to literature values of extracellular GABA capable of inducing inhibitory activity without significant synaptic desensitization.

The efficiency of diffusion decreases with the square of the distance, given by,

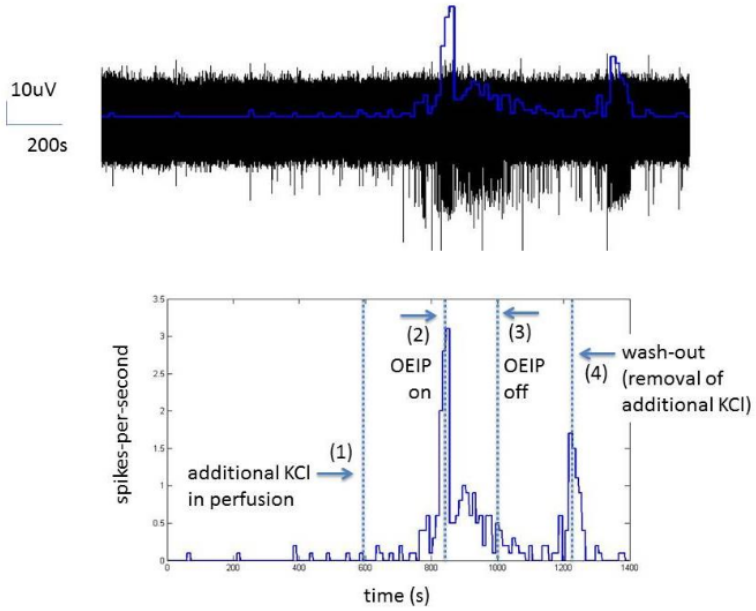

Fig. 2.5 Neuronal activity returns after switching off the OEIP. (top panel) A long baseline recording was taking showing low levels of intermittent spiking from pyramidal neurons in the CA 1 region of the hippocampus (as described in detail in the text of the main article). Hyperexcitabili ty was induced by the addition of KCl to the perfusion and subsequently stopped by the delivery of GABA from the OEIP. After the OEIP was turned off, hyperexcitability returned due to the presence of the additional KCl in the perfusion. Wash - out of the add itional KCl returned activity to its initial low levels of intermittent spiking. (bottom panel) In detail (1) Hyperexcitability was induced by adding 3 mM KCl to the perfusion. A pproximately 3 .5 minutes later, a sharp increase in activity was seen . (2) The OEIP was switched on , delivering GABA , approximately 60s later hyperexcitability was seen to sharply decrease. (3) The OEIP was switched off, and approximately 3 .5 minutes later, a sharp increase in activity was seen. (4) The perfusion was switched to ACS F containing no addition KCl. Over the next several minutes, activity decreased to initial values.

$$t_{diff} = x^2/4D$$

where t diff is the time for the diffusion of a substance through a distance x, which has a diffusion coefficient D in water. The diffusion coefficient of GABA is between 4.0 7.8 x 10^{-6} cm^2 /s . Taking 5 x 10^{-6} cm^2 /s, GABA can diffuse a distance of 245 μm in 30 seconds. We take this distance to be the radius of a half - sphere centered at the pump outlet below the recording electrode. This radius represents the maximum distance a GABA molecule can travel. However, thi s does not mean that all delivered GABA will travel this distance, because of the existence of powerful uptake mechanisms. Regardless, given a GABA delivery of 1.75 picomol/second/outlet, and slightly underestimating the concentration of GABA by not accounting for these uptake mechanisms (using the maximum radius), we arrive at a 4.5 μM concentration This concentration is close to extracellular values previously demonstrated to inhibit neuronal activity, typically between 7 and 20 μM . Hence, at least in vitro, enough GABA was delivered by the pump to control neuronal activity. Since the soma of pyramidal cells is essentially covered with GABAergic synapses and since the site of initiation of action potentials is close to the som a, we located the pump outlet beneath CA1 pyramidal cell somata to guarantee the most efficient control of neuronal output by GABA. The change in K + was similarly calculated and found to be 2.9 mM (3.5 mM increased to 6.4 mM) in the first 30s, also corresponding well to values previously demonstrated to increase neuronal activity, typically between 5 and 9 mM.

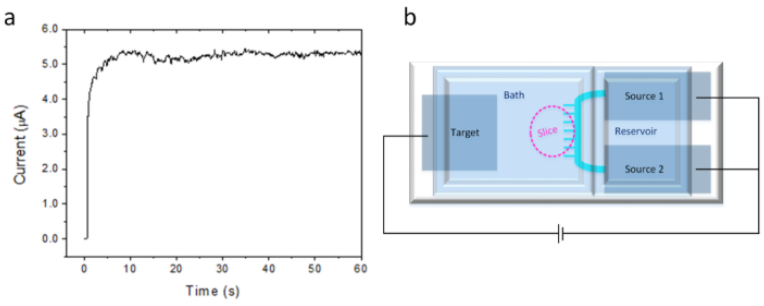

Fig. 2.6 a) Example measured current during device operation. The applied bias was 20 V. b) Schematic top - down view of the CEM during device operation.

Finite - element estimation of GABA concentration at the OEIP outlet was performed for comparison. The GABA concentration at one OEIP outlet that re sults from running a current of 1 μA was modeled using Fick's laws of diffusion. Assuming similar current through all 32 outlets, 1 μA results in 30 nA per outlet, which, assuming transport number 1, yields a flux of 0.3 pmol /second /outlet. The time dependent diffusion equation given this

influx of GABA through a 20 μm 1 μm opening was solved with finite element modeling using COMSOL 5.0. The diffusion coefficient of GABA was set to 5 x 10^{-10} m^2/s. The different time points in the simulation are time points after GABA starts being delivered. in the first 30 s.

2.2 The bioelectronic neural pixel: chemical stimulation and electrical sensing at the same site

2.2.1 Introduction

Recent estimates suggest neurological disorders affect up to 6 % of the global population.[90] The vast majority of treatments generally involves oral administration of pharmaceuticals. When these fail, alternate therapies can include neurosurgery (e.g., in epilepsy) and electrical stimulation via implanted electrodes (e.g., in Parkinson's disease). Pharmaceutical and basic research have identified promising targets and designed potentially efficient drugs for multiple disorders, but such drugs haven't reached patients because of failure during (pre)-clinical tests. There are multiple reasons for such failures. Drugs may be toxic in the periphery [136],[15], they may not cross the blood brain barrier or be pumped back to the blood stream by multi-drug transporters.[104],[59] But the critical factor is the fact that they may have deleterious side effects when they penetrate "healthy" regions, affecting physiological functions such as memory and learning.[123],[94] In addition, since oral administration will lead to a dilution of the drug in the body, there is often a mismatch between the dose necessary to obtain a therapeutic effect in the region to treat and the maximum dose that non-affected body regions can support without side effects.

Providing the drug past the blood brain barrier, where and when it is needed, constitutes the ideal solution. Such delivery would solve all the above-mentioned problems (blood brain barrier crossing, peripheral toxicity, undesirable side effects in healthy regions and effective dose). Devices have been successfully designed to deliver drugs locally.[187] However, the "where" and "when" issues remain to be addressed. Since clinicians may have several spatially distributed regions to treat, or if the volume of the intended treatment region is large, it is important to have multiple drug delivery sites, which would solve the "where" issue. The "when" issue is more difficult to address, as, ideally, a delivery system should act on-demand, when needed (e.g., just before an impending seizure). Since electrophysiological signals can be used to predict incoming pathological events [33], electrical activity should be measured at each delivery site to trigger drug delivery at that specific location. Such local, real-time measure- ment, and precision delivery, would pave the way for closed-loop, fully

automatic, therapeutic devices. Finally, since the size of the region to treat may be small – down to the scale of a single cell – the technology should allow spatial resolution of delivery on the order of micrometers. Interfacing malfunctioning neurological pathways with

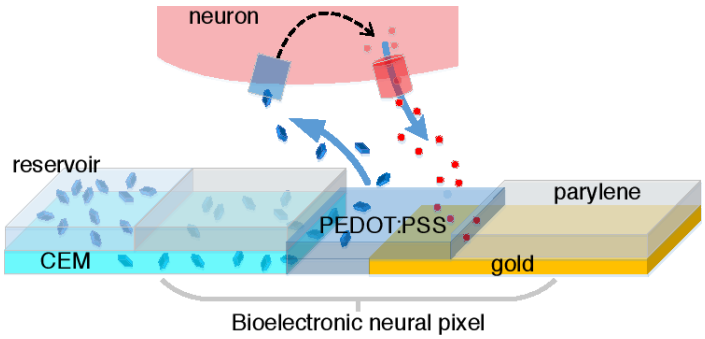

Fig. 2.7 The bioelectronic neural pixel. The OEIP channel outlet (terminating in the PEDOT:PSS) co-localized with the PEDOT:PSS recording electrode forms one neural pixel. The reservoir (left) comprises an aqueous solution of the positively charged compound to be delivered through the cation exchange membrane (CEM) and out through the PEDOT:PSS recording electrode to the neural tissue above the pixel. The biological response, in terms of ion fluxes, is measured locally by the PEDOT:PSS recording electrode co-localized with the OEIP outlet.

spatial resolution and signal specificity approachin those of the cell could provide significant advantages to future therapies. Microelectrode recordings of the field potentials generated by neurons (or even neuronal firing itself) have become routine in investigations of brain function and dysfunction.[31] Small size of recording sites allows for recording of single neurons, and densely packed sites on minimally invasive electrodes enhance the sampling capacity of the probe. Such densely packed probes can be accomplished using conducting polymers, such as poly(3,4- ethylenedioxythiophene) doped with poly(styrenesulfonate) (PEDOT: PSS), without decreasing the quality of the recordings. Conducting polymer electrodes exhibit inherently low impedance characteristics (more than one order of magnitude lower than bare Au, Pt and Ir electrodes of similar dimensions at 1 kHz), with the low impedance being attributed partly to the high porosity, giving an increased electrochemical surface area.[105] Additionally, with their mixed electronic and ionic conductivity and the soft mechanical properties that match those of the neural tissue, conducting polymers are ideally suited to obtain high signal-to-noise ratio recordings at the neural interface.[4],[52] Recently, we have demonstrated microelectrode arrays based on PEDOT:PSS electrodes for in vitro recordings of electrophysiological signals from rat brain slices. [174] These microelectrodes, fabricated at small size and high density, have enabled a good match with the dimensions of neural networks while maintaining high-resolution neural recordings.

We have also demonstrated substance delivery mimicking exocytotic release of neurotransmitters at the neuronal scale by means of the organic electronic ion pump (OEIP).[152], [155] The OEIP utilizes conducting polymer electrodes to electrophoretically "pump" neurotransmitters through a permselective membrane, enabling high spatiotemporal delivery resolution, without necessitating liquid flow. OEIPs have been utilized in vitro to trigger cell signaling[65] and to control epileptiform activity in vitro, as well as in vivo to effect sensory function[155] and as a therapy for pain in awake animals.[78] OEIPs have also been demonstrated in a biosensor-regulated system—on a macroscopic scale—to mimic the chemical-to-electrical-to-chemical signal transduction of neurons. [154] However, none of these devices meet the desired requirement to record and deliver drugs at the same site.

In this article, we engineered a device able to perform electrical sensing of local field potentials and neurotransmitter delivery at the same site. To achieve this co-localized sensing and delivery we developed a system consisting of an array of OEIP delivery points, where each delivery point is integrated with a conducting polymer electrode for recording neuronal activity. Each integrated delivery/sensing pixel is at the single-cell scale and mimics the multifunctionality of a biological neuron: electrical information can be sensed from the local cellular environment, and neuroactive compounds can be delivered diffusively, without liquid flow, at the same location. We report on the development and characterization of this system of "neural pixels", and we demonstrate its use by delivering the endogenous inhibitory neurotransmitter -aminobutyric acid (GABA) to locally affect cells while simultaneously monitoring how the delivery modulates the cells' firing patterns.

2.2.2 Results

Design and Principle

We designed our bioelectronic neural pixel as depicted in Figure 2.7. The charged compound to be delivered is transported from an aqueous reservoir through a cation-conducting channel and through part of the PEDOT:PSS recording electrode before being released to the biological system. In this way, the cells close to the OEIP outlets are affected by the delivery, and the electrodes can record the subsequent modifications in cellular response. The OEIP transports cations by migration; when a potential is applied between an electrode in the reservoir and an electrode in the medium containing the biological system under study, an electric field is established across the cation-conducting channel and a current arises from cation migration from the reservoir to the biological system. In this way, delivery is only achieved when non-zero voltage is applied (see Supplementary Information for more details on on-off switching). The cationconducting channel has a high concentration of fixed

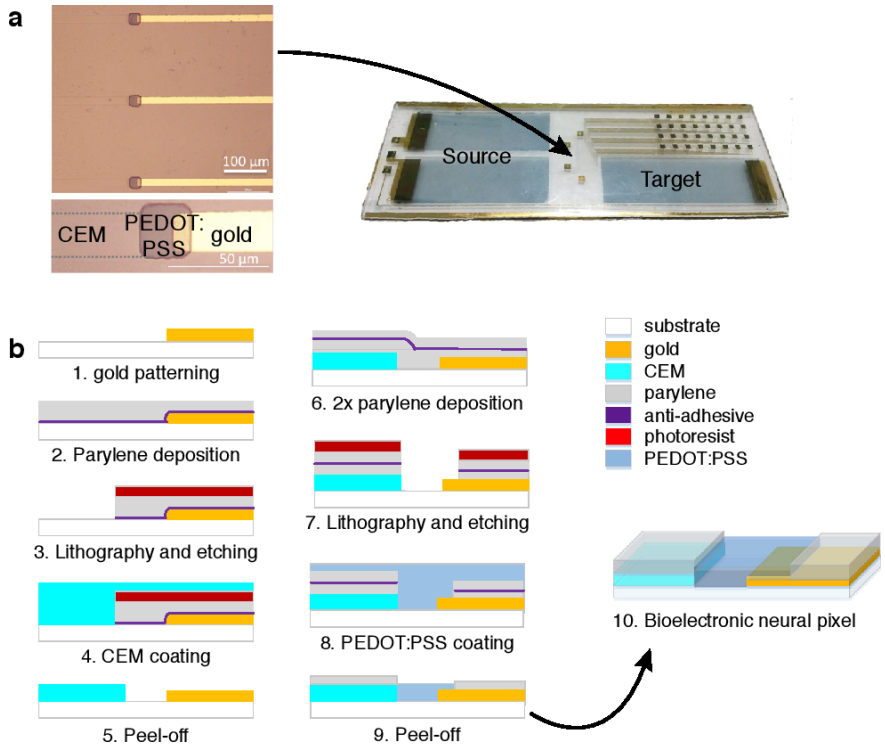

Fig. 2.8 Design and fabrication of the bioelectronic neural pixel. (a)Microscope image of the three adjacent co-localized OEIP outlets and sensing electrodes, and photograph of a typical device. Two source electrodes are depicted, used at equipotential and thus forming effectively one electrode. The reservoir chamber, cut from cured polydimethylsiloxane (PDMS), is affixed to the source and target areas. The source contains the cation solution to be delivered, and the neural tissue is placed on the target region. Supplementary Figure shows the design in more detail. (b) Cross-section schematics showing the photolithographic fabrication process. Gold lines were patterned with photolithography (1), followed by coating of parylene-C with a thin layer of anti-adhesive (2). Photoresist was then cast and exposed, followed by reactive ion etching to define the areas to be filled with CEM (3). The CEM (PSSA-co-MA cross-linked with poly(ethylene glycol)) was patterned into a wide channel that split into 32 separate outlets, each 20 μm wide and spaced by 200 μm by peeling off the sacrificial top layer of parylene-C (4, 5). Two layers of parylene-C were then deposited, separated by a thin layer of anti-adhesive (6). A thick layer of photoresist was then cast, exposed and etched in order to define the areas eventually to be filled with PEDOT:PSS (7). A thick layer of PEDOT:PSS (ca. 400 nm) was spin-cast (8) and the source/target electrodes and the sensing electrodes at the pump outlets were patterned by peeling off the sacrificial top layer of parylene-C (9). The co-localization of an OEIP outlet with the PEDOT:PSS electrode form a neural pixel (10).

negative charges and is therefore permeable to cations but not to anions (Donnan exclusion), and is therefore a form of cation exchange membrane (CEM). Ideally, all the current passed through a CEM, and thus through the device, is due to cation transport, and no anions are transported in the opposite direction. This means that the delivery rate is directly proportional to the current, with 1 A corresponding to a delivery rate of 10 nmol/s. Sustained delivery (constant current) requires nonpolarizable high capacity electrodes that can transfer charge between the electrode and the electrolyte. We used PEDOT:PSS electrodes for this purpose, on top of which were placed the source (reservoir) and target electrolytes (Figure 2.8a). Note that no potential was applied to the recording electrodes at the delivery outlets to control the delivery of ions.

Fabrication and Characterization

The materials and processing of an OEIP and a conducting polymer microelectrode array (MEA) are of similar nature, making it possible to manufacture the two components of the merged device simultaneously on a single glass substrate. To fabricate the bioelectronic neural pixel device, we developed a manufacturing protocol based on standard microfabrication techniques. Device fabrication is depicted Figure 2.8b. First, gold electrodes were patterned on a glass substrate using photolithography and lift-off. Then the main element of the OEIP, the cation exchange membrane (CEM), made from the polyanion poly(styrene sulfonateco- maleic acid) (PSSA-co-MA) cross-linked with poly(ethylene glycol) (PEG), was deposited. The CEM was photolithographically patterned and dry-etched into a wide channel leading to 32 thinner (and thus higher ionic resistance) parallel channels ending in 20 μm-wide delivery outlets. Alternatively, the PSS-co-MA/PEG was patterned by peel-off using parylene (see Methods section). A 2 μm-thick parylene layer, providing the insulating coating of the OEIP and the MEA contacts, was deposited. A thin layer of dilute commercial cleaner was applied as an anti-adhesive coating and a second 2 m-thick parylene layer was deposited. Openings to define the OEIP electrolytes, the microelectrodes, and the contact pads were obtained by further photolithography and plasma etching through the parylene. PEDOT:PSS was then deposited by spin-coating, and the second parylene layer was peeled off to define the OEIP electrolytes and the microelectrodes. The 32 resulting neural pixels thus comprised 20x20 μm PEDOT:PSS recording electrodes at the delivery end of each PSSA-co-MA-based OEIP channel. In this way, substance delivery was achieved through the PEDOT:PSS recording electrode, such that the delivery outlet and the recording electrode were indeed at the same site (Figure 2.7). Finally, a PDMS gasket was cut with openings over the source electrodes, defined the source solution well, and over the 32 neural pixels and target electrode, defining the target solution well.

To characterize the multifunctional device, we first measured the impedance of the recording electrodes separately, and then while running a delivery current through the OEIP to investigate whether running the delivery current through the recording electrodes affected the electrical properties of the recording electrodes. The Bode plot of the mean impedance magnitude of seven randomly picked PEDOT:PSS electrodes of the array is presented in Figure 2.9a. The standard deviation of the impedance magnitude is low, indicating that the fabrication process yielded homogeneous electrode properties within the array. Between 10 kHz and 10 Hz the impedance increased from 16 k to 250 k, and at 1 kHz, the impedance was ca. 19 k, which is similar to our previously reported results (17). To further investigate the influence of OEIP operation on the signal to noise ratio, we compared electrode recordings in the absence and presence of a delivery current (Figure 2.9b). A 100 mM GABA(aq) solution and artificial cerebrospinal fluid (ACSF) were placed on the source and the target side, respectively. The amplitude of the baseline signal measured when the OEIP was off was ca. 10 μV (Figure 2.9b). After 60 s, a positive potential was applied to the OEIP source electrode with respect to the target, and a current of 1 A was run through the device, yielding GABA delivery at the 32 outlets. The electrical signal intensity recorded remained stable. The OEIP was switched off after 60 s without apparent change in signal amplitude. A too high delivery rate could affect the recording electrodes by perturbing the local ion concentration, making cell recordings difficult or impossible. However, as seen in this experiment, constant currents of 1 A or lower are compatible with electrophysiological recordings.

After confirming that cation delivery did not interfere with electrode recordings, we evaluated sensing and stimulation performance of the pixels in a biological system. As the first application of the integrated device could be for epilepsy diagnosis and treatment, we used complete extracted hippocampus preparations from mouse (P7-P12) and triggered epileptiform activity by pharmacological manipulation, namely the addition of 4-aminopyridine (4-AP) to the perfusion. 4-AP is a selective blocker of channels belonging to the Kv1 family of voltage-gated K+ channels. Blocking K+ channels with 4-AP in the perfusion produces epileptiform activity by increasing the time required for a neuron to repolarize (fewer K+ channels are available). Thus, neurons remain above the threshold to fire for a longer period of time, and excitatory neurons consequently continue to deliver glutamate to downstream neighbors. In order to test the efficacy of the device, we chose to deliver GABA. As an endogenous neurotransmitter, GABA activates GABAA receptors, leading to Cl- influx into the cell, which in turn hyperpolarizes the cell membrane (Figure 2.10a). In addition, the opening of these channels decreases the membrane resistance, creating a shunt effect, and limiting the effectiveness of excitatory inputs. The net effect of GABA is therefore a decrease in the firing probability of the cell.[52] With the complete extracted hippocampus

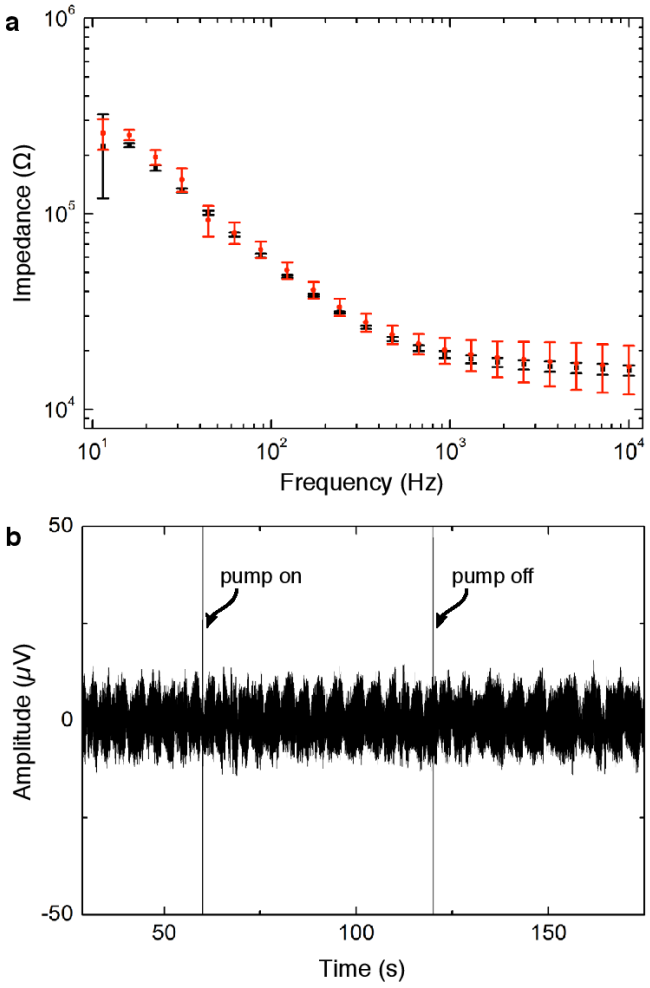

Fig. 2.9 Characterization of sensing electrodes incorporated into neural pixels.(a) Bode plot of impedance versus frequency. The impedance magnitude is an average of seven electrodes. Black squares and red dots are the averaged impedance values while the OEIP is off and the while K+ is delivered (1 A delivery current), respectively. (b)Time trace at a single recording site during GABA delivery ($60 < t < 120$ s) through the sensing electrode to the ACSF target solution.

preparation mounted (and equilibrated) on the target area of the neural pixel system, we induced epileptiform activity with the addition of 4- AP in the perfusion medium. PEDOT:PSS electrodes recorded the subsequent broadband electrophysiological activity (Figure 2.10b). The recordings, which were simultaneously obtained via multiple channels, had signal quality comparable to a conventional tungsten recording electrode, which was located adjacent to the MEA. Moreover, due to multiple recording sites, it is possible to access different forms of activity across the tissue. After ca. one minute of GABA delivery, epileptiform discharges were abolished. Assuming that the delivery is equally distributed between the 32 outlets of the device, 1 A of supply current yields a delivery rate of 0.3 pmol / sec /outlet. This corresponds to a local concentration change of 25 μM at distance of 400 μm from a single pump outlet after 60 s, and is within the known range for GABA to suppress hyperactivity[75] (injection of 250 M GABA in the ACSF-filled bath directly on top of the tissue stopped the hyperactivity almost instantaneously). Previous experiments demonstrated local delivery with OEIPs, and local control of hippocampal networks with a similar device geometry. Taken together, these results demonstrate that the neural pixel system can effectively control the activity of a given network via OEIP delivery, while simultaneously allowing monitoring via the integrated electrodes of both hyperactivity as well as real-time biological response to OEIP operation.

Since GABA is an acid and is transported by the OEIP in its fully protonated form (charge +1), each GABA molecule will release a proton once delivered to the biological system. Therefore, to verify that the observed abolishment of of epileptiform discharges was solely due to GABA delivery, and not to proton delivery, or to the applied potentials and ionic currents, a control experiment delivering protons was performed. The reservoir was filled with aqueous HCl solution, while the target region contained the hippocampus exhibiting hyperactivity. The same current was sourced to the OEIP as for the GABA delivery experiments, however we did not observe any significant change in the electrode recordings upon delivery of H+. This shows that neither proton delivery nor ionic currents (which could cause electrical stimulation) blocked the pathological activity, but that the release of GABA was necessary to to stop epileptiform activity.

2.2.3 Discussion

In the present work, we have demonstrated electrophysiological sensing and chemical stimulation from a single multifunctional “neural pixel”. This is a necessary advancement to achieve highly localized feedback-regulated therapies with future devices. We have previously shown that we could deliver GABA with an OEIP to stop epileptiform activity in a tissue slice. In those experiments, the recording electrode was a tungsten electrode posi-

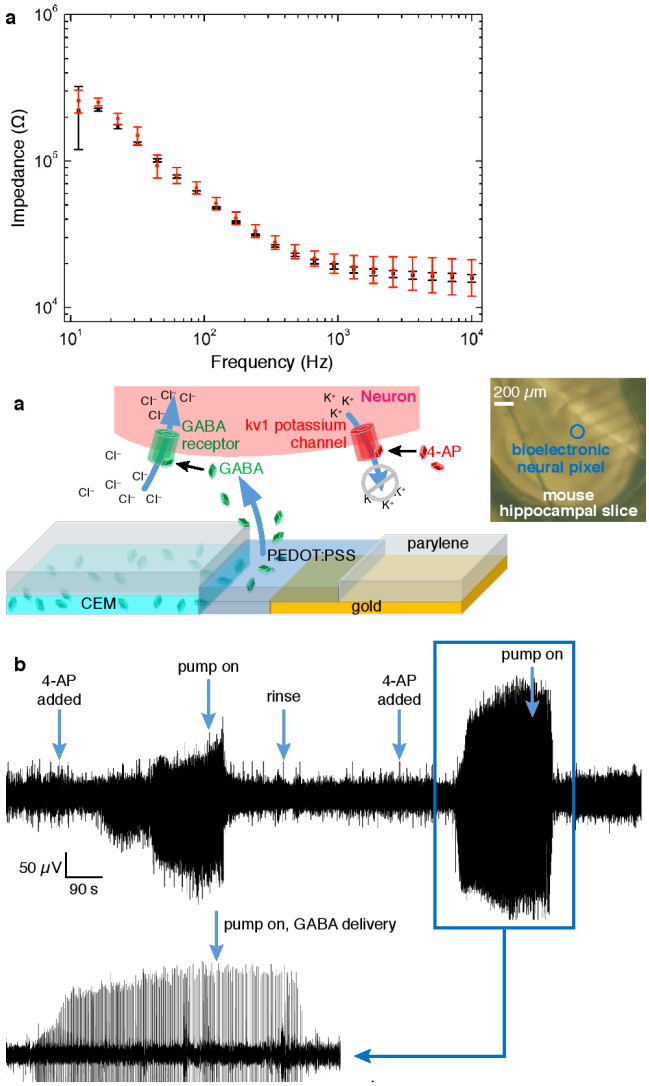

Fig. 2.10 (a) Biochemical pathway for reducing 4-AP-induced epileptiform activity via GABA delivery. The inset shows a mouse hippocampal slice positioned on an array of bioelectronic neural pixels. (b) Epileptiform activity of a complete mouse hippocampal preparation was recorded from a single pixel before and during GABA delivery to the same pixel. Large events are seen at the beginning of the recording approximately 100 s after introducing 4-AP to the bath. Approximately 60 s after the OEIP is switched on, the epileptiform activity stops. This cycle is repeated twice by rinsing the bath with ACSF and treating the tissue with 4-AP. (c)Response of recording electrodes to delivery of H+ .H+ delivery has no observable effect on epileptiform activity. The recorded signal is from the epileptic mouse hippocampal neurons upon delivery of H+ from the OEIP outlets. The activity does not stop when the source reservoir contains HCl and ion pump is operated under the same conditions as with GABA delivery experiment. (c) Negative control: delivery of H+ only. Epileptiform activity was not observed to change.

tioned in the tissue slice in the vicinity of an OEIP outlet. In this work, we suppress the need to align this external recording electrode with the outlets of the OEIP. Instead, delivery occurs through the sensing electrodes, ensuring co-localization of recording and stimulation and eliminating cumbersome experimental setup. The integrated sensing and delivery device stopped externally induced epileptiform activity of a hippocampus by delivering the inhibitory neurotransmitter GABA at the exact sites where epileptic activity was recorded. The low impedance of the conducting polymer electrodes allowed for high signal-to-noise ratio recordings of physiological activity at the site of GABA delivery. In order to efficiently treat an epileptic event, the delivery of GABA should occur as soon as any signs of seizure appear. Many studies have shown local release of compounds using microfluidics, for example Refs. ([154] ,[114]), to name a few. Microfluidics have the ability ot deliver any soluble compound, but such delivery in a carrier fluid induces convection, which risks disrupting fragile biochemical microenvironments . Microfluidic systems also typically require complex setups of valves and pumps. Other groups have demonstrated electrically controlled convectionfree delivery systems, for example Refs. ([162],[4]), that rely on redox-switching of conducting polymers to release an embedded compounds. However, these systems are typically limited in the amount of deliverable compound, a release rate that decreases over time, and a poor on-off ratio. The OEIP-based delivery built into the neural pixel system is electrically controlled, induces no convection, includes a reservoir to increase the deliverable amount, and exhibits a low diffusive off-leakage because of the relatively large distance between the reservoir and the delivery points (see Supplementary Information).

While the electrical signals that turn on the OEIP can be initiated nearly instantaneously, the time required to stop the epileptiform activity after starting GABA delivery was about 60 s. For some applications, this speed may need to be significantly faster. OEIP dynamics are largely governed by the length that ions much traverse from the source electrolyte to the delivery points. In the present geometry, this length is on the scale of several millimeters. We are thus developing devices with significantly faster turn-on by arranging delivery vertically through a thin CEM film, thereby reducing the effective ion path-length to hundreds of nanometers. Likewise, the pixel dimensions in the device described above were 20x20 μm, with the 32-electrode array spanning several hundred microns. This is already on the approximate scale of single neurons, and local neuronal circuits, respectively. While miniaturization is feasible (though difficult), increasing these dimensions to fit different therapeutic targets is also possible.

Another limitation with the present neural pixel system is that it delivers ions simultaneously at the 32 outlets, where each outlet is co-localized with a sensing electrode. An addressable pixel array, where each sensing/delivery site could be individually controlled,

would thus be a significant improvement. Such a system would make it possible to record from an array of electrodes, and then to selectively turn on the delivery at the sites where, for example, epileptiform activity is recorded. A future device, with individually addressable release sites and colocalized recording electrodes, could also be used as an in vitro tool to precisely quantify the kinetics of specific neurochemical signaling. Furthermore, such individually addressed neural pixels could enable multiple connections to a single neuron, similar to the way biological neurons connect with each other. In this way, the dynamics of multiple neural connections could be studied with unprecedented detail.

The lifetime of our device depends on the electrochemical capacity of the electrodes and the delivery rate required for the application. For an in vitro study like the one above, lasting only hours, electrode capacity is not an issue, especially since consumed electrodes can easily be replaced by fresh, free-standing electrodes dipped into the electrolytes. For an implantable in vivo device, however, electrode capacity is crucial. Larger, or more 3D-structured electrodes and delivery in short pulses would increase the lifetime. Another solution would be to incorporate an ion diode-based current rectifier, so that the electrodes could be electrochemically "recycled", increasing the lifetime substantially (31). Likewise, for in vivo applications, the device could be built on flexible substrates, e.g., parylene-C and wrapped onto a tissue, but additional fabrication issues such as long-term mechanical and lamination stability must also be considered. This is something we have not yet explored, however. For applications deeper inside the tissue or organ of interest, neural pixel systems could be constructed into implantable probes, a technique already demonstrated for basic OEIPs.[78],[155]

The ability to sense electrophysiological signals and deliver neuroactive compounds at the same location represents a first step in constructing closed-loop feedback system, capable of monitoring neuronal activity and adjusting local release of neurotransmitters accordingly. Indeed, the system presented above only requires minor modification to the control software to explore this functionality, and we are currently engaged in these experiments. Such a closed-loop system could be used, for example, in epilepsy treatment, to predict or detect an epileptic seizure at an early stage and intervene by delivering inhibitory neurotransmitters. The feedback system would make it possible to stop seizures with a minimal amount of drugs, since the drug release could be stopped as soon as the inhibitory effect is observed.

2.2.4 Methods

Device fabrication

3x1 inch diameter glass slides were cleaned by sonication in soap/water mixture and acetone/IPA mixture. For patterning gold, a photoresist, S1813 (Shipley), was spin-cast on the glass slide, exposed to UV light using a SUSS MJB4 contact aligner, and developed using MF-26 developer. Titanium and gold (100 nm) were evaporated (Alliance Concept EVA450) and patterned using lift-off in acetone. On top of a layer cast from soap/water solution, a 1.5 μm of parylene C was deposited using an SCS Labcoater 2. A 4m of photoresist, AZ9260 was then patterned and etched (300 W, 50 sccm O_2 , 5 min) using Oxford 80 plus. A solution of 3-glycidoxypropyltrimethoxysilane (GOPS, 5 wt%) in a water:ethanol mixture (1:19) was spin coated to improve the adhesion of the PSSA-co-MA on glass. After 15 min, the substrates were rinsed in ethanol to remove excess GOPS. Then the substrates were baked at 110 °C for 20 min. PSSAcoMA (5 wt% in a water:1propanol mixture, 1:1) was mixed with polyethylene glycol (3 wt%, molecular weight 400 gmol /mol) for crosslinking, and then deposited by spin casting at 2000 rpm to obtain a thickness of 300 nm. The film was baked at 110 °C for 1 h. The sacrificial parylene C layer was peeled off to complete the patterning of PSSA-co-MA. Another layer of parylene-C was deposited, reaching a final thickness of 2 μmm, with the use of an adhesion promoting silane. A soap solution (1 wt% in water) was spun and followed by a subsequent parylene-C deposition (2 μm). Finally, the source/target PEDOT:PSS was patterned with the insulating parylene-C using photolithography and a sacrificial peel-off step. A thick layer of AZ9260 (MicroChemicals) photoresist was cast, baked and exposed using a SUSS MJB4 contact aligner, followed by reactive ion etching in an O_2 plasma (160 W, 50 sccm O_2, 15 min) using an Oxford 80 plus plasma etcher. For the preparation of the PEDOT:PSS films, 19 ml of aqueous dispersion (PH 1000 from H.C. Stark) was mixed with 1 ml of ethylene glycol, 50 μl of dodecyl benzene sulfonic acid and 1 wt % of GOPS, and the resulting dispersion was spincoated at 650 rpm, soft baked at 100°C for 60 s, and spun cast at 650 rpm to attain thicker PEDOT:PSS films. The film is patterned by peel-off of the top parylene C film and subsequently baked at 140 °C for 1 h and were immersed in deionized water to remove any excess low molecular weight compounds. The reservoir chambers, cut from cured polydimethylsiloxane, were affixed to the source (reservoir) and target (bath) areas.

Device characterization

Impedance spectra of the electrodes were measured using an Autolab potentiostat equipped with an FRA module. Commercially available Ag/AgCl and Pt electrodes were used as the

counter and reference electrodes. The applied voltage was 0.01 V and the electrolyte solution was aqueous 0.1 M NaCl(aq). The contacts of the OEIP were connected to a Keithley 2400 source/measure unit, and constant current (1 μA or lower) was sourced and voltage was measured using a customized LabVIEW software. Electrode recordings were obtained using a commercially available voltage recording setup, RHD2000 Evaluation System. As the reference electrode, a grounded Ag/AgCl electrode was immersed into the target electrolyte. The recordings were acquired at 20 kHz sampling rate and analyzed using Matlab (Mathworks)-based software with a low-pass filter of 1 kHz and down-sampled by 500.

Electrical recordings and data acqusition

Electrode recordings were obtained using a commercially available voltage recording setup, RHD2000 Evaluation System (Intan Technologies). A 3D printed sample holder was fabricated, containing gold-coated pins in contact with the 32 gold electrode pads of the device. As the reference electrode, a grounded Ag/AgCl electrode was immersed into the target reservoir containing the brain slice. Recordings were acquired at 20 kHz sampling rate and analyzed using MATLAB (Mathworks)-based software with a low-pass filter of 1 kHz and down-sampled by 500.

Hippocampus preparation

All protocols have been approved by the Institutional Animal Care and Use Committee of INSERM. All experiments were repeated twice on different biological samples. After decapitation of anesthetized mice, brains were rapidly extracted (postnatal day 14 to 18). In a chilled and perfused bath, the brain was cut into the left and right hemisphere, and the complete hippocampus including the septum was extracted from each hemisphere. This preparation maintains the whole 3D hippocampal architecture, preserving cellular and axonal integrity. Freshly-extracted preparations were placed in a chamber and perfused with oxygenated (95% O_2 / 5% CO_2) artificial cerebrospinal fluid (ACSF) (126 mM NaCl, 3.5 mM KCl, 2mM CaCl_g , 1.3 mM MgCl_2 , 1.2mM NaH_2PO_4 , 26.2 mM NaHCO_3 , and 10 mM glucose). They were maintained in the chamber at room temperature and allowed to recover for one hour prior to experimental use. After this period of recovery, preparations were transferred with a pipette to the surface of the integrated sensing/delivery device. The chamber containing the hippocampus was continuously perfused with oxygenated ACSF warmed at 33 °C. Tungsten electrodes (with a tip resistance of 1-3 M) were positioned on top the OEIP outlets/ electrode openings. External electrode recordings were made with a World Precision Instruments DAM80 AC amplifier, and acquired using an analog-to-digital con-

verter (Digidata 1322B, Molecular Devices). Analysis was performed using using Clampfit (Molecular Devices) or Matlab (Mathworks)-based software.

2.2.5 Supplementary Information

On-off switching and leakage in OEIPs

When delivery is switched off (after having been switched on for some time) the ion channel is filled with the cation intended for delivery, i.e., GABA in this case, at a concentration of about 1 M. These ions will be exchanged with other cations in the target solution by diffusion, until a linear concentration gradient from the source side of the channel to the target side of the channel is established. Once this situation is reached, the passive leakage from source to target can be described by Fick's first law of diffusion: $j = -D\frac{dc}{dx}$. Where j is the flux of ions per unit time through the outlet area A, D the diffusion coefficient of the ion, and C the concentration of the ion. For an ion channel of length h, given the concentration is approx. 1 M on the source side of the channel and 0 M on the target side, $\frac{dc}{dx} \approx$ - $\frac{1}{h}$. The flux of the ion caused by diffusion is thus $\approx$ D $\frac{dc}{dx}$.

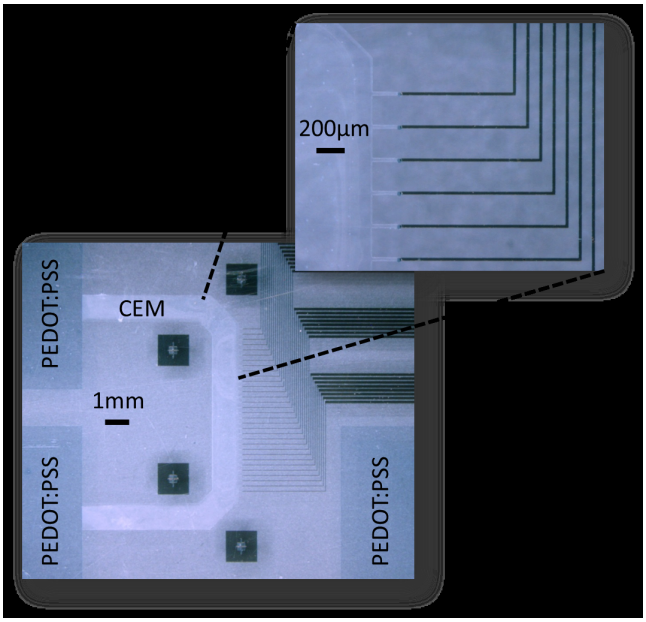

Fig. 2.11 U-shape geometry of the OEIP membrane with its outlets interfacing 32 PEDOT:PSS electrodes and gold interconnects. Also shown is the PEDOT:PSS source and target electrodes of the OEIP.

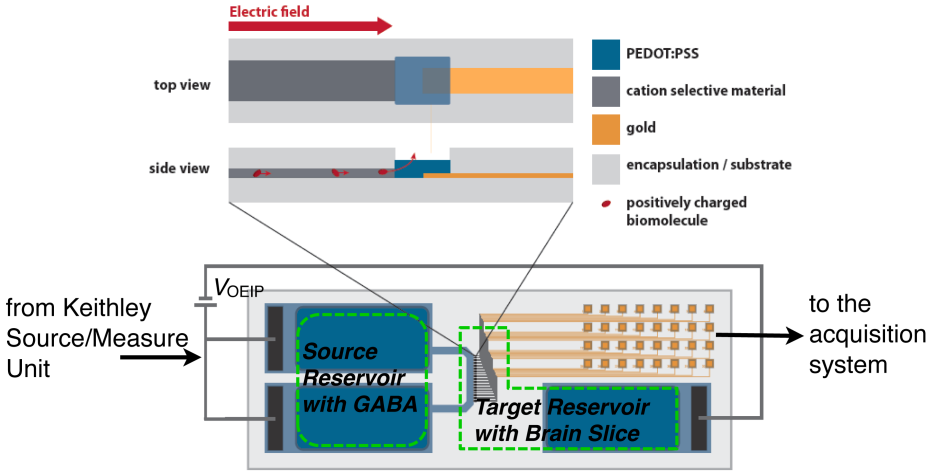

Fig. 2.12 Basic measurement circuit and regions of source and target reservoir wells. The reservoir wells, cut from cured polydimethylsiloxane (PDMS), were affixed to the specific source (reservoir) and target (bath) areas as shown in the figure with green dashed lines.

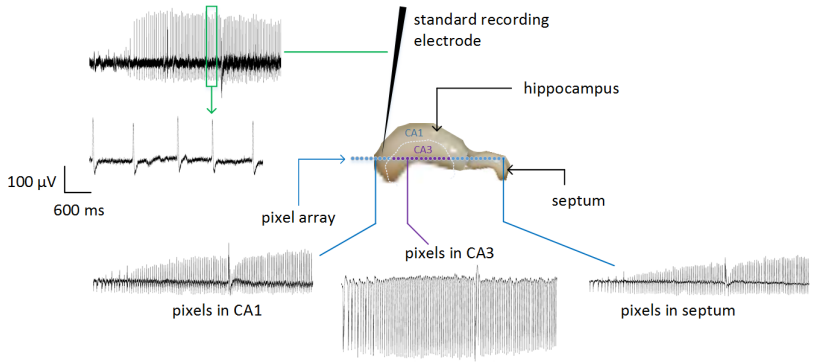

Fig. 2.13 Epileptiform activity is measured by multiple PEDOT:PSS electrodes with a signal to noise ratio comparable to a externally placed tungsten electrode. The standard tungsten electrode was placed in the stratum oriens, just above the stratum pyramidale (the so-called cell layer). This is the typical placement of this type of standard electrode for measuring the activity of a pyramidal neuron extracellularly.

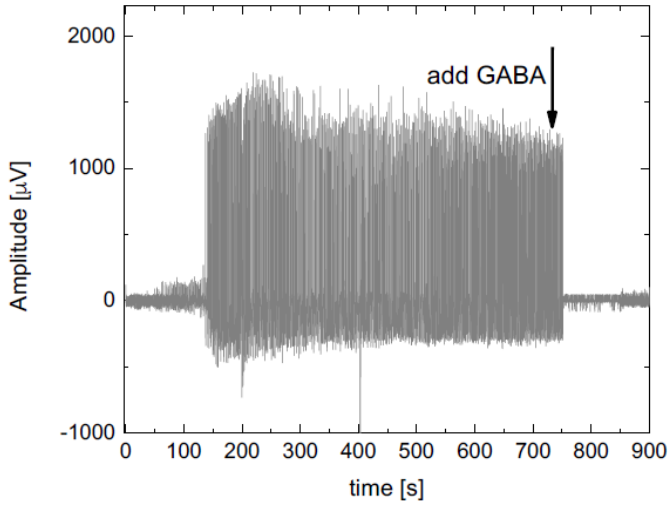

Fig. 2.14 Effect of GABA (250 μM in the bath) injected directly on top of the complete mouse hippocampal preparation exhibiting epileptiform activity, captured by a PEDOT:PSS electrode. Effect of GABA (250 μM in the bath) injected directly on top of the complete mouse

Chapter 3

In Vivo Ion Pumps

3.1 Introduction

Despite the growing efforts in neuroscience, neurological disorders still represent one of the major health concerns worldwide ranging from emotional disorders, such as clinical depression, to movement disorders, such as Parkinson disease. Neurological disorders are estimated to strike millions of people each year, accounting for an annual economic cost of hundreds of millions of dollars due to not only the direct expenses such as hospitalization and prolonged care but also indirect ones caused by the subsequent productivity losses.[1],[56] Treatment of neurological disoders is mainly limited by the method of administration of the pharmaceutically active compounds to their target sites of action inside the body. Most common way is the oral or intravascular introduction, which is particularly challenging as drug molecules are evenly distributed within the body diluting the initial concentration remarkably and their delivery to the brain is often precluded by a variety of physiological and metabolic obstacles such as blood brain barrier (BBB).[104],[59],[149] Increasing the drug dosage can show detrimental effects on organs and healthy tissues that are not involved in the pathological process.[169] With oral/intravascular delivery, the drug release is neither local, nor a desired level of drug at the target area over time can be maintained. It is, therefore, an ongoing focus for the pharmaceutical research to develop novel administration strategies for efficient delivery of drugs to the central nervous system. Strategies that can tackle these challenges are at utmost importance and will have significant clinical implications to provide effective human applications.

Significant amount of research has been made in neurosurgical invasive procedures to deliver therapeutic substances into the brain. The earlier efforts for localized drug delivery systems include convection-enhanced delivery (CED) systems, which are based on drug infusion under high pressure using a intracranial needle or catheter.[16] Direct infusion of the

drug to the target site allows bypassing the BBB and obtaining high local concentrations without side effects that would otherwise have to be introduced by systemic delivery at high toxic levels.[17],[98] Integration of CED into microfluidic systems, with their capability of automated and on demand transport of small liquid quantities, have emerged as a promising platform for designing drug delivery systems.[129],[130],[82] They are maintained to be advanced tools for in vitro interfacing with cells and their application in soft, flexible substrates such as PDMS and parylene C paves the way for their applications in vivo studies by offering improved neural coupling.[55],[46],[117] However, fluid is delivered along with the compound comes with the risk of distorting the biological environment by increasing local pressure inside the brain in the small compartment the device was implanted. Induced shear stress might alter the biochemical properties of the adjacent neural network causing undesired effects.[161] In addition, obtaining good switching capabilities and avoiding backflow requires insertion of valves and actuators, which complicates the device structure and fabrication remarkably.[29]

To avoid such issues, ion pumps based on conductive polymers are promising candiates as they offer precise electrical control over the delivery of ionic molecules, e.g., drugs. The idea employs PEDOT:PSS, the champion material at the bionic interface due to its mixed ionic and electrical conductivity, high biocompatibility and chemical stability.[174],[155] When PEDOT:PSS is overoxidized, either by using chemical agents or exposing the film to high oxidation potentials, the pi-pi conjugation breaks down, leading to a polymer that can conduct only ionic charges, but not electronic ones. [165] Such a film can then act as a "bridge" that physically connects two electrolytes, one being the reservoir for the ions of interest and the other being the target where the ions should be delivered. Under an electrical field, the ions in the reservoir are pumped towards the target area over the over-oxidized PEDOT:PSS bridge. To run an ionic current through the ionic bridge, two electrodes that can convert an electronic current into an ionic current are used. PEDOT:PSS electrodes are typically used as source electrode located in the source reservoir area, and as target electrode correspondingly. This concept was extensively tested in vitro by stimulating neural tissue by the delivery of chemical compounds, in addition it was reported as a therapeutic tool in vivo studies for its on-off switching capabilities, controlled amount of delivery and lack of fluid flow.[66],[78],[65] The design of an efficient implantable ion pump, however, stands as a challenge. The distance charged molecules has to travel is decided by the length of the ionic bridge (overoxidized PEDOT:PSS), which is to be kept long since the reservoir cannot be implanted directly to the brain, as an electrolyte. This led to very slow devices that could start the ion delivery only a certain time after the device is electrically switched ON. Moreover, a long ionic bridge comes along with a higher ionic resistance that needs

to be overcome. This implies a higher operation bias which introduces electrolysis and subsequent ions that are delivered to the target in addition to/instead of the actual ions of interest.

Application of drug delivery devices should be accompanied by recording systems to obtain a direct measure of the effect of the release as well as detecting any irregularities in the neural activity for subsequent manipulation upon pumping. Microelectrode array (MEA) technology is a great candidate for such purposes as the high-density electrodes allow for high-spatial resolution. Conductive polymer coatings of traditional metal electrodes, for having ionic and electrical conductivity and biocompatibility to avoid the mismatch with the soft tissue, improve the recording abilities of these microelectrodes remarkably. High ion uptake and transport within of conductive polymers increase the effective physical "volume" of the recording site by orders of magnitudes.[35],[37] Therefore, the actual size of the electrode can be scaled down with no performance loss enabling the design of densely packed sets of electrodes with high spatial resolution. Such MEAs were reported to exhibit excellent signal-to-noise characteristics when used to record in vivo neural activity spanning from LFPs to action potentials. [85],[83]

Here, we report an ion pump implemented in to an ECOG platform implanted on the surface of the cortex for superficial release of drugs. This device brings the organic ion pump technology to a step further by overcoming the challenges associated with the electrophoretic delviery of ions. Our design borrows the best ideas from the two popular drug delivery concepts: ion pump and microfluidics. The device contains a microfluidic channel that replaces the overoxidized PEDOT:PSS bridge to a large extent. This channel is filled with the fluid which contains the ions to be delivered, overcoming the problem of the placement of the reservoir. The channel is vertically sealed with a thick film of PEDOT:PSS which then allows for the electrophoretic delivery of only solvated ions. PEDOT:PSS at the vertical interface of the fluidic channel with the target area, i.e., the brain, blocks the diffusion of ions, as well as delivery of fluid. Therefore, the ion delivery happens only when a bias is applied between the electrode that is integrated with the device (under the microfluidic channel) and the one that is placed externally in the target area. Furthermore, this device contains PEDOT:PSS based MEAs located around the delivery sites, enabling a feedback regulated delivery system.

3.2 Design and The Fabrication Process

We characterized our devices by evaluating the efficiency of gamma-amino butyric acid (GABA) delivery. Once validated as such in vitro, the same device was used to deliver

potassium (K+) to induce epileptic form activity in rats. Both GABA and K+ can be electrophoretically transported through the negatively charged ion bridge (PEDOT0PSS-) for being positively charged. GABA is an inhibitory neurotransmitter, which suppresses the activity of the neurons it contacts, reducing the probability of firing. Extracellular increase of K+ on the other hand, induces hyper excitability of the neurons. Therefore, it offers a good validation path for observing an increase in the activity on a silent background.

The fabrication is as depicted in the figure 3.1. The microfluidic channel was made of Parylene C and the bottom and the top parts were fabricated separately. For the bottom part of the fluidic channel, gold is patterned on to a 3 um parylene C coated glass substrate using photolithography and lift-off. Subsequently using peel off technique, the PEDOT:PSS was patterned on to the gold. For the top layer, gold was patterned similarly and sandwiched between two parylene C layers. Contacts for the gold electrodes, target electrode and the ion release site were coated with PEDOT:PSS by using peel off method at one single step. Both films were peeled from the glass and stuck together by a 50 um laser cut medical grade tape. Prior to sticking the top part was placed on the glass substrate upside down and the release site was chemically bleached.

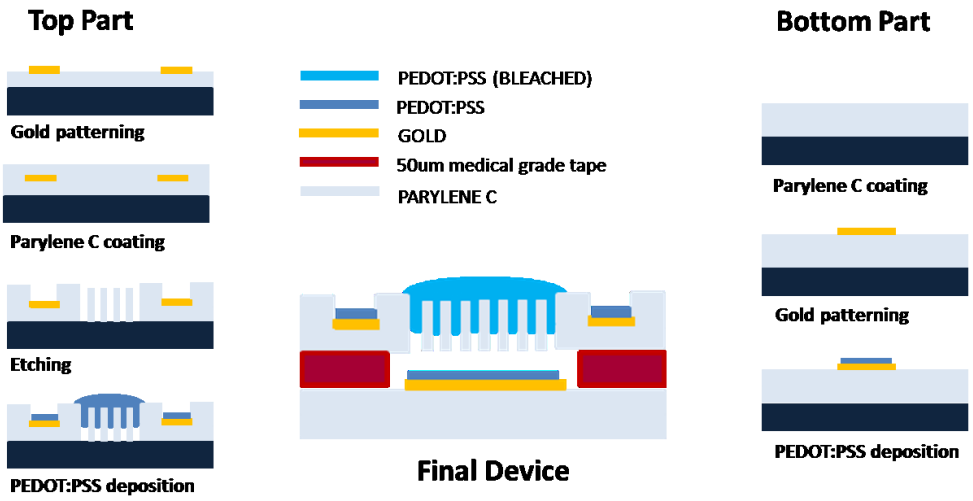

Fig. 3.1 (a) Cross-section schematics showing the photolithographic fabrication process. Gold lines and PEDOT:PSS were patterned using photolithography. Top and bottom parts of the device were fabricated separately and stuck together by a laser cut tape.

The fluidic part of device structure consists of an inlet and outlet interconnected by a parylene C microfluidic channel. The electrolyte is mechanically pumped from the inlet towards outlet to be able to bring the charged molecules as close as possible to the release site. Continuous fluidic channel is essential to avoid bubble formation inside. The area, lying underneath the fluidic channel in contact with the fluid, is completely coated with

gold and PEDOT:PSS and envisaged as the source electrode. In the active area, where the device couples with the tissue, parylene film is etched to have openings as the release sites. The openings consist of 300 holes, each one having 10 μm diameter and fully coated with over oxidized PEDOT:PSS on top. Placing small holes with a big spacing in between allows continuous film deposition, preventing the film to crack and collapse inside the channel. On the active area surrounding the fluidic outlet, there is a set of 15 μm diameter electrodes alternating with a 100 μm spacing. The outer space is PEDOT:PSS coated gold with a surface area of $2\mu m^2$, to be used as the target electrode. (figure 3.2a)

The device operates as follows. The electrolyte including the charged molecule of interest, is filled inside the entire fluidic channel. Upon application of a bias between the source and target electrode, the molecules are driven vertically within the microfluidic channel and drift through the polymer seal towards the target area. For each ion released in the target, the target electrode acquires a random ion from its proximity and therefore gets reduced. Similarly, source electrode gets oxidized as cations are pushed towards the target electrode and this half electrochemical reaction at the electrodes continue until they are completely consumed.

3.3 Results

Using a programmable syringe pump, we first fill in the microfluidic channel with the aqueous GABA solution (0.05M). The target area contains 0.15 M PBS solution, representative of the biological media. Owing to the thin polymeric seal (3 μm in comparison to 1 cm that is typically used in previous designs), the drug delivery starts instantaneously. Moreover the applied potential under only a bias of 0.5V. This value is typically around 10 V for the traditional ion pumps. The profile is completely dominated by the capacitive effect of the source and target electrodes as shown in figure 3.3a. Due to its small surface area, the planar target electrode is consumed within seconds, indicated by the saturated current. After 15 seconds of a voltage of 0.5V applied through the microfluidic, the amount of GABA delivered to the target area is 0.12 nmol. To the best of our knowledge, organic electronic ion pumps could only deliver this much of ions only when they are operated with an order of magnitude higher voltage applied for a longer period. Improving the delivery period, is, however, possible by changing the size of the target electrode. For this purpose we used a stainless steel screw as an external target, which is used as reference for recordings with electrodes in vivo. The screw, coated with PEDOT:PSS, increased the pumping efficiency remarkably, i.e. 1.19 nmol under the same conditions, due to enhanced area of the target electrode. (figure 3.3b) In order to increase the device lifetime, we also employed voltage pulses rather than

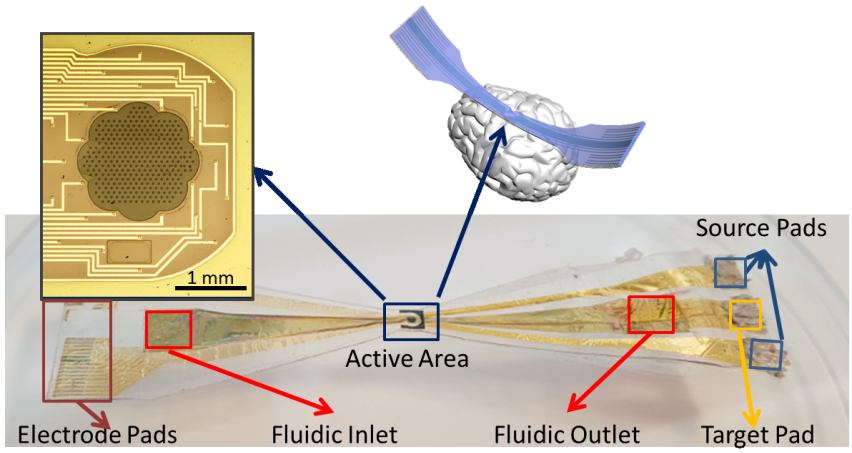

(a)

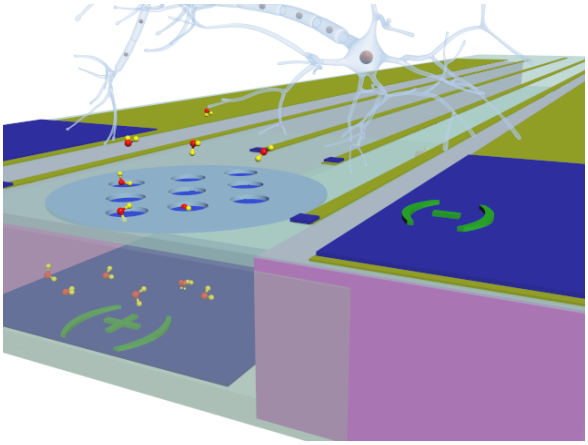

(b)

Fig. 3.2 (a) The fluid is filled by the inlet and outlet of the fluidic channel. The pads for source and target electrodes and for recording electrodes are on two different sides of the device. The device is placed U shape on to the brain as the active area is in the center. The active area of the ECoG array consists of 300 x 10um diameter holes as release site, 32 x 15 um PEDOT:PSS electrodes and the target electrode surrounding them. (b) The operation of the device is achieved upon application of an bias between the source electrode inside the channel and the target electrode.

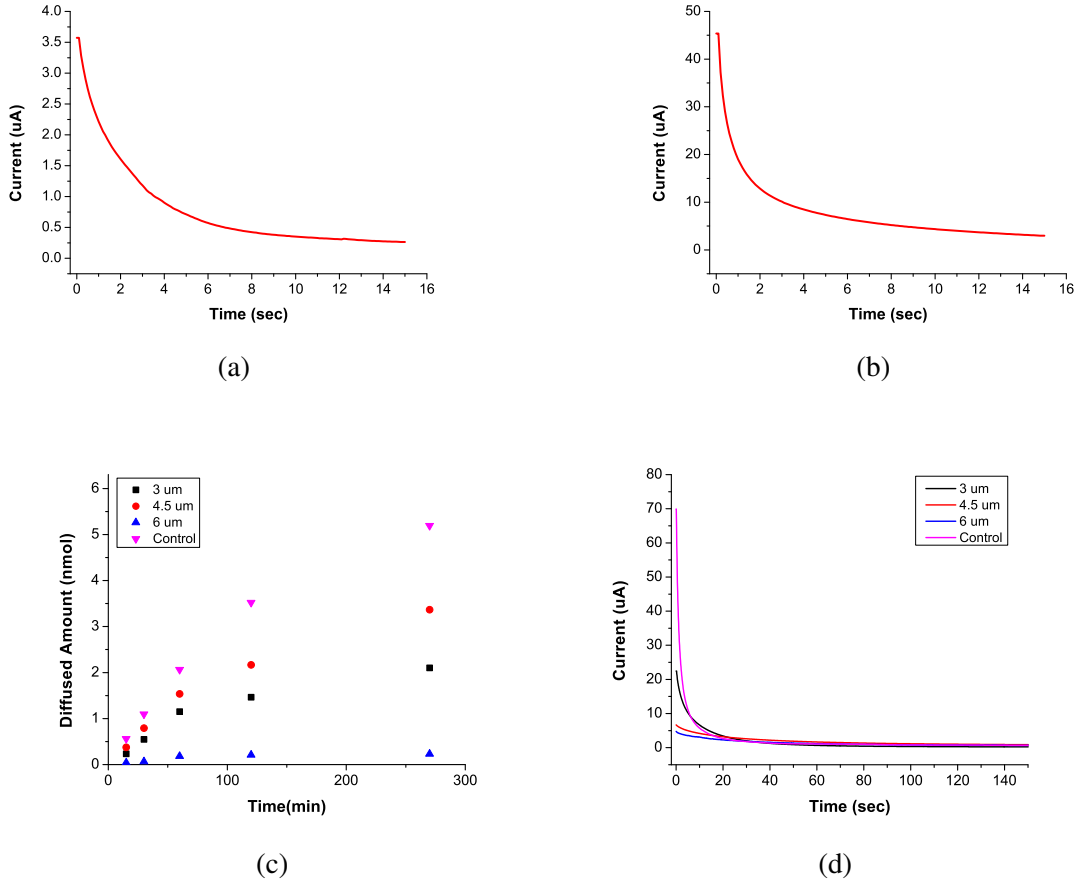

Fig. 3.3 a) and b) Ionic current flowing through the ion pump for an applied voltage of 0.5 V for different target electrodes. c) The diffusson curves of GABA through PEDOT:PSS as a function of time. d) Current-time curves for active pumping.

constant biasing. As oxidation/reduction of PEDOT:PSS film in completely reversible, a long lasting and steady delivery could be achieved via short pulses.

While improving the delivery efficiency by using a microfluidic channel and a thin vertical polymer seal at the interface with the target area, we are challenged with the problem of uncontrolled delivery. Since polymer seal is only a few micrometers, the diffusion is expected to be more of a challenge compared to traditional OEIPs. Therefore, we also designed an experiment to determine whether the collected amount of ions in the target area is partly due to the passive transport- that is diffusion through the polymer. We fabricated devices consisting of only 16 holes and no electrodes to simplify the fabrication steps. The diffusion of GABA molecules was quantified using a commercially available GABA kit relying on ELISA principle (supp info). As polymer thickness is expected to govern the ease of ions to diffuse towards the target site, we prepared devices that contained overoxidized PEDOT:PSS outlets of different thicknesses. We filled the microfluidic channels with an aquoeus GABA solution (0.05M) while the target area contained a constant volume of DI water. Aliquots of sample from the target area was collected over time and analyzed with the kit. As such, we quantified the amount of GABA molecules that were transported to the target area via diffusion for a set of polymer thickness. Figure 3.3c shows that as the polymer thicknesses increases, there is less GABA in the target area. We took the SEM images of each film at the end of the measurement and observed the thinner films to have cracks on the surface.(Figure **??**) Such cracks supplies a diffusion path for the molecules, thus increase the off current. We could obtain the least diffusion, accordingly crack-free and softer PEDOT:PSS films above 4 μm of thickness. Same devices were tested for active pumping of GABA by employing a PEDOT:PSS/gold coated polyimide film as target electrode with a surface area of 4x4 μm_2. The pumped amount was measured and the ratio between the on state and off state of the pump for the same time domain was calculated to be around 250, proving that the thick coating supplies a good barrier for ion diffusion, while not disrupting the active delivery upon biasing for the ionic diffusion.

In our previous in vitro OEIPs, we used a PSS based copolymer as the ion bridge. This device was used to deliver a high concentration of GABA (under an applied bias of 20 V) that could control locally hippocampal networks.(Chapter 2) However, for such designs the current obtained upon application of a bias does not completely correspond to the delivered amount at the target area. The trapped charges inside the long polymeric chain as well as the induced protons due to high applied potential, can travel in effect of the bias, thus reducing the efficiency. In order to correlate the current values that are recorded during biasing with the actual number of GABA ions that are collected in the target area, we operated our device for 150 seconds and quantified the delivered amount using the GABA kit. The current that

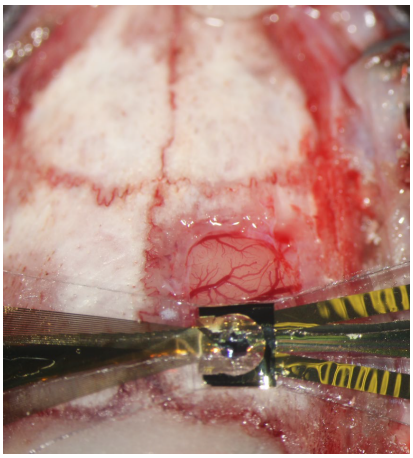

(a)

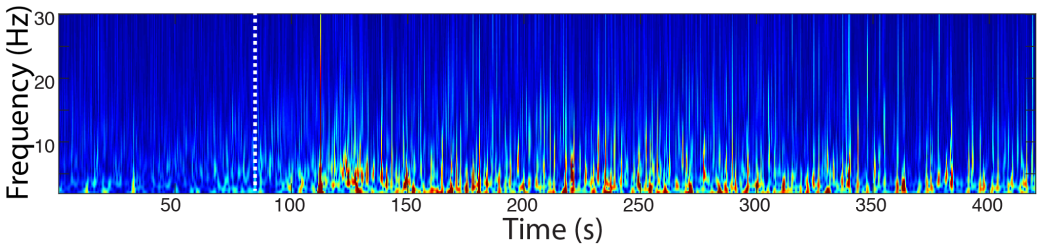

(b)

Fig. 3.4 a)In Vivo implantation of the ECoG ion pumps. b)Intensity of spiking activity over time.

is integrated over time gives us an estimation of the GABA molecules that are delivered-for each cation delivered, one electron is extracted. This value is 2.17 nmol, in contrast to 1.98 nmol obtained via the chemical analysis. Here, the diffusion within 150 seconds is negligible (see Figure 3.3c). Overall, the efficiency of GABA delivery is over 90 %. (Fig. 3.3d)

Electrodes were characterized using the electrochemical impedance spectra as described in the Experimental Section. Impedance at 1 kHz , being the benchmark for the characterization of neural electrodes, as this frequency corresponds to recording spiking activity, was measured to be 10 kOhm. (Figure 3.6)

To test the feasibility of this concept, we used the as the in vivo experimental platform, the design is tested in rats. A small craniotomy (3x3 mm) was performed over the cortex and the device was laid over the surface of the brain with the help of a brush. A reference tungsten was implanted next to the active area of ECoG array to be able to monitor the activity in deeper regions. (Fig. 3.4a)

The tungsten reference was initially set to record the background activity indicating a low/zero epileptic form activity. After the activation of the pump shown by the dashed line, the spikes emerged as a result of K+ increase. The activity starts only in matter of seconds proving the capabilities of the design.(Fig. 3.4b)

3.4 Conclusion

The approach presented here fulfills several important, previously unachievable requirements for drug delivery systems. The device can convert electrical signals into a precise ionic current with an efficiency order of magnitude higher than the existing studies. Low voltage requirements of the system , owing to the thin membrane, offers it a a promising tool for applications in vivo. The PEDOT:PSS sealing supplies minimizes he off current of the system. Moreover, the OEIP can be processed using standard photolithography and printing techniques that are easily integrated with other organic or inorganic solid-state systems. Taken together, these developments represent a significant step forwards in biology&technology interfacing, and promise to pioneer further symbiosis of electronics and living systems.

3.5 Experimental

3.5.1 Device Fabrication

Glass sides with dimensions of 1x3 inch are cleaned upon sonication in first 2 % water soap solution and then in acetone. The cleaned substrates were deposited with a 1.7 um parylene C film using a SCS Labcoater 2. For top part, S1813 (Shipley) photoresist was spincoated on the film and exposed to UV light SUSS MJB4 contact aligner, using the mask required for gold patterning. MF-26 developer is employed for development. The samples are evaporated with first a 10nm layer of chromium for adhesion and 100 nm of gold by Alliance Concept EVA450 and subsequently patterned by a lift off process in acetone. A second parylene C was coated using silane as adhesion promoter. The films were coated with photoresist AZ9260, exposed and developed using MF26A followed by reactive ion etching by an Oxford 80 plus plasma etcher to obtain the outline of the probe. Another layer of parylene C deposited using 2 % soap solution to minimize the adhesion. The samples were again coated with AZ9260, exposed and delevoped. Subsequent to the etching and aqueous dispersion of PEDOT:PSS (PH 1000 from H.C. Stark) was mixed with 5 % of ethylene glycol, 1 % dodecyl benzene sulfonic acid and 1 wt % of GOPS, was spincoated on

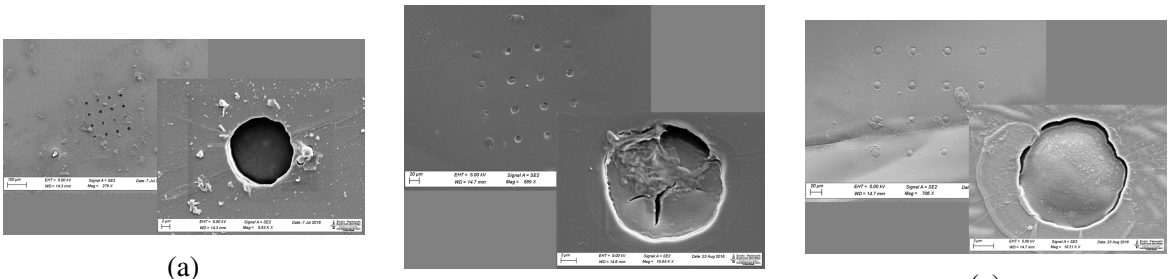

(a) (b) (c)

Fig. 3.5 SEM images of the devices. a) control b) thick film (5 um) c) thin film (3 um)

the substrates 7 times with a 1 minute step of soft baking in between at 110 degrees. Finally the sacrificial layer of parylene C was peeled of to complete the patterning of PEDOT:PSS. For the bottom layer, a second layer of parylene C was coated on the first one with silane. Gold and PEDOT:PSS patterning on top of the 3 um film of parylene C was achieved using the same methods as the top part.

3.5.2 Device Characterization

Impedance spectra of the electrodes were measured using an Autolab potentiostat equipped with an FRA module. As counter and reference electrodes commercially available Ag/AgCl and Pt electrodes were employed inside a 0.1 M NaCl solution. The characterization of ion pumps were done by using a keithley 2000 source measuring unit and a customized Labview software. The current was measured by applying 0.5 V constant bias as a function of time.

3.6 Supplementary Information

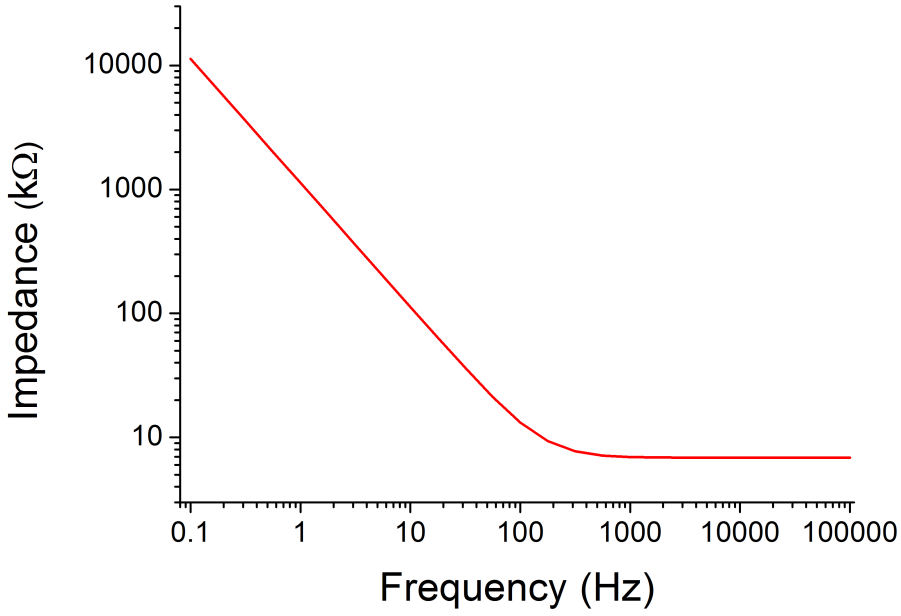

Fig. 3.6 Impedance spectra of the electrodes.

Chapter 4

Minimally Invasive Recordings of Brain Activity using Organic Transistors

4.1 Introduction

Over the past decades, recordings of the neural activity from the surface of the brain [i.e., electrocorticography (ECoG)] have become recognized as a promising platform to conduct the basic neuroscientific investigations.[148] ECoG approach, compared to non-invasive systems such as Electroencephalography (EEG), has advantageous characteristics such as high spatial resolution, more resistance to noise, high fidelity and broader frequency band, making it suitable for applications in neuroscience.[147] Important data carrying information about the states of the brain is coded in different time or frequency domain components and their interactions. Capturing sufficient amounts of that information requires an high density array of electrodes placed on the brain. Abilities to extract this data has strong clinical implications. Examples include treatment of neurological disorders and studies on brain machine interfaces. Surgical treatment of epilepsy requires the epileptogenic zone to be removed or disconnected, which is the area of the cortex responsible of initiation of seizures. The success of the operation is highly dependent on accurate identification of the epileptogenic zone.[62] Due to its high spatial and temporal resolution ECoG arrays are widely employed for such purposes. In addition ECoG based brain-machine interfaces are reported as promising tools for neuroprostetic studies. ECoG systems can record high frequency (i.e. gamma) activity offering movement related information, which is absent in EEG. [137],[32]

The invasivity of the recording system directly relates the quality of recordings from the adjacent site. Motivated by that, initial devices for neural recordings and stimulation were based on an array of sharpened metallic electrodes which were designed to penetrate inside the brain. They were shown to provide an high resolution recording and

were effectively used for BMI studies in humans.[62],[24] One major issue for in vivo interfacing of neurons with invasive metal electrodes is the foreign body response upon implantation.[125],[173],[45] In addition to neural loss, inflammatory response leads to glial scarring around the implanted electrodes which may act as an insulating layer between electrogenic cells and the electronics. This challenges the maintenance of an effective neural interface, ultimately prevents the communication of the electronics with the target neurons, and gradually limits the function of the device, especially for chronic applications.[10] In most cases, the devices lose their ability to record neural activity or require higher stimulation currents to trigger neural response. [6],[20] While the insertion injury cannot be fully eliminated, the biological response to the device should be kept minimal for electrically vital devices.

Highly flexible arrays of subdural electrodes have unique advantages over penetrating microelectrode arrays in that they are able to maintain signal quality over extended periods of time with minimized irritation and injury to brain tissues. Owing to usage of highly conformal materials, the array can conform onto a curvilinear surface of the brain, thus providing an advanced coupling.[177] When it comes to interface the nervous system, conducting polymer coatings have the potential to provide superior performance in comparison to conventional metals.[184], [53] These materials allow for a more seamless coupling between electronic devices and living organisms due to a unique set of features.[54] In addition to biological compatibility, the inherently soft and flexible nature of polymers dampens the mechanical mismatch with the soft tissue, and therefore elicits a minimal foreign body response.[190] The ability of the material to transport both ionic and electronic charges, on the other hand, leads to low impedance electrodes. This allows not only for efficient transduction of signals of biological origin, but also enables a reduced implant size with a denser array of recording sites, leading to less tissue damage. In fact, compared to metal electrodes of the same geometry, conducting polymer electrodes have been shown to be able to record in vivo signals from rat cortical neurons more efficiently and for a longer time. Moreover, conducting polymer electrodes can counteract the tissue damage upon implantation. They can be incorporated with anti-inflammatory agents or 2 neurotrophins through synthetic efforts or surface functionalization techniques, which aids better neural interfacing. Poly(3,4-ethylenedioxythiophene) doped with poly(styrene sulfonate) (PEDOT:PSS) is considered to be one of the most promising conducting polymer candidate for neural interfacing. PEDOT maintains its electrical and chemical stability in an oxygenated, hydrated, i.e., in vivo-like environment.[54],[37] As an assembly of a polyanion and conjugated polymer, the material supports transport of ions in addition to electronic charges, which has led to novel concepts for bioelectronic devices.

Electrocorticography (ECoG) technique generally involves a surgical operation that removes the meninges, the fluid-filled sac which surrounds the brain and provides both a protective cushion and a means of waste removal. The two outermost layers of the meninges, i.e. the dura mater and the arachnoid, follow the inside of the skull and are separated from the third layer, the pia mater,by continuously flowing cerebrospinal fluid. Rupturing these layers of the meninges during implantation can have extraordinarily detrimental effects to the patient such as inflammation and possible infection. Considering such practical challenges associated with the implantation of these electrodes on the cortical surface, we aimed a less invasive approach relying on high performance of PEDOT:PSS devices by placing the arrays on top of the duramater (outermost layer of the meninges).

4.2 Design and The Fabrication Process

The fabrication process of the ECoG arrays are depicted in figure 4.1. A 1.5 μm parylene C film is used as the substrate to fabricate the array on which is coated on to a glass slide. The gold lines (150 nm) are patterned on the parylene C film by a standard lift-off process and insulated by a second 1.5 μm parylene C film. The extra parylene around the array is etched to define the outline of the probe. A final sacrificial layer of parylene C is coated on and small holes are etched selectively on the film for PEDOT:PSS deposition to define the structure of electrodes. Finally, a 200 nm layer of PEDOT:PSS is coated and the sacrificial layer of parylene C is peeled, to achieve the patterning of PEDOT:PSS.

The process described above yielded electrode arrays with a total thickness of 3 μm, with the Au interconnects and the PEDOT:PSS located at the neutral mechanical plane. The layout of an array is shown in Figure 4.2a. The arrays had a hole in the middle (through the parylene film), in order to allow the simultaneous insertion of a silicon probe (see below). Two sets of 32 electrodes each were placed on either side of this hole. Each set consisted of two subsets of 16 electrodes each, placed on a hexagonal lattice, with individual electrodes having an area of 20 μm $\times$ 20 μm and a center-to-center distance of 60 μm. This particular design provides a fi ne surface map of the electrical activity of a brain region of interest, while at the same time it allows depth-recordings from a silicon probe to be performed. Owing to the good mechanical properties of parylene C, array can be spread on a place i.e. on the surface of a brain easily with the help of a brush and can gold pads can be connected to the electronics by clipping with a zero insertion force socket.

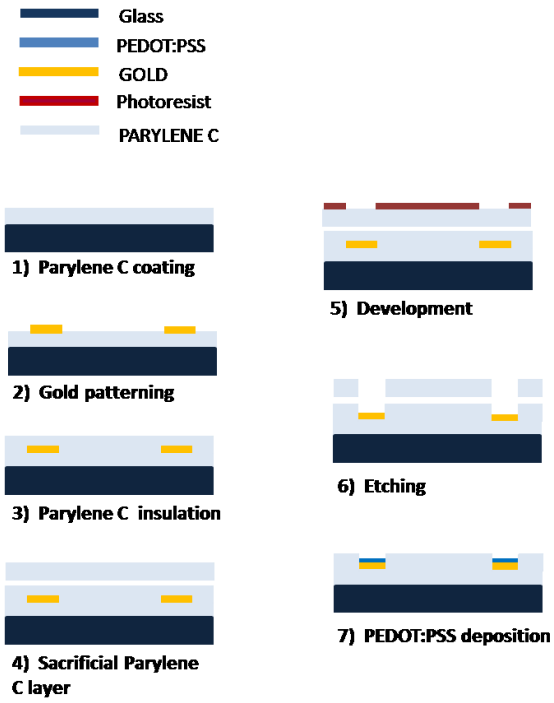

Fig. 4.1 Fabrication steps of the conformable PEDOT:PSS based ECoG array.

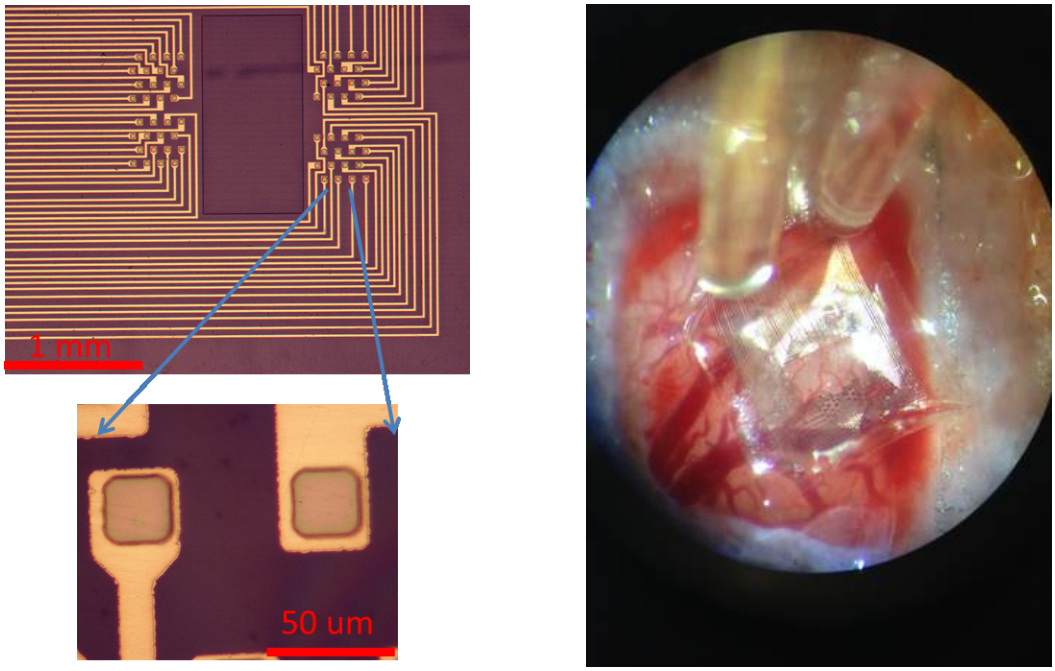

(a) (b)

Fig. 4.2 (a) The layout of the PEDOT:PSS electrode arrays consisting of 32 electrodes. (b) The array placed on the small craniotomy over the somatosensory cortex of an anesthetized rat.

4.3 Results

In vivo validation of the PEDOT:PSS ECoG array

For validation of the PEDOT:PSS array in vivo and prove that it can record signals of biological origin, the following experiment was performed. The Wistar Han rats (400-500g) were deeply anesthetized with Urethane 25% (1,25g/kg IP) and a mixture of Ketamine-Xylazine (50mg/kg and 5 mg/kg IM respectively). The physiological constants were monitored and kept constant during all the experiment. Once on the stereotaxic frame, a 3x3mm craniotomy was performed above the somatosensory cortex and the brain was exposed. The ECoG devices and the control tungsten electrode were placed subduraly in a close distance to each other. The signals from both devices were simultaneously acquired and sampled at a 32kHz rate by a DigitalLynx recording system (Neuralynx). At the end of the recording session, the animals were euthanized by injecting a lethal dose of Pentobarbital Na (200 mg/kg IP). The Tungsten electrode being a standard device to collect the neurophysiological activity, it was chosen as a control device to estimate the recording quality of the PEDOT:PSS device. (Figure 4.2.)

The data collected by both devices showed the same slow oscillations (1Hz) activity. The slow waves recorded by the PEDOT:PSS passive ECoG device were of similar amplitude (481.17 ± 52.43 mV) as compared to the Tungsten electrode (461.13 ± 51.73 mV). The baseline activities did not differ between both signals (std baseline tungsten = 13.42 mV ; std baseline PEDOT:PSS = 14.35 mV). (Figure 4.3a)

We computed the power spectra of both signals. The spectra were again very similar (same peak in the 1-2 Hz range, indicating the presence of the slow oscillations, and a 10 Hz peak characteristic of the somatosensory cortex in this state of anesthesia) and displayed high values of coherence (i.e. similitude of the spectra), indicating that both devices recorded with the same spectral definition the ongoing activity. Unlike in the epidural condition, the PEDOT:PSS spectrum was not different from the Tungsten signal spectrum over all the frequency range (mean power PEDOT:PSS = 10.48 ± 4.03 dB; Tungsten = 9.71 ± 4.04 dB), showing here no significant improvement by the PEDOT:PSS device. Finally, the SNR for the PEDOT:PSS passive device was not significantly different from the Tungsten device SNR (Tungsten SNR = 2.41; PEDOT:PSS SNR = 2.60). Altogether, the ECoG PEDOT:PSS passive device showed identical recordings abilities as compared to a classical ECoG electrode when the signal is collected directly at the surface of the brain. (Figure 4.3b)

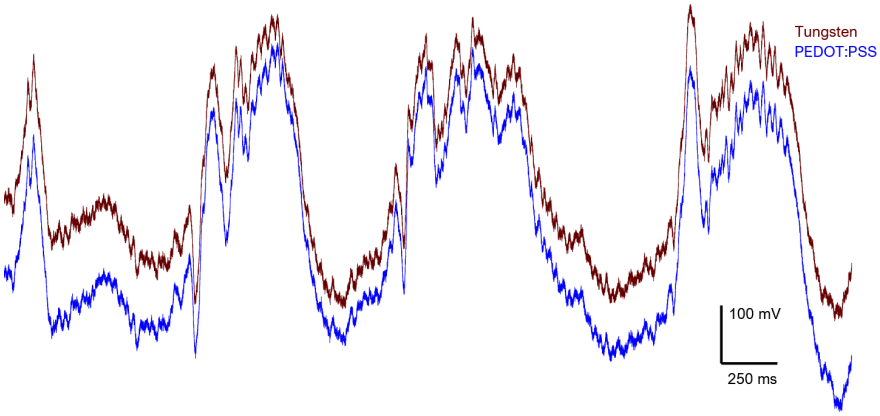

(a)

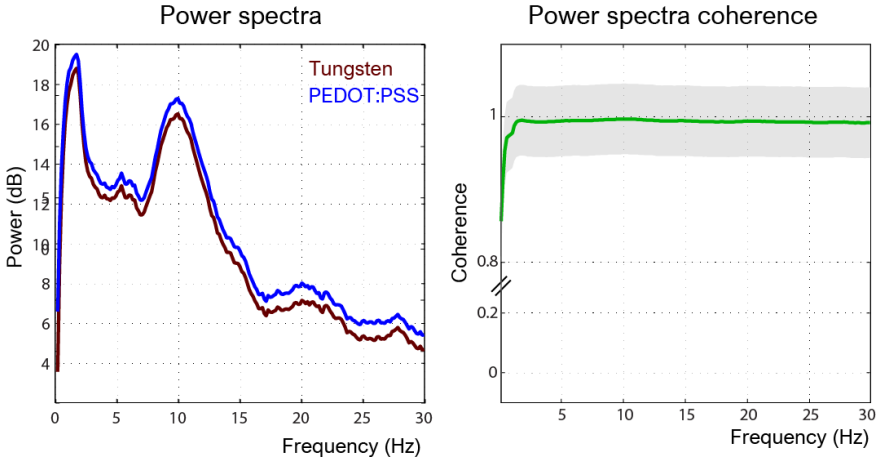

(b)

Fig. 4.3 (a) SWS recordings using subdural PEDOT:PSS electrode arrays. (b) Power spectra of the recordings.

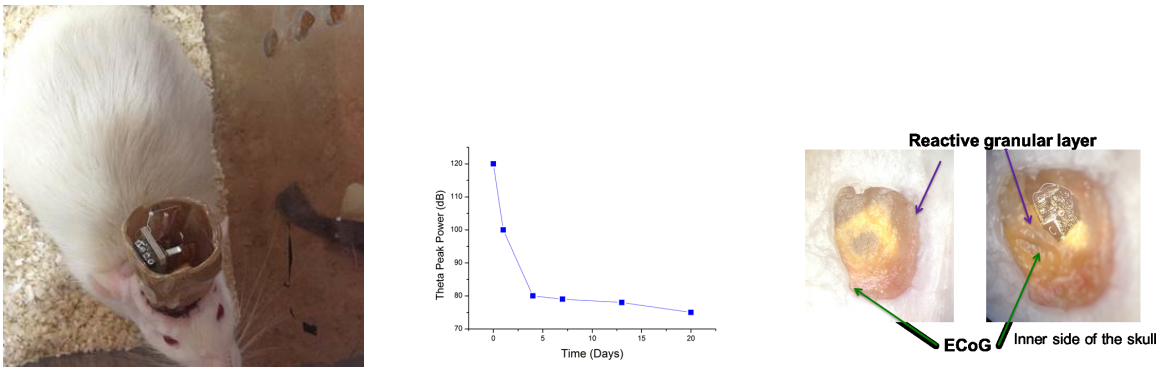

(a) (b) (c)

Fig. 4.4 a) The chronic implantation of PEDOT:PSS based electrode arrays in vivo. b) Quality of recording over time. (ac) Histogram of the rat brain 3 weeks after implantation showing the inflommatory tissue growth.

Subdural chronic recordings

The ultimate aim of the study is to employ the system for research for diagnosis of neurological problems or BMI. All the possible applications require the chronic implantation of such arrays. To further explore the of the capabilites of the approach, we recorded quiet immobility activity in a freely-moving rat. Briefly, a Wistar Han male rat was anesthetized, and a craniotomy was performed over the somato-sensory cortex. The recording grid (see Figure **??**a) was gently laid subsequent to the removal of dura mater. The device was then recovered with a silicon-based artificial dura and dental cement. The grid was connected to a ZIF/Omnetics connector and fixed inside a rigid hat anchored on the head of the animal. The hat was built out of a copper mesh, we acts as a faraday cage during recordings. The animal was allowed to recover during one week before recordings were performed. The signal was recorded while the animal was awake and immobile in its homecage. The quality of signal showed a major decrease in a matter of 3 days described by the decrease in theta power density in figure **??**b. Histology was performed 20 days after the implantation showed an 1 mm inflammatory tissue growth. This caused the array to lose the contact with the area of recordings, thus the ability to record the brain activity. (Figure **??**c)

Epidural acute recordings with PEDOT:PSS electrodes

Considering such practical challenges associated with the implantation of these electrodes on the cortical surface, we aimed a less invasive approach relying on high performance of

PEDOT:PSS devices by placing the arrays on top of the duramater (outermost layer of the meninges). Such an approach prevents in the inflammation response of the body, as the surgery does not breach the duramater. Moreover, the surgery for placing the ECoG array causes the neurons on the upper layers of the brain at the vicinity of the surgery zone to die. Cortex consists of layers each one containing a characteristic distribution of neuronal cell types and connections with other cortical and subcortical regions.

- Layer I, the molecular layer, contains few scattered neurons and consists mainly of extensions of apical dendritic tufts of pyramidal neurons and horizontally oriented axons, as well as glial cells.
- Layer II, the external granular layer, contains small pyramidal neurons and numerous stellate neurons.
- Layer III, the external pyramidal layer, contains predominantly small and medium-size pyramidal neurons, as well as non-pyramidal neurons.
- Layer IV, the internal granular layer, contains different types of stellate and pyramidal neurons,
- Layer V, the internal pyramidal layer, contains large pyramidal neurons which give rise to axons leaving the cortex and running down to subcortical structures .

Removal of duramater causes irreversible damage especially on the neurons layer 1 and layer 2 in a depth of 200 μm. Avoiding the rupture of duramater would enable monitoring the activity on these regions. For this purpose, the PEDOT:PSS device and the Tungsten electrode were placed gently over the intact dura matter. The data collected by both devices showed typical slow oscillations (1Hz), a marker of slow-wave sleep- like activity obtained under deep anesthesia. (Figure 4.5a)

The neurophysiological signal is a convolution of different frequency bands. Depending of the network activity, different bands are present in the spectrum of the signal. In order to compare the recording range of the devices in the spectral domain, we computed the power spectra (Fast Fourier Transform) of the signals. The spectra were very similar (same peak in the 1-2 Hz range, indicating the presence of the slow oscillations) and displayed high values of coherence (i.e. similitude of the spectra), indicating that both devices recorded with the same spectral definition the ongoing activity. However, the PEDOT:PSS spectrum was stronger over all the frequency range (mean power PEDOT:PSS = 3.32 ± 4.85 dB; Tungsten = -4.37 ± 5.35 dB), showing again that the PEDOT:PSS device signal was amplified as

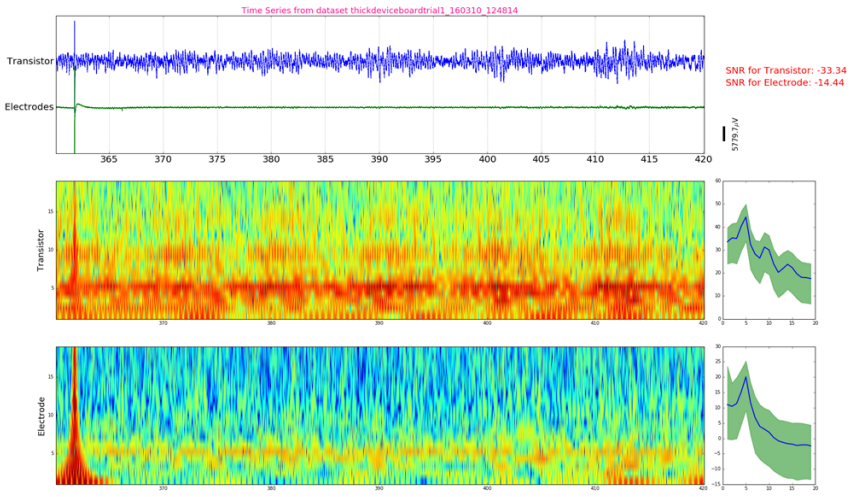

(a)

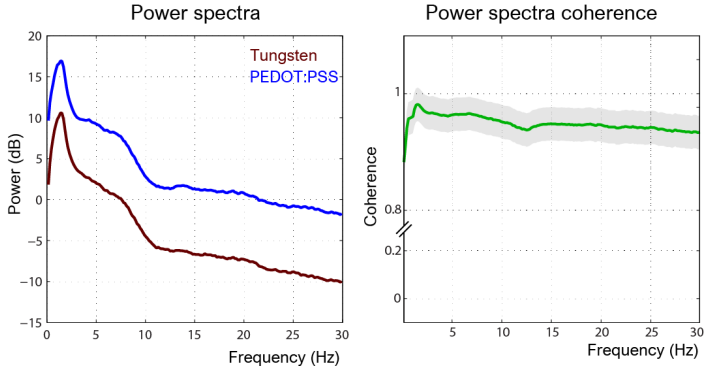

(b)

Fig. 4.5 (a) SWS recordings using epidural PEDOT:PSS electrode arrays. (b) Power spectra of the recordings.

compared to the Tungsten electrode. The SNR of the signal collected by the Tungsten electrode and the PEDOT:PSS passive device were then calculated as the ratio of the standard deviation of the full signal recorded (for 30 min) and the standard deviation of the baseline (without slow oscillations). As expected, the SNR for the PEDOT:PSS passive device was twice that one of the Tungsten device (Tungsten SNR = 5.03; PEDOT:PSS SNR = 11.88. Altogether, the ECoG PEDOT:PSS passive device showed superior recordings abilities as compared to a classical ECoG electrode when the signal is collected above the dura matter. This is important since the preservation of the dura matter could allow longer-term and more physiological recordings. (Figure 4.5b)

Epidural acute recordings with PEDOT:PSS OECTs

To enhance the performance further, one characteristic example is an organic electrochemical transistor (OECT), which operates in contact with biological media at low operating voltages (lt;1 V). As the ions of electrolyte penetrate inside the transistor channel, i.e. PEDOT:PSS, the conductivity of the channel is drastically modulated (Figure 1a). [12] OECTs are, therefore, efficient transducers of ionic-to-electronic signals, ideal for recording neural activity from single cell level to local field potentials or for electrical stimulation of electrogenic cells. [84] The work with PEDOT:PSS based OECT arrays has demonstrated great success in acute studies in rats and recently expanded to trials with human brain. [85] These OECTs recorded both local field potentials and action potentials from superficial cortical neurons without penetrating the brain surface of patients.

The design is illustrated in figure 4.6a. The array consists of 12 OECTs with 10x5 μm channel with a total area of 150 μm2. Each OECT has an adjacent electrode with 13x13 μm size, corresponding to the same surface area as the OECTs. The OECTs are powered separately by a bias of -0.6 V. The source contacts are short circuited and grounded. OECTs are tuned to have their maximum transconductance at 0 bias between gate and source terminals. Therefore, the common source is etched and coated with PEDOT:PSS to serve as gate with an opening of 500x500 μm. As it is grounded, it can as well be employed as reference for the PEDOT:PSS electrodes. It was demonstrated before that dependence of transconductance on channel thickness can be used to tune transistor performance. Volumetric capacitance of PEDOT:PSS channel defines the cutoff frequency of the channel. Here, we aim to record delta (1-3 Hz) and theta (4-7 Hz) oscillations as they give information of the sleep states of the anesthetized rat. By observing the activity in these frequency bands, we can identify the slow wave sleep (deep sleep) or rapid eye movement sleep (REM), the dream state of the brain. Considering both states occur at low frequency bands, we adjusted the channel thickness to be 250 nm, leading a low cutoff frequency at around 100 Hz.

To achieve the right working parameters with the OECTs, prier to an in vivo implantation, devices were characterized in vivo. The arrays were placed on the cortex of the rat and by employing a stainless screw fixed in the skull, the drain current was measured as a function of gate and drain voltage. (Figure 4.8) The value of transconductance, which governs the amplification level of the signal, is decided by he working regime of the device. Different PEDOT:PSS thicknesses and channel geometries were tested and for the 10x5 um channel with a 250 nm thickness was observed to perform the best. The design showed an 8 mS transconductance with a drain bias of -0.6 and zero bias between source and drain. (Both grounded)

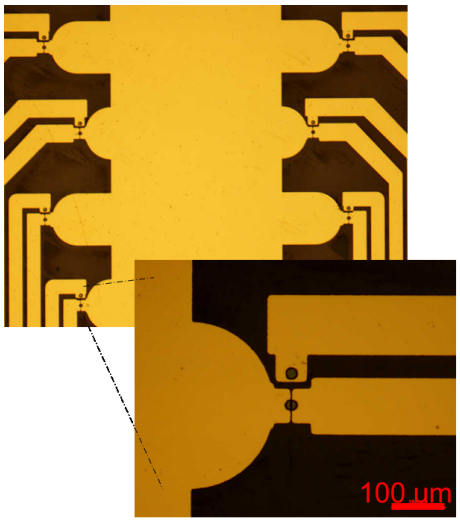

(a)

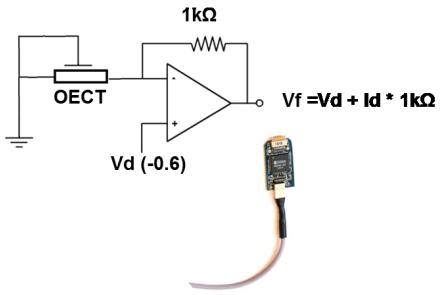

(b)

Fig. 4.6 (a) The layout of the hybrid probe consisting of 12 OECTs and 12 electrodes. (b) The IV conversion stage for simultaneous recordings.

In vivo application of OECTs employ biological signal as the gate to modulate the drain current in the channel. The output signal of an OECT is current, whereas it is voltage in case of electrodes. That requires using separate recording systems for simultaneous recordings, which is crucial to evaluate the performance accurately. However, that comes with the risk of inducing noise and synchronization problems. Here, we used a transimpedance amplifier to convert the current output of OECTs to voltage to be able to record it by using the same measurement system. The diagram is illustrated in figure . The current is ran over a resistor connected between the minus input and output of an operational amplifier (Opamp). Opamp floats the output based on the current flowing through to channel to maintain a steady drain voltage at -0.6 V. The change in the output voltage is a direct translation of the modulations in the drain current. Using this approach we recorded all the OECTs and electrodes simultaneously. (Figure 4.6b)

The hybrid array was implanted in a similar fashion as described before. (Figure 4.7) These OECTs based on poly (3,4-ethylenedioxythiophene): poly (styrenesulfonate) (PEDOT:PSS) are able to record not only pathological seizure-like neural activity but also the transition from SWS to REM with a rich spectrum. On the contrary, identically fabricated PEDOT:PSS electrodes or conventional metal electrodes can reach such high SNR only subdurally implanted, demonstrating the potential of OECTs as minimally-invasive neural probes.

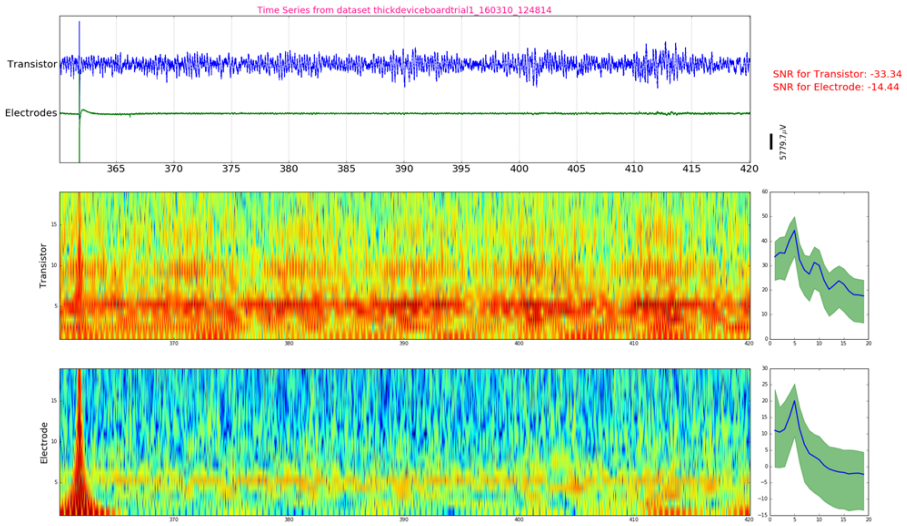

Fig. 4.7 Time frequency analysis of the recordings shows OECTs outperform electrodes.

4.4 Conclusion

Here, we aimed to minimize the invasivity of the ECoG approach by keeping the SNR high relying on the high performance of OECTs. OECTs transforms voltage modulations in the gate to current modulations it the channel forming an voltage controlled current amplifier. The small 50 mV fluctuations caught by the electrodes are transformed into 400 μA current deviations in the output. Such preamplification carries the capabilities of electrodes further by allowing epidural high performance recordings.

For applications that need to employ electrical recordings, in vivo OECTs constitutes a major breakthrough. The high SNR they exhibit, allows recordings small and more local activities from the surface of the brain , beyond the capabilities of electrodes. Such arrays would be used in treatment and diagnosis of neural diseases as they offer a less invasive way of monitoring brain activity. In addition, superior capacity to decode the frequency components would have implications on BMI studies.

4.5 Supplementary Information

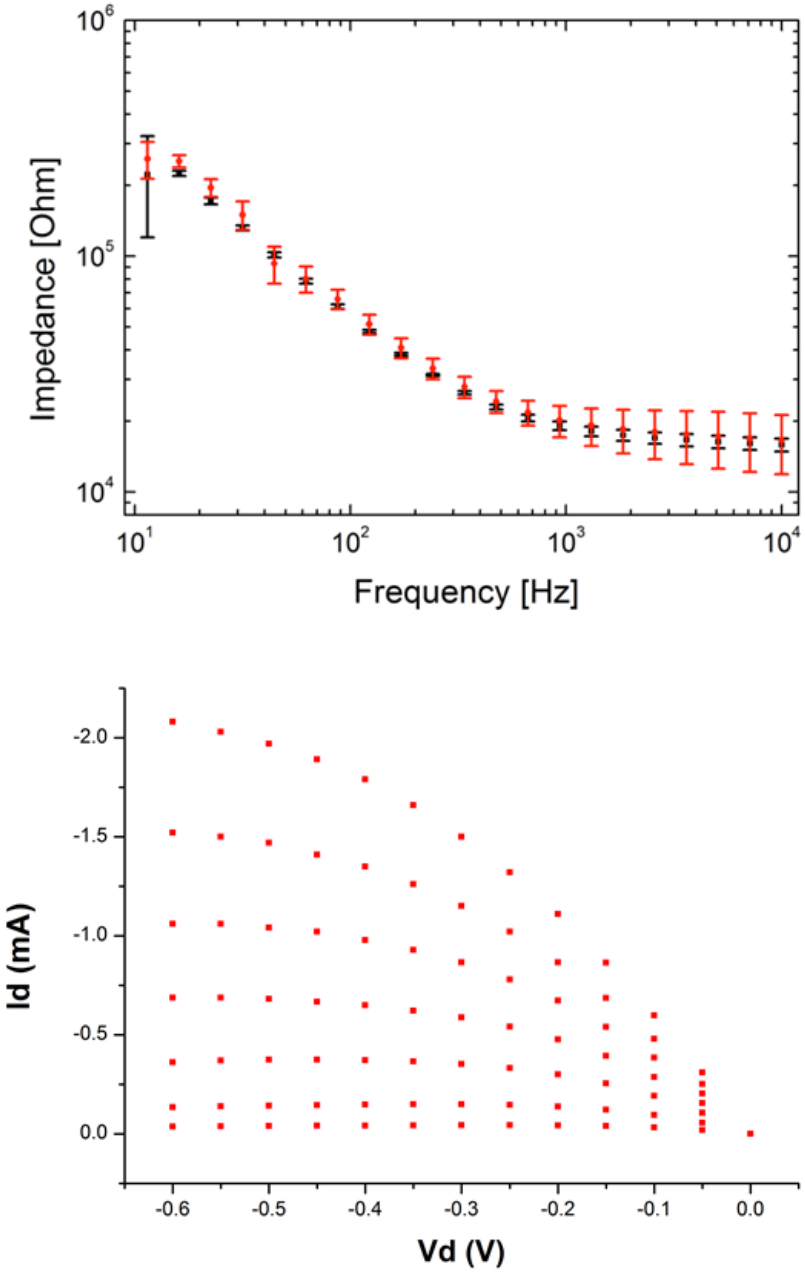

Fig. 4.8 In vivo characterization of OECTs and invitro characterization of electrodes.

Chapter 5

Sterilization of PEDOT:PSS electrophysiology devices

5.1 Introduction

The biological applications of organic electronic materials are currently attracting a great deal of interest.[135],[11],[101] One key thematic area encompasses the development of new devices for electrophysiology – devices that interface with cells by means of electrical recording and stimulation. Historically, interest in organics stems from their soft nature, which decreases the mechanical properties mismatch with tissue. Another property that makes organics attractive to electrophysiology is their mixed electronic/ionic conductivity. Indeed, organic coatings are shown to decrease the electrochemical impedance at the biotic/abiotic interface and lead to better recordings and more efficient stimulation compared to traditional metal electrodes.[135] In addition to making better electrodes, mixed conductivity is leveraged to design novel devices with state-of-the-art properties. One such example is the organic electrochemical transistor (OECT), a device that uses an organic film as the transistor channel.[White et al.] When used in vivo, ions from the cerebrospinal fluid, set in motion by neural firing, penetrate into the volume of the film and change its doping level. As a result of this volumetric response, OECTs act as efficient signal amplifiers and are being used to record brain activity with unprecedented signal-to-noise ratio.[84]

The prototypical material used in organic-based electrophysiology devices is the conducting polymer poly(3,4-ethylenedioxythiophene) doped with polystyrene sulfonate (PEDOT:PSS). It is commercially available as an aqueous dispersion, and can be easily processed into films that are biocompatible and show high hole and ion conductivity.[132] PEDOT:PSS electrodes and OECTs are also used in in vitro diagnostics to monitor the health of cultures and tissue slices,[152] and have been integrated with both rigid and flexible sub-

strates to yield devices that interface with electrically active tissues in animal models.[74], [83] Deposited on thin films of parylene, they make arrays that conform well to the surface of the brain and yield stable, high signal-to-noise ratio cortical recordings in animal models as well as in humans.[20] Finally, PEDOT:PSS has been used in the fabrication of OECTs with record-high transconductance, used for electrophysiological recordings in animal models and in humans.[23],[133] These efforts generate a great deal of potential for the realization of high quality neural interfaces using organic materials. Such interfaces can be used to understand the brain, treat neurological diseases including epilepsy and Parkinson's, and yield stable brain/computer interfaces.

In order to transition these technologies to the clinic, effective sterilization that renders the devices free of pathogenic agents needs to be demonstrated. Several methods exist for the sterilization of medical devices, relying on heat, chemicals or radiation to destroy potential pathogens. Among these, autoclaving is the most-frequently used. The device to be sterilized is placed in a chamber and exposed to high pressure steam typically at a temperature of 121 °C for several minutes. The simplicity of the procedure and low cost of the equipment make this method widely available among biology laboratories and clinics worldwide. Unfortunately, however, autoclaving is not suitable for heat and moisture sensitive materials, which, a priori precludes its use with the vast majority of organic electronic devices. Indeed, few examples of organic-based devices can survive such a process, due to failure modes that include intrinsic materials degradation, morphological/structural changes, or mechanical damage due to thermal expansion.[93] It is worth noting that the first (and only so far)[20] clinical application of PEDOT:PSS relied on ethylene oxide sterilization, a method that is used for sterilization of disposable plasticware in bulk, and not directly available in most hospitals. A successful use of autoclaving would constitute an important step towards transitioning PEDOT:PSS devices from the lab to the clinic.

In this chapter we show that sterilization of PEDOT:PSS electrophysiology devices can be performed using an autoclave. In a parallel study, conducted simultaneously in two laboratories in Gardanne (France) and in San Diego (California), we fabricated, sterilized, and tested PEDOT:PSS microelectrode and transistor arrays. We find that autoclaving is a viable sterilization method, leaving morphology unaltered and causing only minor changes in electrical properties. These results pave the way for the widespread utilization of PEDOT:PSS electrophysiology devices in the clinic.

5.2 Results

PEDOT:PSS microelectrode and OECT arrays were fabricated using lithography, as detailed in the Experimental Section. Each array consisted of a parylene substrate, Au pads/ interconnects/ electrodes, PEDOT:PSS islands and a parylene layer insulating the metal interconnects. In Gardanne, each array comprised 64 microelectrodes with sizes of 10x10, 20x20 and 40x40 μm2, or 13 OECTs with a channel length of 5 µm and width of 10 μm. The thickness of the PEDOT:PSS film was 220 nm. In San Diego, each array comprised 15 microelectrodes of 15x15 μm2 (Figure 5.1). The thickness of the PEDOT:PSS film was 280 nm. The arrays were autoclaved by exposure to steam at a temperature of 121 °C for 20 min. We evaluated the efficacy of the sterilization process by intentionally inoculating a portion of the arrays with Escherichia coli (E. coli, ATCC 25922) before sterilization, as described in the Experimental Section. Immediately after sterilization, all arrays were incubated in culture media. After 24 hours, the optical density (OD) of the media at 600 nm (OD600 is a common method for estimating the concentration of bacteria in media) was measured. We defined boundary conditions by measuring the OD of autoclaved media (reference 1 – sterile) and of media containing bacteria (reference 2 – non-sterile), respectively. The results are summarized in Table 5.1. Array 1 was neither exposed to E. coli nor sterilized. Media in which the array was incubated showed an OD above the baseline, consistent with the array being non-sterile. Array 2 was not exposed to E. coli but was sterilized, resulting into optically clear media, consistent with the array being sterile. Array 3 was exposed to E. coli but was subsequently sterilized. Media in which the array was incubated was also clear, consistent with the array being sterile. These results, therefore, show that autoclaving renders the arrays sterile.

	E.coli exposure	Sterilization	OD at 600nm	Sterile?
Reference 1		+	0.05 ± 0.01	Yes
Reference 2	+		1.68 ± 0.05	No
Array 1		+	0.12 ± 0.01	No
Array 2		+	0.05 ± 0.01	Yes
Array 3	+		0.05 ± 0.01	Yes

Table 5.1 Results of the autoclave sterilization assay. N=3 solution samples taken from each.

We next investigated the influence of autoclave sterilization on the morphological stability of the microelectrodes by optical microscopy, scanning electron microscopy (SEM), and atomic force microscopy (AFM). The overall structure of the arrays is shown in Figure 5.1a. Optical images of the same microelectrode before (Figure 5.1b) and after (Figure 5.1c) au-

toclaving showed no evident morphological changes (the same holds for the whole device – no visible change was observed after sterilization). Similarly, SEM images on the same PEDOT:PSS microelectrode before (Figure 5.1d) and after (Figure 5.1e) autoclaving showed no evident delamination, cuts, or other observable morphological changes. To look further at the surface topography of the PEDOT:PSS at a higher resolution, we conducted AFM topography before (Figure 5.1f) and after (Figure 5.1g) autoclaving on the same 5×5m2 PEDOT:PSS location. The AFM images showed that the PEDOT:PSS morphology is generally conserved with a root mean square surface roughness of 3.41 nm before and 3.47 nm after autoclave.

We next evaluated the impact of the sterilization process on the electrical performance of the electrodes and OECTs. For the electrodes, we measured the electrochemical impedance spectra as described in the Experimental Section. Impedance at 1 kHz is used as the benchmark for the characterization of neural electrodes, as this frequency allows recording simultaneously from local field potentials and spiking activity, if any.[22] Figure 5.2a shows a histogram of impedance values before and after sterilization, for electrodes with an area of 10x10 μm2 made and measured in Gardanne. The data show that the distribution moves slightly to higher values, with the average value changing from 49.7±3.6 k before sterilization to 53.2±3.4 k after. Similar results were obtained in San Diego, where average impedance values at 1 kHz changed from 57.7 ± 7.2 k before sterilization to 58.7 ± 7.3 k after sterilization.

For the OECTs, we measured the transfer curves as described in the Experimental Section and extracted transconductance. The transconductance is the key parameter that determines the performance of OECTs in electrophysiology, as it relates to signal amplification.[134] Figure 5.2b shows a histogram of transconductance values before and after sterilization, for devices made and measured in Gardanne. As with impedance, the change of the transconductance was very little after sterilization, from 7.4±0.2 mS to 7.3±0.2 mS. Furthermore, the resistance of the OECT channels was found to decrease by 4% after sterilization, indicating that materials degradation, changes in mobility/doping, and/or delamination from contacts might be underlying the changes in impedance and transconductance. These changes are, however, small, and the devices remain functional after autoclave sterilization.

The observed stability of the PEDOT:PSS electrophysiology devices to autoclaving can be attributed partly to the intrinsic thermal stability of their components and partly to the use of a crosslinker. Indeed, the devices are already baked during fabrication at 140 °C for 1 h in ambient conditions, a temperature that all components of the device can sustain. Moreover, the crosslinker 3-glycidoxypropyltrimethoxysilane (GOPS) renders the PEDOT:PSS film insoluble to water. Devices made without GOPS do not survive autoclave sterilization, as

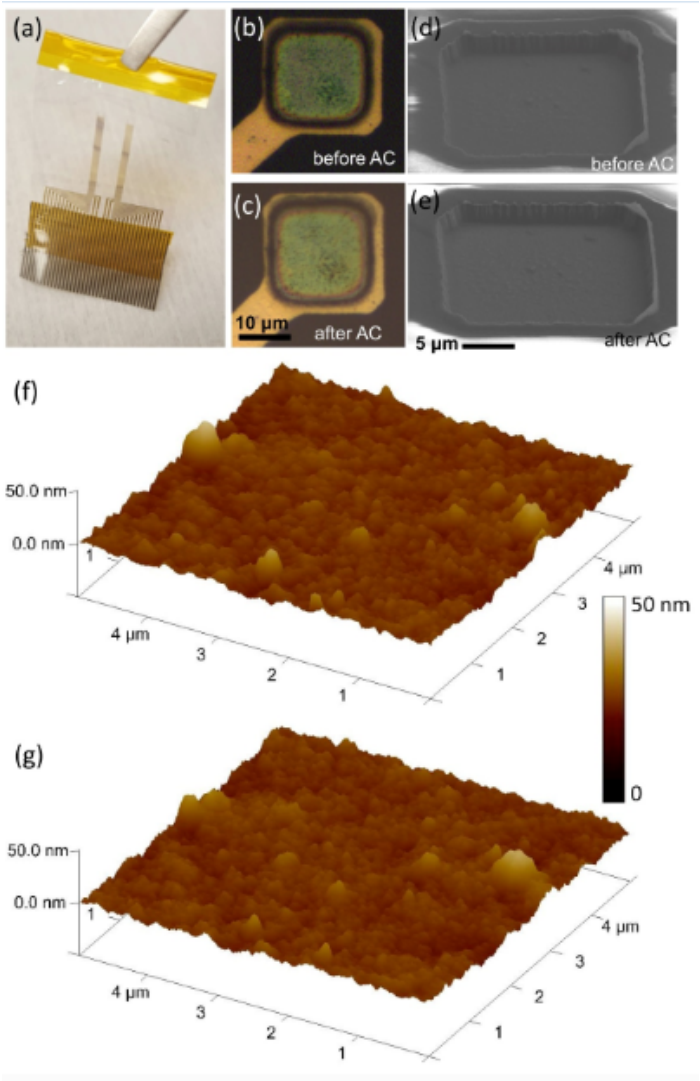

Fig. 5.1 . (a) Picture of test geometry with 2 arrays, each containing 15 PEDOT:PSS microelectrodes. Optical micrographs of the same microelectrode (b) before and (c) after autoclave. 45° angle view SEM images of the same microelectrode (d) before and (e) after autoclave. AFM topography images on a 5×5m2 area at the same location of PEDOT:PSS before (f) and after (g) autoclave.

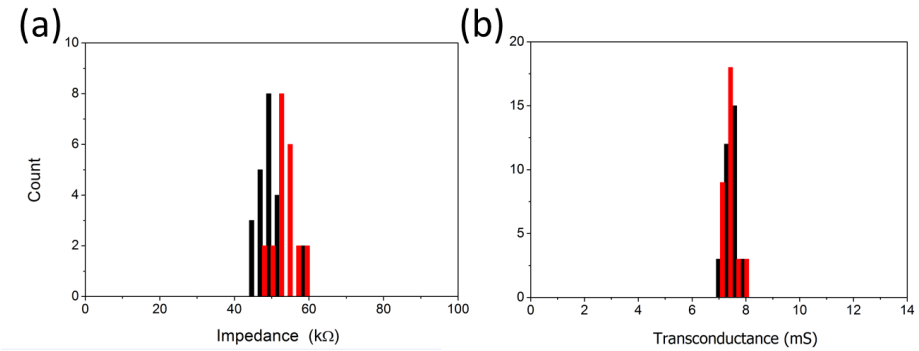

Fig. 5.2 (a) Histogram showing the distribution in electrode impedance at 1 kHz before (black) and after (red) sterilization. (b) Histogram showing the distribution in OECT transconductance before (black) and after (red) sterilization.

the PEDOT:PSS film falls apart. It should be noted that sterilization by autoclave does not seem to change the mechanical properties of parylene (Figure **??**) and sterilized devices conform well to a 1:1 model of a rat brain (Figure **??**) and show the ability to record brain activity (Figure **??**).

While autoclaving showed no significant influence in the morphology and electrical characteristics of PEDOT:PSS devices, this is not a general case for all sterilization methods. As an example to the contrary we show results from chemical sterilization using the Sterrad system. This system destroys pathogens through exposure to a H_2O_2 gas plasma. Since the process does not typically exceed 50 °C, this method is particularly well-suited to heat and moisture sensitive devices. However, Sterrad sterilization imparted extensive damage to PEDOT:PSS microelectrodes. As shown in Figure 5.3a, it resulted in non-functional devices, manifested by large impedance values. SEM and optical images in Figure 5.3b and Figure 5.3c, respectively, depict severe morphological changes in the PEDOT:PSS film. By utilizing focused-ion beam (FIB) to section a PEDOT:PSS microelectrode before and after Sterrad sterilization (Figures 5.3d and 5.3e), we observed clear delamination of the PEDOT:PSS from the Ti/Au metal lead at the center of the microelectrode and from the parylene at the edge of the microelectrode after the Sterrad process. This result points to the fact that for each sterilization method, a systematic study needs to be undertaken to ensure suitability to a particular device.

In conclusion, we investigated the impact of sterilization methods on PEDOT:PSS microelectrodes and electrochemical transistors integrated on thin parylene supports. We show that devices inoculated with E. coli are effectively sterilized using autoclaving. The process does not alter appreciably the morphology of PEDOT:PSS films, while the electrical characteristics of microelectrodes and transistors show only minor degradation after exposure to steam. Sterrad sterilization, in contrast, causes large morphological changes in the PE-

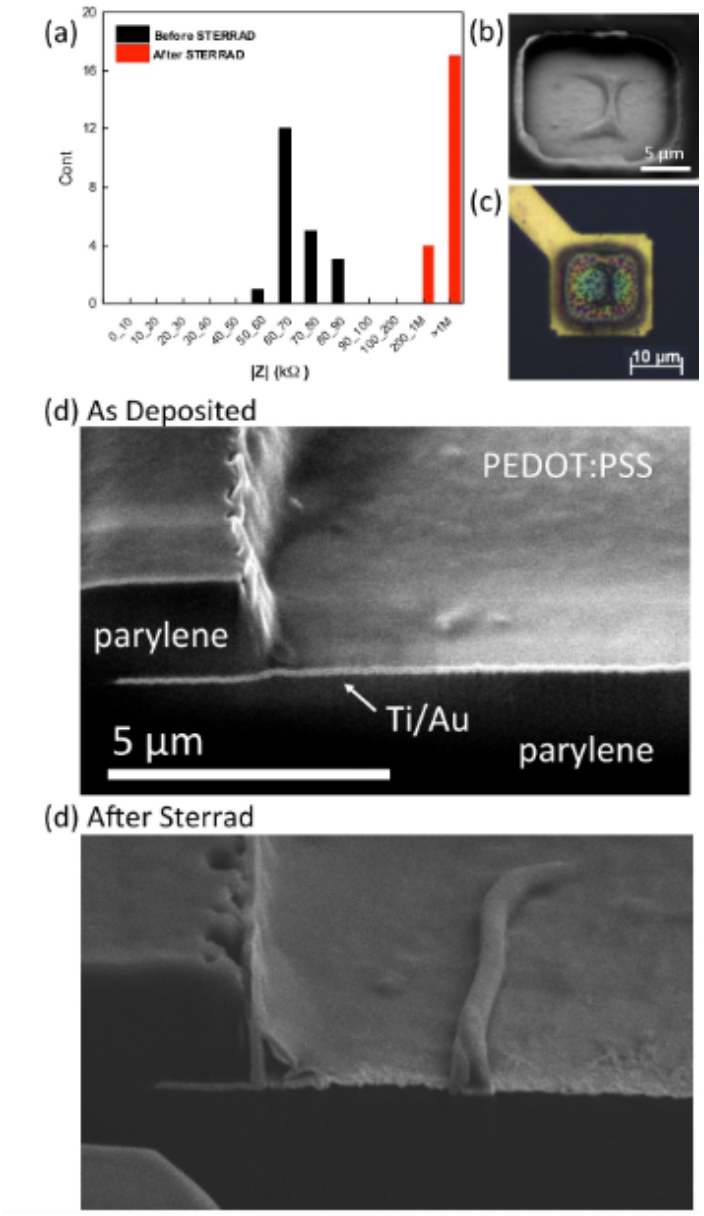

Fig. 5.3 . (a) Impedance histogram at 1 kHz showing mostly open circuit devices after Sterrad sterilization. (b) SEM image and (c) optical image of a typical PEDOT:PSS microelectrode after Sterrad sterilization, showing clear delamination of the PEDOT:PSS microelectrode from Ti/Au near the edge and near the center after Sterrad sterilization. (d) and (e) FIB cuts of the same electrode before and after sterilization.

DOT:PSS films and results in non-functional devices. The results show that autoclaving, which is readily available in most biological laboratories, is a viable sterilization method for PEDOT:PSS electrophysiology devices. This finding represents a significant step towards the widespread introduction of these devices to the clinic.

5.3 Experimental section

Fabrication

The fabrication of PEDOT:PSS-based electrodes and OECTs followed previously published processes. In Gardanne, glass slides with dimensions of 7.62×2.54 cm2 for OECTs and 4×4 cm2 for electrodes, were cleaned by sonication in soap/water mixture and then in acetone/IPA mixture for 30 min. They were coated with 2 µm of parylene-C using an SCS Labcoater 2. For patterning Au interconnects, S1813 (Shipley) photoresist was spin-coated on the glass slide, exposed to UV light using a SUSS MJB4 contact aligner, and developed using MF-26 developer. A thin (10 nm) Cr adhesion layer, followed by a Au film (100 nm) was deposited (Alliance Concept EVA450) and patterned using lift-off in acetone. A 1.8 μm of parylene-C was deposited, acting as the insulation layer, and an additional, sacrificial layer of parylene-C (2 µm) was deposited, with a layer of soap in between. A 3.5 μm of photoresist, AZ9260, was then patterned and etched using oxygen plasma with an Oxford 80 plus. Aqueous dispersion of PEDOT:PSS (PH 1000 from H.C. Stark) was mixed with ethylene glycol (EG, 5 vol%), dodecyl benzene sulfonic acid (DBSA, 0.2 vol%), and 3-glycidoxypropyltrimethoxysilane (GOPS, 1 wt%). The dispersion was spun cast at 650 rpm for 30 seconds and the resulting film was patterned by peel-off of the top parylene-C film. The arrays were subsequently baked at 140 °C for 1 h and were immersed in deionized water to remove any excess low molecular weight compounds. In San Diego, glass slides (3×3.5 cm2) were used as substrate carriers for a thin parylene-C layer. The glass wafers were rinsed with acetone/IPA/water/IPA, sonicated for 5 min in IPA, and then rinsed again with acetone/IPA/water/IPA. Anti-adhesion promoter (Micro 90) was spin-coated at 650 rpm on the glass wafer to facilitate peeling-off the array at final step. A first parylene-C layer (3 μm) was deposited using PDS 2010 Parylene Coater system. Ti/Au (10 nm/100 nm) metal leads were defined using a lift-off process in acetone with a NR9-3000 negative resist for photolithography and a Temescal BJD 1800 electron beam evaporator for the 10 nm Ti adhesion layer and 100 nm Au layer deposition. Prior to the second parylene-C deposition, an adhesion promoter (Silane A-174:H2O:IPA with 1:200:200) was applied. The encapsulating parylene-C layer (2.2 μm) was then deposited and coated with another Micro 90 anti-

adhesion film. A third layer parylene-C was then deposited, followed by the spin-coating of a thick 2010 SU-8 layer, which was exposed using a Karl Suss MA6 Mask Aligner and developed with SU-8 developer. Oxygen plasma (Oxford Plasmalab 80 RIE) was used to etch and define the openings for the subsequent PEDOT:PSS layer. Aqueous dispersion of PEDOT:PSS (PH 1000 from Clevios) was mixed with ethylene glycol (EG, 5 vol%), dodecyl benzene sulfonic acid (DBSA, 0.2 vol%), and 3-glycidoxypropyltrimethoxysilane (GOPS, 1 wt%). The solution was spin-coated at 650 rpm for 30 seconds and pre-baked at 95 °C for 1 min. The third parylene-C layer was peeled-off to pattern the PEDOT:PSS on top of the electrode sites. Finally, the arrays were cured at 140 °C for 1 hour and immersed in DI water to remove any excessive components from the PEDOT:PSS.

Characterization

FEI SFEG UHR SEM was used to take high resolution images at 10 kV with 4702× magnification. For sample preparation, a thin layer of the Ti (15 nm) has been deposited at back of the array in order to reduce the charging effects during the imaging. A Veeco Scanning Probe Microscope was used to take atomic force microscopy (AFM) images in tapping mode. Electrochemical impedance spectroscopy (EIS) was performed using a GAMRY interface 1000E in phosphate buffer saline (PBS) solution, using three electrode configuration, i.e., Ag/AgCl electrode as a reference, platinum as a counter, and PEDOT:PSS a working electrode. Sinusoidal signals with 10 mV rms AC voltage and zero DC voltage were applied and the frequency was swept from 100 KHz to 1 Hz to achieve complete capacitive and faradaic domains. In Gardanne, impedance spectra were measured with an Autolab PGSTAT equipped with an FRA module. The measurements were carried out in PBS using a three electrode configuration using the same parameters as in San Diego. The OECTs were characterized in PBS with a Ag/AgCl gate electrode, using a Keithley 2612A dual SourceMeter and customized LabVIEW software. The transconductance reported here was measured at a drain voltage of -0.6 V and a gate voltage of 0 V.

Sterilization

In Gardanne, sterilization of the devices was achieved using a Tuttnauer Model 3150EL autoclave. The samples were placed into autoclave pouches and sealed prior to exposure to steam. A 20 minute treatment with saturated steam at 121 °C was followed by a 15 minutes evaporative drying step. Some of the devices were inoculated with 200 μL pre-culture (Escherichia coli ATCC 25922), sterilized by autoclave and placed in pre-sterilized flasks that contained Luria-Bertani media (Sigma). The arrays were incubated for 24 hours at 37

°C. The optical density of the resultant microbial population was measured at a wavelength of 600 nm using a TECAN M1000 spectrophotometer. In San Diego, autoclave sterilization was performed using a SUN series autoclave (Class B). Arrays were directly exposed to water vapor at 121 °C for 20 minutes. Sterrad sterilization was performed by exposing arrays to hydrogen peroxide vapor at 50 °C for 47 minutes, at UCSD's Thornton Hospital, while the arrays were kept in appropriate sterilization pouches.

5.4 Supplementary Information

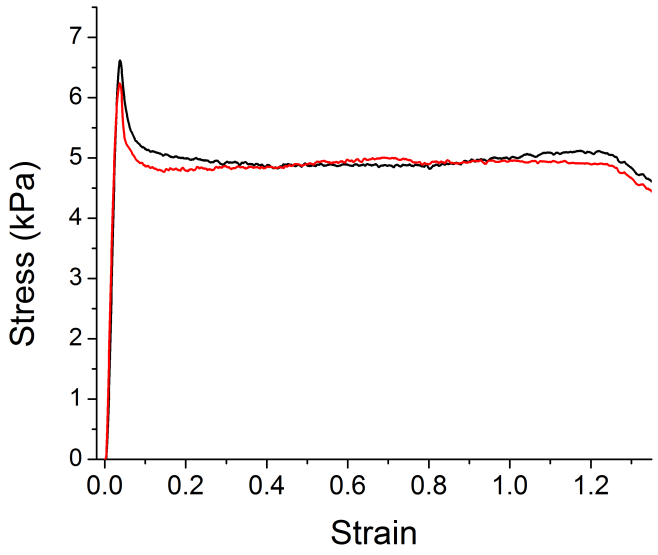

Fig. 5.4 Stress vs. strain curves for 3 m thick parylene films before (black) and after (red) autoclaving, measured with a 3665 Instron. Each curve is the average of 3 experiments. After the yield point is reached the materials goes to the plastic stage and extends irreversibly till it ruptures, which occurrs at similar extension levels for all films.

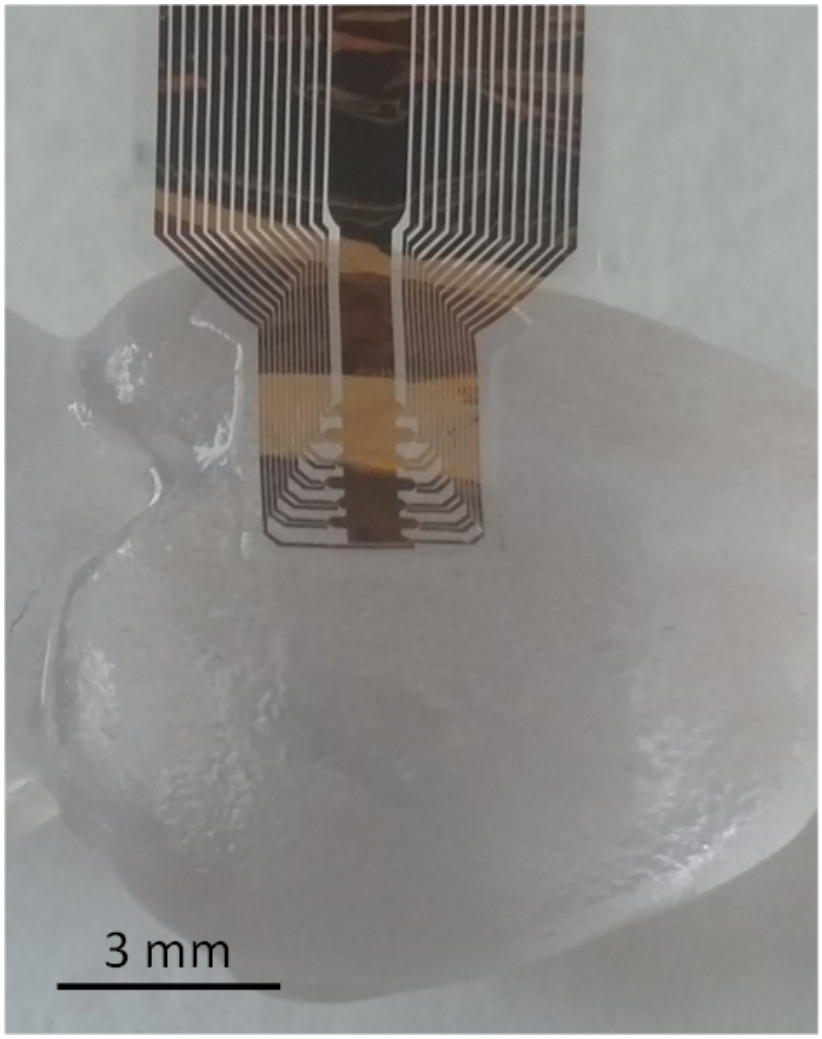

Fig. 5.5 Image of a device containing transistors conforming to the surface of a 3D printed model of a rat brain (1:1 scale). The device was sterilized with autoclaving.

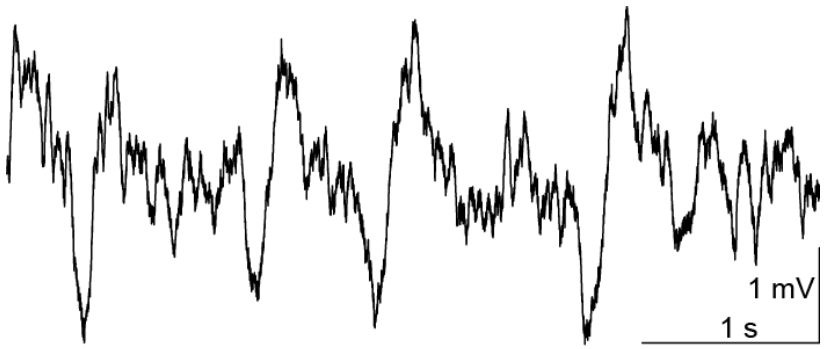

Fig. 5.6 Quiet immobility activity recorded in a freely-moving rat. Briefly, a Wistar Han male rat was anesthetized, and a craniotomy was performed over the somato-sensory cortex. The recording grid (see Figure S2) was gently laid over the dura mater. The device was then recovered with a silicon-based artificial dura and dental cement. The grid was connected to a ZIF/Omnetics connector and fixed inside a rigid hat anchored on the head of the animal. The animal was allowed to recover during one week before recordings were performed. The transistors were powered and the source-drain current converted in voltage. The signal shown here was obtained while the animal was awake and immobile in its homecage. Note the excellent signal-to-noise ratio despite the fact that the grid was above the dura mater, and not directly in contact with the cortex.

Chapter 6

Conclusion

6.1 Conclusion

In conclusion, we fabricated OEIPs using the conducting polymer PEDOT:PSS and a polyanionic copolymer. We used these devices to deliver GABA to tissue slices and demonstrated that epileptiform activity, induced using three different models, can be successfully controlled. These results show that OEIPs represent a technological breakthrough for local and timed delivery of active molecules cannot be delivered in a systematic way. Combining the approach with PEDOT:PSS electrodes enables the capability to sense electrophysiological signals and deliver neuroactive compounds at the same location. It represents a first step in constructing closed-loop feedback system, capable of monitoring neuronal activity and adjusting local release of neurotransmitters accordingly. Such a closed-loop system could be used, for example, in epilepsy treatment, to predict or detect an epileptic seizure at an early stage and intervene by delivering inhibitory neurotransmitters. The feedback system would make it possible to stop seizures with a minimal amount of drugs, since the drug release could be stopped as soon as the inhibitory effect is observed. We further explored the innovations OEIP offers but integrating it into an ECoG platform. Combining the electrophoretic delivery with a microfluidic channel and a vertical overoxidized PEDOT:PSS seal, boosted the pumping efficiency remarkably. The high ionic current and low voltage requirements offer it as a promising tool for in vivo studies for modulating mammalian sensory function by precise delivery of neurotransmitters.

In addition, we developed a generic process for incorporating conducting polymer electrodes on highly conformable substrates. Arrays of PEDOT:PSS electrodes were fabricated on parylene substrates, and their total thickness of 3 um endowed them with high conformability. Their use in electrocorticography was demonstrated and validated against a silicon probe, and they were shown to outperform Au electrodes of similar geometry. OECTs, on

the other hand, carried the detection capabilites of the PEDOT:PSS electrodes even further through the high local amplification they have. Implanted epidurally, they were able to decode the frequency components of brain activity with high precision, demonstrating the potential of OECTs as minimally-invasive neural probes.

To explore the applications of such arrays in humans, we investigated the impact of sterilization methods on PEDOT:PSS microelectrodes and electrochemical transistors integrated on thin parylene supports. We show that devices inoculated with E. coli are effectively sterilized using autoclaving. The process does not alter appreciably the morphology of PEDOT:PSS films, while the electrical characteristics of microelectrodes and transistors show only minor degradation after exposure to steam. Sterrad sterilization, in contrast, causes large morphological changes in the PEDOT:PSS films and results in non-functional devices. The results show that autoclaving, which is readily available in most biological laboratories, is a viable sterilization method for PEDOT:PSS electrophysiology devices. This finding represents a significant step towards the widespread introduction of these devices to the clinic.

References

[1] (2007). Neurological disorders affect millions globally: Who report. Technical report.

[2] Abbott, N. J., Ronnback, L., and Hansson, E. (2006). Astrocyte-endothelial interactions at the blood-brain barrier. *Nat Rev Neurosci*, 7(1):41–53.

[3] Abdelhamid, M. E., O'Mullane, A. P., and Snook, G. A. (2015). Storing energy in plastics: a review on conducting polymers their role in electrochemical energy storage. *RSC Adv.*, 5:11611–11626.

[4] Abidian, M., Kim, D.-H., and Martin, D. (2006). Conducting-polymer nanotubes for controlled drug release. *Advanced Materials*, 18(4):405–409.

[5] Albus, K., Wahab, A., and Heinemann, U. (2008). Standard antiepileptic drugs fail to block epileptiform activity in rat organotypic hippocampal slice cultures. *Br J Pharmacol*, 154(3):724. 18414393[pmid].

[6] Aregueta-Robles, U. A., Woolley, A. J., Poole-Warren, L. A., Lovell, N. H., and Green, R. A. (2014). Organic electrode coatings for next-generation neural interfaces. *Frontiers in Neuroengineering*, 7:15.

[7] Aregueta-Robles, Ulises A, W. A. J. P.-W. L. A. L. N. H. G. R. A. (2014). Organic electrode coatings for next-generation neural interfaces. *Frontiers in Neuroengineering*, 7.

[8] Arshak, K., Ajina, A., and Egan, D. (2001). Development of screen-printed polymer thick film planner transformer using mn–zn ferrite as core material. *Microelectronics Journal*, 32(2):113 – 116.

[9] Asano, E., Juhász, C., Shah, A., Muzik, O., Chugani, D. C., Shah, J., Sood, S., and Chugani, H. T. (2005). Origin and propagation of epileptic spasms delineated on electrocorticography. *Epilepsia*, 46(7):1086–1097.

[10] Barrese, J. C., Rao, N., Paroo, K., Triebwasser, C., Vargas-Irwin, C., Franquemont, L., and Donoghue, J. P. (2013). Failure mode analysis of silicon-based intracortical microelectrode arrays in non-human primates. *Journal of Neural Engineering*, 10(6):066014.

[11] Berggren, M. and Richter-Dahlfors, A. (2007). Organic bioelectronics. *Advanced Materials*, 19(20):3201–3213.

[12] Bernards, D. and Malliaras, G. (2007). Steady-state and transient behavior of organic electrochemical transistors. *Advanced Functional Materials*, 17(17):3538–3544.

[13] Bernards, D. A., Macaya, D. J., Nikolou, M., DeFranco, J. A., Takamatsu, S., and Malliaras, G. G. (2008). Enzymatic sensing with organic electrochemical transistors. *J. Mater. Chem.*, 18:116–120.

[14] Bhagwat, N., Kiick, K. L., and Martin, D. C. (2014). Electrochemical deposition and characterization of carboxylic acid functionalized pedot copolymers. *Journal of Materials Research*, 29:2835–2844.

[15] Bialer, M. and White, H. S. (2010). Key factors in the discovery and development of new antiepileptic drugs. *Nat Rev Drug Discov*, 9(1):68–82.

[16] Bobo, R. H., Laske, D. W., Akbasak, A., Morrison, P. F., Dedrick, R. L., and Oldfield, E. H. (1994a). Convection-enhanced delivery of macromolecules in the brain. *Proceedings of the National Academy of Sciences*, 91(6):2076–2080.

[17] Bobo, R. H., Laske, D. W., Akbasak, A., Morrison, P. F., Dedrick, R. L., and Oldfield, E. H. (1994b). Convection-enhanced delivery of macromolecules in the brain. *Proc Natl Acad Sci U S A*, 91(6):2076–2080. 8134351[pmid].

[18] Bolts, J. M. and Wrighton, M. S. (1979). Chemically derivatized n-type semiconducting gallium arsenide photoelectrodes. thermodynamically uphill oxidation of surface-attached ferrocene centers. *Journal of the American Chemical Society*, 101(21):6179–6184.

[19] Bormann, J. (XXXX). Electrophysiology of gaba_a and gaba_b receptor subtypes. *Trends in Neurosciences*, 11(3):112–116.

[20] Branner, A., Stein, R. B., Fernandez, E., Aoyagi, Y., and Normann, R. A. (2004). Long-term stimulation and recording with a penetrating microelectrode array in cat sciatic nerve. *IEEE Transactions on Biomedical Engineering*, 51(1):146–157.

[21] Brinker, C., Frye, G., Hurd, A., and Ashley, C. (1991). Fundamentals of sol-gel dip coating. *Thin Solid Films*, 201(1):97 – 108.

[22] Buzsáki, G., Anastassiou, C. A., and Koch, C. (2012). The origin of extracellular fields and currents. *Nat Rev Neurosci*, 13(6):407–420.

[23] Campana, A., Cramer, T., Simon, D. T., Berggren, M., and Biscarini, F. (2014). Electrocardiographic recording with conformable organic electrochemical transistor fabricated on resorbable bioscaffold. *Advanced Materials*, 26(23):3874–3878.

[24] Campbell, P. K., Jones, K. E., Huber, R. J., Horch, K. W., and Normann, R. A. (1991). A silicon-based, three-dimensional neural interface: manufacturing processes for an intracortical electrode array. *IEEE Transactions on Biomedical Engineering*, 38(8):758–768.

[25] Cao, W. and Xue, J. (2014). Recent progress in organic photovoltaics: device architecture and optical design. *Energy Environ. Sci.*, 7:2123–2144.

[26] Carrasquillo, K. V. and Pinto, N. J. (2012). Tunable schottky diodes fabricated from crossed electrospun sno2/pedot-pssa nanoribbons. *Materials Science and Engineering: B*, 177(11):805 – 809.

[27] Cecchelli, R., Berezowski, V., Lundquist, S., Culot, M., Renftel, M., Dehouck, M.-P., and Fenart, L. (2007). Modelling of the blood-brain barrier in drug discovery and development. *Nat Rev Drug Discov*, 6(8):650–661.

[28] Chandrasekhar, P. (1999). *Conducting Polymers, Fundamentals and Applications: A Practical Approach*. Springer US.

[29] Chen, C. S., Tan, J., and Tien, J. (2004). Mechanotransduction at cell-matrix and cell-cell contacts. *Annual Review of Biomedical Engineering*, 6(1):275–302. PMID: 15255771.

[30] Chestek, C. A., Gilja, V., Nuyujukian, P., Foster, J. D., Fan, J. M., Kaufman, M. T., Churchland, M. M., Rivera-Alvidrez, Z., Cunningham, J. P., Ryu, S. I., and Shenoy, K. V. (2011). Long-term stability of neural prosthetic control signals from silicon cortical arrays in rhesus macaque motor cortex. *Journal of Neural Engineering*, 8(4):045005.

[31] Cogan, S. F. (2008). Neural stimulation and recording electrodes. *Annual Review of Biomedical Engineering*, 10(1):275–309. PMID: 18429704.

[32] Collinger, J., Vinjamuri, R., Degenhart, A., Weber, D., Sudre, G., Boninger, M., Tyler-Kabara, E., and Wang, W. (2014). Motor-related brain activity during action observation: a neural substrate for electrocorticographic brain-computer interfaces after spinal cord injury. *Frontiers in Integrative Neuroscience*, 8:17.

[33] Cook, M. J., O'Brien, T. J., Berkovic, S. F., Murphy, M., Morokoff, A., Fabinyi, G., D'Souza, W., Yerra, R., Archer, J., Litewka, L., Hosking, S., Lightfoot, P., Ruedebusch, V., Sheffield, W. D., Snyder, D., Leyde, K., and Himes, D. (XXXX). Prediction of seizure likelihood with a long-term, implanted seizure advisory system in patients with drug-resistant epilepsy: a first-in-man study. *The Lancet Neurology*, 12(6):563–571.

[34] Cossart, R., Bernard, C., and Ben-Ari, Y. (XXXX). Multiple facets of gabaergic neurons and synapses: multiple fates of gaba signalling in epilepsies. *Trends in Neurosciences*, 28(2):108–115.

[35] Cui, X., Hetke, J. F., Wiler, J. A., Anderson, D. J., and Martin, D. C. (2001a). Electrochemical deposition and characterization of conducting polymer polypyrrole/pss on multichannel neural probes. *Sensors and Actuators A: Physical*, 93(1):8 – 18.

[36] Cui, X., Lee, V. A., Raphael, Y., Wiler, J. A., Hetke, J. F., Anderson, D. J., and Martin, D. C. (2001b). Surface modification of neural recording electrodes with conducting polymer/biomolecule blends. *Journal of Biomedical Materials Research*, 56(2):261–272.

[37] Cui, X. and Martin, D. C. (2003). Electrochemical deposition and characterization of poly(3,4-ethylenedioxythiophene) on neural microelectrode arrays. *Sensors and Actuators B: Chemical*, 89(1–2):92 – 102.

[38] Das, T. K. and Prusty, S. (2012). Review on conducting polymers and their applications. *Polymer-Plastics Technology and Engineering*, 51(14):1487–1500.

[39] DAVID OGDEN, P. S. (2007). *Patch clamp techniques for single channel and whole-cell recording*. London.

[40] Douglas B. Chrisey, G. K. H. (1994). *Pulsed Laser Deposition of Thin Films*. Wiley-Interscience, New York, first edition.

[41] Eric R. Kandel, Editor, J. H. S. E.-T. M. J. E. S. A. S. A. J. H. (2013). *Principles of Neural Science, Fifth Editon*.

[42] Fang, Y., Li, X., and Fang, Y. (2015). Organic bioelectronics for neural interfaces. *J. Mater. Chem. C*, 3:6424–6430.

[43] Farrell, M. S., Pei, Y., Wan, Y., Yadav, P. N., Daigle, T. L., Urban, D. J., Lee, H.-M., Sciaky, N., Simmons, A., Nonneman, R. J., Huang, X.-P., Hufeisen, S. J., Guettier, J.-M., Moy, S. S., Wess, J., Caron, M. G., Calakos, N., and Roth, B. L. (2013). A g[alpha]s dreadd mouse for selective modulation of camp production in striatopallidal neurons. *Neuropsychopharmacology*, 38(5):854–862.

[44] Ferguson, S. M. and Neumaier, J. F. (2012). Grateful dreadds: Engineered receptors reveal how neural circuits regulate behavior. *Neuropsychopharmacology*, 37(1):296–297. 22157861[pmid].

[45] Fernández, E., Greger, B., House, P. A., Aranda, I., Botella, C., Albisua, J., Soto-Sánchez, C., Alfaro, A., and Normann, R. A. (2014). Acute human brain responses to intracortical microelectrode arrays: challenges and future prospects. *Frontiers in Neuroengineering*, 7:24.

[46] Foley, C. P., Nishimura, N., Neeves, K. B., Schaffer, C. B., and Olbricht, W. L. (2009). Flexible microfluidic devices supported by biodegradable insertion scaffolds for convection-enhanced neural drug delivery. *Biomedical Microdevices*, 11(4):915–924.

[47] Fromherz, P., Offenhausser, A., Vetter, T., and Weis, J. (1991). A neuron-silicon junction: a retzius cell of the leech on an insulated-gate field-effect transistor. *Science*, 252(5010):1290–1293.

[48] Fujita, K., Ishikawa, T., and Tsutsui, T. (2002). Novel method for polymer thin film preparation: Spray deposition of highly diluted polymer solutions. *Japanese Journal of Applied Physics*, 41(1A):L70.

[Gary S. Aston-Jones] Gary S. Aston-Jones, G. R. S. Electrophysiology.

[50] Gleason, K. K. (2015). *CVD Polymers: Fabrication of Organic Surfaces and Devices*. Wiley-VCH.

[51] GM, X. Y. K. E. Z. X.-M. R. J. P. M. W. (1996). Complex optical surfaces formed by replica molding against elastomeric masters. *Science*, 273:347–349.

[52] Green, R. A., Lovell, N. H., Wallace, G. G., and Poole-Warren, L. A. (2008a). Conducting polymers for neural interfaces: Challenges in developing an effective long-term implant. *Biomaterials*, 29(24–25):3393 – 3399.

[53] Green, R. A., Lovell, N. H., Wallace, G. G., and Poole-Warren, L. A. (2008b). Conducting polymers for neural interfaces: Challenges in developing an effective long-term implant. *Biomaterials*, 29(24–25):3393 – 3399.

[54] Green, R. A., Matteucci, P. B., Hassarati, R. T., Giraud, B., Dodds, C. W. D., Chen, S., Byrnes-Preston, P. J., Suaning, G. J., Poole-Warren, L. A., and Lovell, N. H. (2013). Performance of conducting polymer electrodes for stimulating neuroprosthetics. *Journal of Neural Engineering*, 10(1):016009.

[55] Gu, W., Zhu, X., Futai, N., Cho, B. S., and Takayama, S. (2004). Computerized microfluidic cell culture using elastomeric channels and braille displays. *Proceedings of the National Academy of Sciences of the United States of America*, 101(45):15861–15866.

[56] Gustavsson, A., Svensson, M., Jacobi, F., Allgulander, C., Alonso, J., Beghi, E., Dodel, R., Ekman, M., Faravelli, C., Fratiglioni, L., Gannon, B., Jones, D. H., Jennum, P., Jordanova, A., Jönsson, L., Karampampa, K., Knapp, M., Kobelt, G., Kurth, T., Lieb, R., Linde, M., Ljungcrantz, C., Maercker, A., Melin, B., Moscarelli, M., Musayev, A., Norwood, F., Preisig, M., Pugliatti, M., Rehm, J., Salvador-Carulla, L., Schlehofer, B., Simon, R., Steinhausen, H.-C., Stovner, L. J., Vallat, J.-M., den Bergh, P. V., van Os, J., Vos, P., Xu, W., Wittchen, H.-U., Jönsson, B., and Olesen, J. (XXXX). Cost of disorders of the brain in europe 2010. *European Neuropsychopharmacology*, 21(10):718–779.

[57] HajjHassan Mohamad, Chodavarapu, V. M. S. (2008). Neuromems: Neural probe microtechnologies. *Sensors (Basel, Switzerland)*, pages 6704–6726.

[58] Hemm, S. and Wårdell, K. (2010). Stereotactic implantation of deep brain stimulation electrodes: a review of technical systems, methods and emerging tools. *Medical & Biological Engineering & Computing*, 48(7):611–624.

[59] Higgins, C. F. (2007). Multiple molecular mechanisms for multidrug resistance transporters. *Nature*, 446(7137):749–757.

[60] Hill N Jeremy, Gupta Disha, B. P. G. A. A. M. A. R. A. S. G. (2012). Recording human electrocorticographic (ecog) signals for neuroscientific research and real-time functional cortical mapping. *Epilepsia*, 64.

[61] HJ, Y. (2013). Additive effect of poly(4-vinylphenol) gate dielectric in organic thin film transistor at low temperature process. *Journal of Nanoscience and Nanotechnology*.

[62] Hochberg, L. R., Serruya, M. D., Friehs, G. M., Mukand, J. A., Saleh, M., Caplan, A. H., Branner, A., Chen, D., Penn, R. D., and Donoghue, J. P. (2006). Neuronal ensemble control of prosthetic devices by a human with tetraplegia. *Nature*, 442(7099):164–171.

[63] Horowitz, G. (1998). Organic field-effect transistors. *Advanced Materials*, 10(5):365–377.

[64] Inzelt, G. (2012). *Conducting Polymers*. Springer-Verlag Berlin Heidelberg.

[65] Isaksson, J., Kjall, P., Nilsson, D., Robinson, N., Berggren, M., and Richter-Dahlfors, A. (2007). Electronic control of ca2+ signalling in neuronal cells using an organic electronic ion pump. *Nat Mater*, 6(9):673–679.

[66] Isaksson, J., Nilsson, D., Kjäll, P., Robinson, N. D., Richter-Dahlfors, A., and Berggren, M. (2008). Electronically controlled ph gradients and proton oscillations. *Organic Electronics*, 9(3):303 – 309.

[67] Islam, A., Rabbani, M., Bappy, M. H., Miah, M. A. R., and Sakib, N. (2013). A review on fabrication process of organic light emitting diodes. In *Informatics, Electronics Vision (ICIEV), 2013 International Conference on*, pages 1–5.

[68] Itamar Willner, E. K., editor (2005). *Bioelectronics: From Theory to Applications*. Wiley-VCH, Weinheim.

[69] Jaeger, R. C. (2002). *Introduction to Microelectronic Fabrication: Volume 5 of Modular Series on Solid State Devices*. Academic Press.

[70] Jagur-Grodzinski, J. (1999). Biomedical application of functional polymers. *Reactive and Functional Polymers*, 39(2):99 – 138.

[71] Jirsa, V. K., Stacey, W. C., Quilichini, P. P., Ivanov, A. I., and Bernard, C. (2014). On the nature of seizure dynamics. *Brain*, 137(8):2210–2230.

[72] John E. McMurry, R. C. F. (2000). *Chemistry: Annotated Instructor's Edition*. Pearson Education.

[73] John Huguenard, David McCormick (2008). *Electrophysiology of the Neuron*. http://tonto.stanford.edu/eotn/.

[74] Johnson, M. D., Franklin, R. K., Gibson, M. D., Brown, R. B., and Kipke, D. R. (2008). Implantable microelectrode arrays for simultaneous electrophysiological and neurochemical recordings. *Journal of Neuroscience Methods*, 174(1):62 – 70.

[75] Jones, M. V., Jonas, P., Sahara, Y., and Westbrook, G. L. (XXXX). Microscopic kinetics and energetics distinguish gaba_a receptor agonists from antagonists. *Biophysical Journal*, 81(5):2660–2670.

[76] Jones, M. V. and Westbrook, G. L. (1996). The impact of receptor desensitization on fast synaptic transmission. *Trends in Neurosciences*, 19(3):96 – 101.

[77] Jones, M. V. and Westbrook, G. L. (XXXX). Desensitized states prolong gaba_a channel responses to brief agonist pulses. *Neuron*, 15(1):181–191.

[78] Jonsson, A., Song, Z., Nilsson, D., Meyerson, B. A., Simon, D. T., Linderoth, B., and Berggren, M. (2015). Therapy using implanted organic bioelectronics. *Science Advances*, 1(4).

[79] Jou, J.-H., Kumar, S., Agrawal, A., Li, T.-H., and Sahoo, S. (2015). Approaches for fabricating high efficiency organic light emitting diodes. *J. Mater. Chem. C*, 3:2974–3002.

[80] Kandel ER, Schwartz JH, J. T. (2000). *Principles of Neural Science. McGraw-Hill Professional*. McGraw-Hill Professional.

[81] Kergoat, L., Piro, B., Simon, D. T., Pham, M.-C., Noël, V., and Berggren, M. (2014). Detection of glutamate and acetylcholine with organic electrochemical transistors based on conducting polymer/platinum nanoparticle composites. *Advanced Materials*, 26(32):5658–5664.

[82] Khan, I. U., Serra, C. A., Anton, N., and Vandamme, T. (2013). Microfluidics: A focus on improved cancer targeted drug delivery systems. *Journal of Controlled Release*, 172(3):1065 – 1074.

[83] Khodagholy, D., Doublet, T., Gurfinkel, M., Quilichini, P., Ismailova, E., Leleux, P., Herve, T., Sanaur, S., Bernard, C., and Malliaras, G. G. (2011). Highly conformable conducting polymer electrodes for in vivo recordings. *Advanced Materials*, 23(36):H268–H272.

[84] Khodagholy, Dion, D. T. Q. P. G. M. L. P. G. A. I. E. H. T. S. S. B. C. M. G. G. (2013). In vivo recordings of brain activity using organic transistors. *Nature Communications*, 4.

[85] Khodagholy, Dion, G. J. N. T. T. D. W. D. O. M. G. G. B. G. (2014). Neurogrid: recording action potentials from the surface of the brain. *Nature Neuroscience*, 18:310–315.

[86] Kim, Y., Lee, J., Kang, H., Kim, G., Kim, N., and Lee, K. (2012). Controlled electrospray deposition of highly conductive pedot:pss films. *Solar Energy Materials and Solar Cells*, 98:39 – 45.

[87] Kittel, C. (2004). *Introduction to Solid State Physics, 8th Edition*. Wiley.

[88] Kofuji, P. and Newman, E. (2004). Potassium buffering in the central nervous system. *Neuroscience*, 129(4):1043 – 1054. Brain Water Homeostasis.

[89] Kotov, N. A., Winter, J. O., Clements, I. P., Jan, E., Timko, B. P., Campidelli, S., Pathak, S., Mazzatenta, A., Lieber, C. M., Prato, M., Bellamkonda, R. V., Silva, G. A., Kam, N. W. S., Patolsky, F., and Ballerini, L. (2009). Nanomaterials for neural interfaces. *Advanced Materials*, 21(40):3970–4004.

[90] Kringelbach, M. L., Jenkinson, N., Owen, S. L. F., and Aziz, T. Z. (2007). Translational principles of deep brain stimulation. *Nat Rev Neurosci*, 8(8):623–635.

[91] Krook-Magnuson, E., Armstrong, C., Oijala, M., and Soltesz, I. (2013). On-demand optogenetic control of spontaneous seizures in temporal lobe epilepsy. *Nat Commun*, 4:1376.

[92] Kullmann, D. M., Schorge, S., Walker, M. C., and Wykes, R. C. (2014). Gene therapy in epilepsy[mdash]is it time for clinical trials? *Nat Rev Neurol*, 10(5):300–304. Perspectives.

[93] Kuribara, K., Wang, H., Uchiyama, N., Fukuda, K., Yokota, T., Zschieschang, U., Jaye, C., Fischer, D., Klauk, H., Yamamoto, T., Takimiya, K., Ikeda, M., Kuwabara, H., Sekitani, T., Loo, Y.-L., and Someya, T. (2012). Organic transistors with high thermal stability for medical applications. *Nat Commun*, 3:723.

[94] Kwan, P. and Brodie, M. J. (XXXX). Neuropsychological effects of epilepsy and antiepileptic drugs. *The Lancet*, 357(9251):216–222.

[95] Kwan, P., Schachter, S. C., and Brodie, M. J. (2011). Drug-resistant epilepsy. *New England Journal of Medicine*, 365(10):919–926. PMID: 21899452.

[96] Kymissis, I., Dimitrakopoulos, C. D., and Purushothaman, S. (2002). Patterning pentacene organic thin film transistors. *Journal of Vacuum Science Technology B*, 20(3).

[97] LaVan, D. A., McGuire, T., and Langer, R. (2003). Small-scale systems for in vivo drug delivery. *Nat Biotech*, 21(10):1184–1191.

[98] Lewis, O., Woolley, M., Johnson, D., Rosser, A., Barua, N. U., Bienemann, A. S., Gill, S. S., and Evans, S. (2016). Chronic, intermittent convection-enhanced delivery devices. *Journal of Neuroscience Methods*, 259:47 – 56.

[99] Li, Y., Neoh, K. G., and Kang, E. T. (2005). Controlled release of heparin from polypyrrole-poly(vinyl alcohol) assembly by electrical stimulation. *Journal of Biomedical Materials Research Part A*, 73A(2):171–181.

[100] liang Feng, C., hong Xu, Y., and min Song, L. (2000). Study on highly sensitive potentiometric igg immunosensor. *Sensors and Actuators B: Chemical*, 66(1–3):190 – 192.

[101] Liao, C., Zhang, M., Yao, M. Y., Hua, T., Li, L., and Yan, F. (2015). Flexible organic electronics in biology: Materials and devices. *Advanced Materials*, 27(46):7493–7527.

[Lodish H] Lodish H, Berk A, Z. S. e. a. *Molecular Cell Biology. 4th edition. Section 21.1, Overview of Neuron Structure and Function.* http://www.ncbi.nlm.nih.gov/books/NBK21535/, New York.

[103] Loscher, W., Klitgaard, H., Twyman, R. E., and Schmidt, D. (2013). New avenues for anti-epileptic drug discovery and development. *Nat Rev Drug Discov*, 12(10):757–776. Review.

[104] Loscher, W. and Potschka, H. (2005). Drug resistance in brain diseases and the role of drug efflux transporters. *Nat Rev Neurosci*, 6(8):591–602.

[105] Ludwig, K. A., Uram, J. D., Yang, J., Martin, D. C., and Kipke, D. R. (2006). Chronic neural recordings using silicon microelectrode arrays electrochemically deposited with a poly(3,4-ethylenedioxythiophene) (pedot) film. *Journal of Neural Engineering*, 3(1):59.

[106] Luo, X. and Cui, X. T. (2011). Electrochemical deposition of conducting polymer coatings on magnesium surfaces in ionic liquid. *Acta Biomaterialia*, 7(1):441 – 446.

[107] Madsen, K. K., White, H. S., and Schousboe, A. (2010). Neuronal and non-neuronal {GABA} transporters as targets for antiepileptic drugs. *Pharmacology Therapeutics*, 125(3):394 – 401.

[108] Malhotra, B. D., Chaubey, A., and Singh, S. (2006). Prospects of conducting polymers in biosensors. *Analytica Chimica Acta*, 578(1):59 – 74. Pacifichem {SIImmobilization} and Applications ofFunctional Proteins, Nucleic Acids andCells at Solid Interfaces.

[109] Mannerbro, R., Ranlöf, M., Robinson, N., and Forchheimer, R. (2008). Inkjet printed electrochemical organic electronics. *Synthetic Metals*, 158(13):556 – 560.

[110] Mark W Barnett, P. M. L. (2007). The action potential. *Pract Neurol*, pages 192–197.

[111] Maruyama, T. and Shionoya, J. (1989). Silicon dioxide thin films prepared by chemical vapor deposition from silicon tetraacetate. *Japanese Journal of Applied Physics*, 28(12A):L2253.

[112] Merrill, D. R., Bikson, M., and Jefferys, J. G. (2005). Electrical stimulation of excitable tissue: design of efficacious and safe protocols. *Journal of Neuroscience Methods*, 141(2):171 – 198.

[113] Michel A Aegerter, M. M. (2004). *Sol-Gel Technologies for Glass Producers and Users*. Springer US, New York.

[114] Minev, I. R., Musienko, P., Hirsch, A., Barraud, Q., Wenger, N., Moraud, E. M., Gandar, J., Capogrosso, M., Milekovic, T., Asboth, L., Torres, R. F., Vachicouras, N., Liu, Q., Pavlova, N., Duis, S., Larmagnac, A., Vörös, J., Micera, S., Suo, Z., Courtine, G., and Lacour, S. P. (2015). Electronic dura mater for long-term multimodal neural interfaces. *Science*, 347(6218):159–163.

[115] Nelson, J. (2011). Polymer:fullerene bulk heterojunction solar cells. *Materials Today*, 14(10):462 – 470.

[116] Nüesch, F., Upadhyaya, H., Razykov, T., and Tiwari, A. (2011). Introduction to the special issue on organic photovoltaics and dye sensitized solar cells. *Solar Energy*, 85(6):1171 –. Organic photovoltaics and dye sensitized solar cells.

[117] Ng, J. M. K., Gitlin, I., Stroock, A. D., and Whitesides, G. M. (2002). Components for integrated poly(dimethylsiloxane) microfluidic systems. *ELECTROPHORESIS*, 23(20):3461–3473.

[118] Nikolou, M. and Malliaras, G. G. (2008). Applications of poly(3,4-ethylenedioxythiophene) doped with poly(styrene sulfonic acid) transistors in chemical and biological sensors. *The Chemical Record*, 8(1):13–22.

[119] Obien, M. E. J., Deligkaris, K., Bullmann, T., Bakkum, D. J., and Frey, U. (2015). Revealing neuronal function through microelectrode array recordings. *Frontiers in Neuroscience*, 8:423.

[120] Padeste, C., Grubelnik, A., and Tiefenauer, L. (1998). Amperometric immunosensing using microperoxidase mp-11 antibody conjugates. *Analytica Chimica Acta*, 374(2–3):167 – 176.

[121] Pauling, L. (1931). The nature of the chemical bond. application of results obtained from the quantum mechanics and from a theory of paramagnetic susceptibility to the structure of molecules. *Journal of the American Chemical Society*, 53(4):1367–1400.

[122] Paz, J. T., Davidson, T. J., Frechette, E. S., Delord, B., Parada, I., Peng, K., Deisseroth, K., and Huguenard, J. R. (2013). Closed-loop optogenetic control of thalamus as a tool for interrupting seizures after cortical injury. *Nat Neurosci*, 16(1):64–70.

[123] Perucca, P. and Gilliam, F. G. (XXXX). Adverse effects of antiepileptic drugs. *The Lancet Neurology*, 11(9):792–802.

[124] Pettit, G. H. and Sauerbrey, R. (1993). Pulsed ultraviolet laser ablation. *Applied Physics A*, 56(1):51–63.

[125] Prodanov, D. and Delbeke, J. (2016). Mechanical and biological interactions of implants with the brain and their impact on implant design. *Frontiers in Neuroscience*, 10:11.

[126] Qin, Dong, X. Y. W. G. M. (2010). Soft lithography for micro- and nanoscale patterning. *Nature Protocols*, 5(3):491–502.

[127] Reeja-Jayan, B., Kovacik, P., Yang, R., Sojoudi, H., Ugur, A., Kim, D. H., Petruczok, C. D., Wang, X., Liu, A., and Gleason, K. K. (2014). A route towards sustainability through engineered polymeric interfaces. *Advanced Materials Interfaces*, 1(4):n/a–n/a. 1400117.

[128] Reese, C., Roberts, M., mang Ling, M., and Bao, Z. (2004). Organic thin film transistors. *Materials Today*, 7(9):20 – 27.

[129] Riahi, R., Tamayol, A., Shaegh, S. A. M., Ghaemmaghami, A. M., Dokmeci, M. R., and Khademhosseini, A. (2015a). Microfluidics for advanced drug delivery systems. *Current Opinion in Chemical Engineering*, 7:101 – 112.

[130] Riahi, R., Tamayol, A., Shaegh, S. A. M., Ghaemmaghami, A. M., Dokmeci, M. R., and Khademhosseini, A. (2015b). Microfluidics for advanced drug delivery systems. *Current Opinion in Chemical Engineering*, 7:101 – 112.

[131] Richardson, R. T., Wise, A. K., Thompson, B. C., Flynn, B. O., Atkinson, P. J., Fretwell, N. J., Fallon, J. B., Wallace, G. G., Shepherd, R. K., Clark, G. M., and O'Leary, S. J. (2009). Polypyrrole-coated electrodes for the delivery of charge and neurotrophins to cochlear neurons. *Biomaterials*, 30(13):2614 – 2624.

[132] Rivnay, J., Inal, S., Collins, B. A., Sessolo, M., Stavrinidou, E., Strakosas, X., Tassone, C., Delongchamp, D. M., and Malliaras, G. G. (2016). Structural control of mixed ionic and electronic transport in conducting polymers. *Nat Commun*, 7:11287. 27090156[pmid].

[133] Rivnay, J., Leleux, P., Ferro, M., Sessolo, M., Williamson, A., Koutsouras, D. A., Khodagholy, D., Ramuz, M., Strakosas, X., Owens, R. M., Benar, C., Badier, J.-M., Bernard, C., and Malliaras, G. G. (2015). High-performance transistors for bioelectronics through tuning of channel thickness. *Science Advances*, 1(4).

[134] Rivnay, J., Leleux, P., Sessolo, M., Khodagholy, D., Hervé, T., Fiocchi, M., and Malliaras, G. G. (2013). Organic electrochemical transistors with maximum transconductance at zero gate bias. *Advanced Materials*, 25(48):7010–7014.

[135] Rivnay, J., Owens, R. M., and Malliaras, G. G. (2014). The rise of organic bioelectronics. *Chemistry of Materials*, 26(1):679–685.

[136] Rogawski, M. A. and Loscher, W. (2004). The neurobiology of antiepileptic drugs. *Nat Rev Neurosci*, 5(7):553–564.

[137] Rouse, A. G., Williams, J. J., Wheeler, J. J., and Moran, D. W. (2013). Cortical adaptation to a chronic micro-electrocorticographic brain computer interface. *The Journal of Neuroscience*, 33(4):1326–1330.

[138] Rousseau, T., Cravino, A., Bura, T., Ulrich, G., Ziessel, R., and Roncali, J. (2009a). Bodipy derivatives as donor materials for bulk heterojunction solar cells. *Chem. Commun.*, pages 1673–1675.

[139] Rousseau, T., Cravino, A., Bura, T., Ulrich, G., Ziessel, R., and Roncali, J. (2009b). Bodipy derivatives as donor materials for bulk heterojunction solar cells. *Chem. Commun.*, pages 1673–1675.

[140] Rousseau, T., Cravino, A., Bura, T., Ulrich, G., Ziessel, R., and Roncali, J. (2009c). Multi-donor molecular bulk heterojunction solar cells: improving conversion efficiency by synergistic dye combinations. *J. Mater. Chem.*, 19:2298–2300.

[141] Rutecki, P. A., Lebeda, F. J., and Johnston, D. (1985). Epileptiform activity induced by changes in extracellular potassium in hippocampus. *Journal of Neurophysiology*, 54(5):1363–1374.

[142] Saltzman, W. M. and Olbricht, W. L. (2002). Building drug delivery into tissue engineering design. *Nat Rev Drug Discov*, 1(3):177–186.

[143] Sambandan, S. (2012). *Non-Crystalline Semiconductors*. CRC Press.

[144] Sandro Carrara, K. I. (2008). *Handbook of Bioelectronics Directly Interfacing Electronics and Biological Systems*. Cambridge University Press.

[145] Scanziani, Massimo, H. M. (2009). Electrophysiology in the age of light. *Nature*, pages 930–939.

[146] Schaaf, P. (2010). *Laser Processing of Materials*. Springer-Verlag Berlin Heidelberg, first edition.

[147] Schalk, G. (2010). Can electrocorticography (ecog) support robust and powerful brain-computer interfaces? *Frontiers in Neuroengineering*, 3:9.

[148] Schalk, G. and Leuthardt, E. C. (2011). Brain-computer interfaces using electrocorticographic signals. *IEEE Reviews in Biomedical Engineering*, 4:140–154.

[149] Scheld, W. M. (1989). Drug delivery to the central nervous system: General principles and relevance to therapy for infections of the central nervous system. *Reviews of Infectious Diseases*, 11:S1669–S1690.

[150] Schevon, C. A., Weiss, S. A., McKhann, G., Goodman, R. R., Yuste, R., Emerson, R. G., and Trevelyan, A. J. (2012). Evidence of an inhibitory restraint of seizure activity in humans. *Nat Commun*, 3:1060.

[151] Semyanov, A., Walker, M. C., and Kullmann, D. M. (2003). Gaba uptake regulates cortical excitability via cell type-specific tonic inhibition. *Nat Neurosci*, 6(5):484–490.

[152] Sessolo, M., Khodagholy, D., Rivnay, J., Maddalena, F., Gleyzes, M., Steidl, E., Buisson, B., and Malliaras, G. G. (2013). Easy-to-fabricate conducting polymer microelectrode arrays. *Advanced Materials*, 25(15):2135–2139.

[153] Simon, D. T., Kurup, S., Larsson, K. C., Hori, R., Tybrandt, K., Goiny, M., Jager, E. W. H., Berggren, M., Canlon, B., and Richter-Dahlfors, A. (2009). Organic electronics for precise delivery of neurotransmitters to modulate mammalian sensory function. *Nat Mater*, 8(9):742–746.

[154] Simon, D. T., Larsson, K. C., Nilsson, D., Burström, G., Galter, D., Berggren, M., and Richter-Dahlfors, A. (2015). An organic electronic biomimetic neuron enables auto-regulated neuromodulation. *Biosensors and Bioelectronics*, 71:359 – 364.

[155] Simon, Daniel T., K. S. L. K. C. H. R. T. K. G. M. J. E. W. H. B. M. C. B. R.-D. A. (2009). Organic electronics for precise delivery of neurotransmitters to modulate mammalian sensory function. *Nature Materials*, 8(9):742–746.

[156] Sirringhaus, H. (2014). 25th anniversary article: Organic field-effect transistors: The path beyond amorphous silicon. *Advanced Materials*, 26(9):1319–1335.

[157] Spira, Micha E., H. A. (2013a). Multi-electrode array technologies for neuroscience and cardiology. *Nature Nanotechnology*, pages 83–94.

[158] Spira, Micha E., H. A. (2013b). Multi-electrode array technologies for neuroscience and cardiology. *Nature Nanotehcnology*, 8:83–94.

[159] Stavrinidou, E., Leleux, P., Rajaona, H., Khodagholy, D., Rivnay, J., Lindau, M., Sanaur, S., and Malliaras, G. G. (2013). Direct measurement of ion mobility in a conducting polymer. *Advanced Materials*, 25(32):4488–4493.

[160] Stringer, J. L. and Lothman, E. W. (1988). Epileptiform discharges induced by altering extracellular potassium and calcium in the rat hippocampal slice. *Experimental Neurology*, 101(1):147 – 157.

[161] Suzuki, H. and Yoneyama, R. (2003). Integrated microfluidic system with electrochemically actuated on-chip pumps and valves. *Sensors and Actuators B: Chemical*, 96(1–2):38 – 45.

[162] Svirskis, D., Travas-Sejdic, J., Rodgers, A., and Garg, S. (2010). Electrochemically controlled drug delivery based on intrinsically conducting polymers. *Journal of Controlled Release*, 146(1):6 – 15.

[163] Tang, H., Yan, F., Lin, P., Xu, J., and Chan, H. L. W. (2011). Highly sensitive glucose biosensors based on organic electrochemical transistors using platinum gate electrodes modified with enzyme and nanomaterials. *Advanced Functional Materials*, 21(12):2264–2272.

[164] Tarasov, A., Wipf, M., Stoop, R. L., Bedner, K., Fu, W., Guzenko, V. A., Knopfmacher, O., Calame, M., and Schönenberger, C. (2012). Understanding the electrolyte background for biochemical sensing with ion-sensitive field-effect transistors. *ACS Nano*, 6(10):9291–9298. PMID: 23016890.

[165] Tehrani, P., Robinson, N. D., Kugler, T., Remonen, T., Hennerdal, L.-O., Häll, J., Malmström, A., Leenders, L., and Berggren, M. (2005). Patterning polythiophene films using electrochemical over-oxidation. *Smart Materials and Structures*, 14(4):N21.

[166] Teichler, A., Perelaer, J., and Schubert, U. S. (2013). Inkjet printing of organic electronics - comparison of deposition techniques and state-of-the-art developments. *J. Mater. Chem. C*, 1:1910–1925.

[Thakor] Thakor, N. Building brain machine interfaces – neuroprosthetic control with electrocorticographic signals.

[168] Thompson, J.A., L. D. I. N. A. A. (2014). Clinical implications of local field potentials for understanding and treating movement disorders. *Stereotactic and Functional Neurosurgery*, pages 251–263.

[169] Torchilin, V. P. (2000). Drug targeting. *European Journal of Pharmaceutical Sciences*, 11, Supplement 2:S81 – S91. Frontiers in Biopharmacy.

[170] Trevelyan, A. J. (2009). The direct relationship between inhibitory currents and local field potentials. *The Journal of Neuroscience*, 29(48):15299–15307.

[171] Trevelyan, A. J., Sussillo, D., Watson, B. O., and Yuste, R. (2006). Modular propagation of epileptiform activity: Evidence for an inhibitory veto in neocortex. *The Journal of Neuroscience*, 26(48):12447–12455.

[172] Tsumura, A., Koezuka, H., and Ando, T. (1986). Macromolecular electronic device: Field-effect transistor with a polythiophene thin film. *Applied Physics Letters*, 49(18).

[173] Turner, J., Shain, W., Szarowski, D., Andersen, M., Martins, S., Isaacson, M., and Craighead, H. (1999). Cerebral astrocyte response to micromachined silicon implants. *Experimental Neurology*, 156(1):33 – 49.

[174] Tybrandt, K., Larsson, K. C., Kurup, S., Simon, D. T., Kjäll, P., Isaksson, J., Sandberg, M., Jager, E. W. H., Richter-Dahlfors, A., and Berggren, M. (2009). Translating electronic currents to precise acetylcholine–induced neuronal signaling using an organic electrophoretic delivery device. *Advanced Materials*, 21(44):4442–4446.

[175] Tye, K. M. and Deisseroth, K. (2012). Optogenetic investigation of neural circuits underlying brain disease in animal models. *Nat Rev Neurosci*, 13(4):251–266.

[176] V.B. Gupta, V. K. (2012). *Manufactured Fibre Technology*. Springer Science Business Media.

[177] Viventi, J., Kim, D.-H., Vigeland, L., Frechette, E. S., Blanco, J. A., Kim, Y.-S., Avrin, A. E., Tiruvadi, V. R., Hwang, S.-W., Vanleer, A. C., Wulsin, D. F., Davis, K., Gelber, C. E., Palmer, L., Van der Spiegel, J., Wu, J., Xiao, J., Huang, Y., Contreras, D., Rogers, J. A., and Litt, B. (2011). Flexible, foldable, actively multiplexed, high-density electrode array for mapping brain activity in vivo. *Nat Neurosci*, 14(12):1599–1605.

[178] Vorotilov, K., Petrovsky, V., and Vasiljev, V. (1995). Spin coating process of sol-gel silicate films deposition: Effect of spin speed and processing temperature. *Journal of Sol-Gel Science and Technology*, 5(3):173–183.

[179] Wadhwa, R., Lagenaur, C. F., and Cui, X. T. (2006a). Electrochemically controlled release of dexamethasone from conducting polymer polypyrrole coated electrode. *Journal of Controlled Release*, 110(3):531 – 541.

[180] Wadhwa, R., Lagenaur, C. F., and Cui, X. T. (2006b). Electrochemically controlled release of dexamethasone from conducting polymer polypyrrole coated electrode. *Journal of Controlled Release*, 110(3):531 – 541.

[181] Wahab, A., Albus, K., Gabriel, S., and Heinemann, U. (2010). In search of models of pharmacoresistant epilepsy. *Epilepsia*, 51:154–159.

[White et al.] White, H. S., Kittlesen, G. P., and Wrighton, M. S.

[183] White, S. P., Dorfman, K. D., and Frisbie, C. D. (2016). Operating and sensing mechanism of electrolyte-gated transistors with floating gates: Building a platform for amplified biodetection. *The Journal of Physical Chemistry C*, 120(1):108–117.

[184] Wilks, S., Richardson-Burn, S., Hendricks, J., Martin, D., and Otto, K. (2009). Poly(3,4-ethylene dioxythiophene) (pedot) as a micro-neural interface material for electrostimulation. *Frontiers in Neuroengineering*, 2:7.

[185] Willner, I. and Katz, E. (2005). *Bioelectronics – An Introduction*, pages 1–13. Wiley-VCH Verlag GmbH Co. KGaA.

[186] Willson, C. G., Dammel, R. R., and Reiser, A. (1997). Photoresist materials: a historical perspective. *Proc. SPIE*, 3049:28–41.

[187] Wolinsky, J. B., Colson, Y. L., and Grinstaff, M. W. (2012). Local drug delivery strategies for cancer treatment: Gels, nanoparticles, polymeric films, rods, and wafers. *Journal of Controlled Release*, 159(1):14 – 26.

[188] Wykes, R. C., Heeroma, J. H., Mantoan, L., Zheng, K., MacDonald, D. C., Deisseroth, K., Hashemi, K. S., Walker, M. C., Schorge, S., and Kullmann, D. M. (2012). Optogenetic and potassium channel gene therapy in a rodent model of focal neocortical epilepsy. *Science Translational Medicine*, 4(161):161ra152–161ra152.

[189] Xia, Y., Kim, E., Mrksich, M., , and Whitesides*, G. M. (1996). Microcontact printing of alkanethiols on copper and its application in microfabrication. *Chemistry of Materials*, 8(3):601–603.

[190] Yang, J. and Martin, D. C. (2006). Impedance spectroscopy and nanoindentation of conducting poly(3,4-ethylenedioxythiophene) coatings on microfabricated neural prosthetic devices. *Journal of Materials Research*, 21(5):1124–1132.

[191] Zhao XM, Xia YN, W. G. (1996). Fabrication of three-dimensional micro-structures: Microtransfer molding. *Advanced Materials*, 8(10):837–840.

[192] Zimmermann, K. A. (March 2016). Nervous system: Facts, function diseases.

École Nationale Supérieure des Mines
de Saint-Étienne

NNT : **2016LYSEM027**

Ilke UGUZ

Organic Implantable Probes for in vivo Recordings of Electrophysciological Activity and Drug Delivery

Speciality : Microelectronics / Bioelectronics

Keywords : Bioelectronics, Implantable biomedical devices, Organic electronics, Organic electrochemical transistors, Organic electrophoretic ion pumps...

Abstract :

Recordings and stimulation of in vivo neural activity are necessary for diagnostic purposes and for brain-machine interfaces. Organic electronic devices constitute a promising candidate due to their mechanical flexibility and biocompatibility. Local control of neuronal activity is central to many therapeutic strategies aiming to treat neurological disorders. Arguably, the best solution would make use of endogenous highly localized and specialized regulatory mechanisms of neuronal activity, and an ideal therapeutic technology should sense activity and deliver endogenous molecules simultaneously to achieve the most efficient feedback regulation. Thus, there is a need for novel devices to specifically interface nerve cells. Here, we demonstrate an organic electronic device capable of precisely delivering neurotransmitters in vitro and in vivo. In converting electronic addressing into delivery of neurotransmitters, the device mimics the nerve synapse. The inhibitory neurotransmitter, -aminobutyric acid (GABA), was actively delivered and stopped epileptiform activity, recorded simultaneously and colocally. These multifunctional devices create a range of opportunities, including implantable therapeutic devices with automated feedback, where locally recorded signals regulate local release of specific therapeutic agents. In addition, we demonstrate the engineering of an organic electrochemical transistor embedded in an ultrathin organic film designed to record electrophysiological signals on the surface of the brain. The device was applied in vivo and epidurally implanted could reach capabilities beyond similar sized electrodes allowing minimally invasive monitoring of brain activity.

École Nationale Supérieure des Mines
de Saint-Étienne

NNT : **2016LYSEM027**

Ilke UGUZ

Sondes organiques implantables pour l'enregistrement in vivo de l'activité électrophysiologique et le relarguage de drogues

Spécialité: Microelectronique/bioelectronique

Mots clefs : Bioélectronique, Dispositifs Biomédicaux Implantables, Electronique organique, Transistor organique électrochimique, Pompe ionique organique, ...

Résumé :

L'enregistrement et la stimulation in vivo de l'activité neuronale peuvent aussi bien servir pour la recherche médicale que pour les interfaces cerveau-machine. Les dispositifs à base d'électronique organique sont de prometteurs candidats pour ce faire, grâce à leur flexibilité et leur biocompatibilité. Le contrôle local de l'activité neuronale est la clé de nombreuses stratégies thérapeutiques visant à traiter les troubles neurologiques. Une solution idéale serait donc de fabriquer un dispositif capable de détecter l'activité neuronale et, en réponse, d'injecter des molécules endogènes. L'un des objectifs de cette thèse est de s'attaquer à cette problématique à l'aide d'un dispositif permettant à la fois de stimuler les cellules, et de mesurer l'activité neuronale, au même endroit, à l'échelle cellulaire. Nous présentons un dispositif organique capable de délivrer précisément des neurotransmetteurs in vitro et in vivo. En convertissant un signal électrique en la délivrance de neurotransmetteurs, le dispositif mime le fonctionnement d'une synapse. Le neurotransmetteur inhibiteur, l'acide γ- aminobutyrique (GABA), est relargué au niveau des électrodes d'enregistrement par l'activation d'une pompe ionique électronique. L'injection du GABA engendre l'arrêt de l'activité épileptique qui a été enregistré au niveau des électrodes. Des dispositifs multifonctionnels ouvrent de nombreuses possibilités, incluant des dispositifs thérapeutiques avec des boucles de retour, avec lesquels l'enregistrement local de signaux régule la délivrance d'agents thérapeutiques. De plus, nous avons également réalisé pendant cette thèse l'intégration de transistors organiques sur un film organique ultra fin, pour mesurer les signaux électrophysiologiques in vivo à la surface d'un cerveau de rat. Le dispositif, implanté de façon épidurale, montre des résultats surpassant certains dispositifs subduraux de taille similaire, permettant ainsi une approche moins invasive et efficace pour mesurer l'activité neuronale.